EXPLORING DYNAMICS AND STEREOCHEMISTRY IN MECHANICALLY-INTERLOCKED COMPOUNDS

Scott A. VIGNON[1] and J. Fraser STODDART[2,*]

California NanoSystems Institute and Department of Chemistry and Biochemistry, University of California, Los Angeles, 405 Hilgard Avenue, Los Angeles, CA 90095-1569, U.S.A.; e-mail: [1] scvignon@chem.ucla.edu, [2] stoddart@chem.ucla.edu

Received May 4, 2005
Accepted June 15, 2005

1. Introduction 1494
1.1. History 1494
1.2. Dynamics 1496
1.3. Stereochemistry 1503
2. Dynamics and Stereochemistry of Donor–Acceptor [2]Catenanes 1506
2.1. Background 1506
2.2. Dynamics 1507
2.3. Stereochemistry 1514
2.4. Conclusions 1521
3. Dynamics and Switching of Tetrathiafulvalene-Containing Catenanes and Rotaxanes 1522
3.1. Background 1522
3.2. Dynamics 1524
3.3. Switching 1531
3.4. Conclusions 1540
4. Dynamics and Switching of Donor-Acceptor Neutral Rotaxanes 1541
4.1. Background 1541
4.2. Dynamics 1545
4.3. Switching 1551
4.4. Conclusions 1555
5. Dynamics and Switching in Self-Complexes and Pretzelanes 1556
5.1. Background 1556
5.2. Dynamics 1558
5.3. Switching 1566
5.4. Conclusions 1568
6. References and Notes 1569

The advent of self-assembly and template-directed synthetic protocols has led to a tremendous surge in the number of mechanically-interlocked compounds being prepared and studied. As these investigations are being carried out, it is becoming increasingly apparent that many of these compounds, known as catenanes and rotaxanes, possess unique dynamic and stereochemical properties. In addition, the drive to create molecular switches and machines

for nanotechnological applications has generated a need to understand how to control those properties in condensed phases. Here, we present an overview of the field with regard to the solution dynamics and stereochemistry of mechanically-interlocked compounds – as well as to some related structural types – and review the recent results from our own research in some detail. ^{1}H NMR spectroscopy has proven to be a powerful tool for probing both degenerate and nondegenerate dynamic processes in these compounds, as well as for identifying stereoisomers if they are present in solution. The results of several variable temperature NMR investigations on the effects of structural changes upon the dynamic processes and stimulated relative motions of components in catenanes and rotaxanes, as well as in some self-complexes and pretzelanes, are discussed. A review with 90 references.

Keywords: Catenanes; Donor–acceptor; Dynamic stereochemistry; Molecular machines; NMR dynamics; Pretzelanes; Rotaxanes; Self-complexing; Tetrathiafulvalenes; Macrocycles.

1. INTRODUCTION

1.1. History

The concept of a mechanical bond is one we are familiar with in the macroscopic world. In medieval times, mechanically-interlocked metal loops were used for defense in the form of chain-mail and for offense in the shape of the flexible component of a flail. In more recent times, macroscopic mechanical bonds can be found in everyday life – for example, interconnected carabiners used by mountain climbers or the rings of a keychain (Fig. 1). Although the concept of two macroscopic objects linked together by a me-

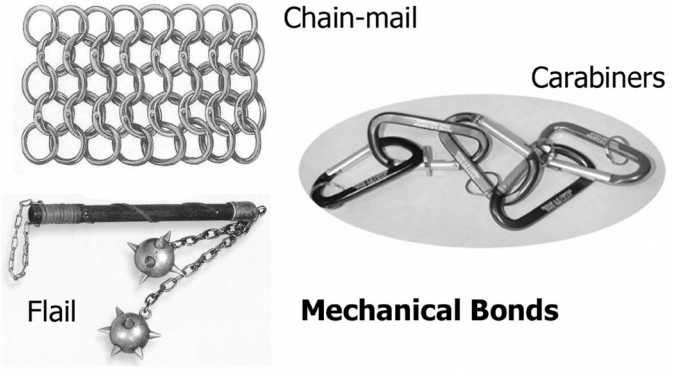

FIG. 1
Three examples of macroscopic objects containing mechanical bonds – a small piece of chain-mail armor, the chain in a medieval flail and five interconnected carabiners used for mountain climbing

chanical bond seems as natural to us as any other form of connection, the molecular equivalent has taken many decades to reach the point where such systems are easily accessible. Indeed, new and interesting chemistry arising from mechanically-interlocked compounds is still being discovered to this day.

In 1960, Wasserman[1] reported what is generally accepted today to be the first wholly synthetic catenane – a molecule composed of two interlocking rings with no covalent bonds connecting them. Because these rings are inseparable without cutting one ring or the other, they are said to be joined by a mechanical bond. As a result of this important discovery, chemists began to realize that it was also important to consider topology, in addition to atom connectivity and bond geometries, when describing a molecule. Frisch and Wasserman[2] published a landmark paper in 1961 discussing this topic of chemical topology, in which a variety of topologically interesting structures were proposed. Many of these structures, such as higher-order catenanes[3], trefoil knots[4], and the Borromean rings[5], have since been synthesized, largely on account of new developments in synthetic methodology.

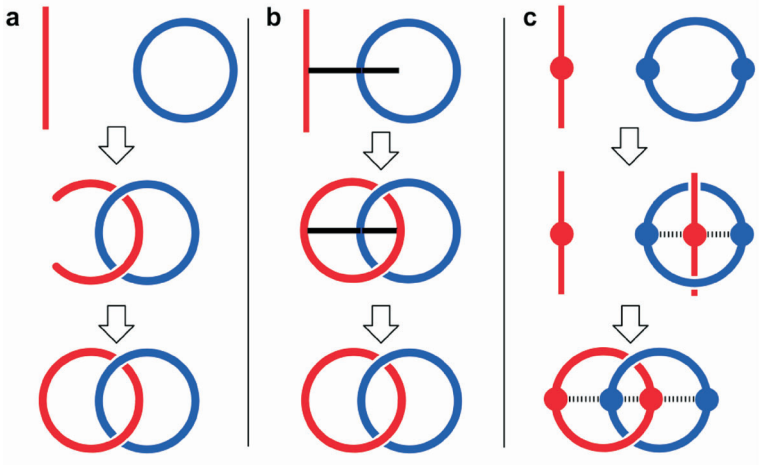

FIG. 2
Three different synthetic schemes for constructing a [2]catenane, including **a** the statistical method, where the catenane is formed by the chance macrocyclization of a thread while it resides within another ring, **b** covalent bond-directed synthesis, in which the ring and thread are joined by one or more covalent bonds that are cleaved after macrocyclization, and **c** noncovalent bond template-directed synthesis, with one ring acting as a noncovalent template during formation of the second ring

The first catenanes and rotaxanes – mechanically interlocked compounds composed of a ring component trapped on a rod-like component by bulky stoppers – were synthesized (Fig. 2a) using statistical methods. For example, catenanes can be formed by the chance closing of a thread, while it resides momentarily inside another macrocycle. As expected, low yields were the usual outcome of such statistical schemes. An alternative method, namely, covalent-directed synthesis (Fig. 2b), was demonstrated[6] in 1964. In this method, the first component, either a ring or rod, is linked via a covalent bond to the second ring-forming component, and cleavage of the link after macrocyclization produces the catenane or rotaxane. While orders of magnitude improvements in yields were obtained using this covalent bond-directed method, further improvements were later achieved via the use of template-directed synthesis involving coordinative and/or noncovalent bonds.

Templates, which can be ions, transition metals, other molecules, etc., act in the opposite way from which a traditional mold works. The new entity which is being formed wraps around the template to assume a complementary shape, and then it is fixed in its new location as a result of the formation of one or more covalent bonds. During catenation, for example, one ring can be used to template the formation (Fig. 2c) of the other ring, greatly improving the yield of the catenane. Since many reviews have been written describing the use of template-directed synthesis[7] and self-assembly[8] in mechanically-interlocked systems[9], the details will not be presented here. Suffice it to say that, once these compounds became more available in terms of quantity and diversity, researchers began to explore the unique and potentially useful properties that arise from incorporation of mechanical bonds into molecules.

1.2. Dynamics

One of the side-effects of the popular template-directed synthetic scheme employed for the construction of catenanes and rotaxanes arises because the interactions used during their synthesis usually live on after the product has been isolated. These interactions have an influence on the co-conformers[10] adopted and the dynamic processes that occur involving the mechanical bond(s) in these molecules. Both degenerate and non-degenerate processes can arise as a result. The investigation of these processes has been the subject of considerable attention on account of their potential applications in the creation of artificial molecular machines and switches[11].

To date, the mechanically-interlocked compounds that are the most often synthesized and investigated are [2]catenanes and [2]rotaxanes, where the number in square brackets indicates the number of interlocked components, i.e., two rings or one ring and one dumbbell-shaped component, respectively. In addition to the usual dynamic processes involving torsions around covalent bonds present in the vast majority of molecules, the presence of a mechanical bond in these molecules opens up the possibility for the existence of additional dynamic processes, such as circumrotation, rocking and shuttling. An example of each will now be presented here briefly.

In catenanes, the most commonly observed mechanical motion[12] is circumrotation, or pirouetting, which involves rotation of one ring through, or around, the other ring. Leigh et al.[13] reported observing circumrotation (Fig. 3b) in an amide-based [2]catenane (Fig. 3a) using variable temperature (VT) NMR spectroscopy. The circumrotation process causes exchange to occur between two degenerate co-conformers, which are stabilized by hydrogen bonding between the amide nitrogens, carbonyl oxygens and pyridine nitrogens. This process occurs (Fig. 3b) with a barrier[14] of

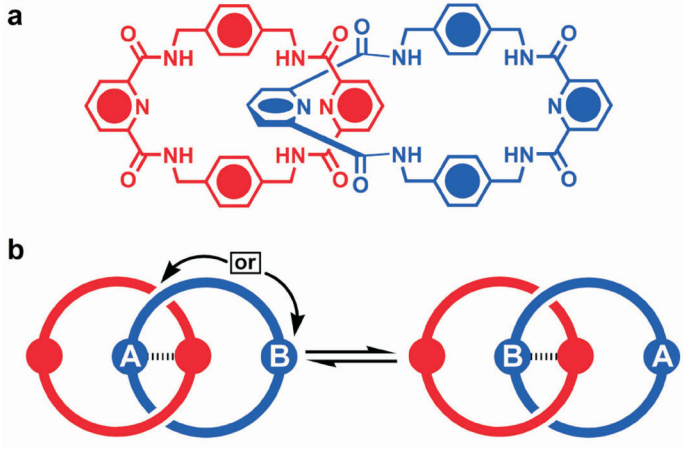

FIG. 3
a The structural formula of an amide-based [2]catenane. **b** A schematic representation of circumrotation in a degenerate [2]catenane. One ring rotates through the other ring, in either direction, to exchange sites A and B

18 kcal mol^{-1} at 377 K in CD_3SOCD_3. Further studies were also performed to (i) assess the sensitivity of this barrier to the environment[15] and (ii) to explore[16] the mechanism by computational chemistry.

If the angle between the planes that contain the rings of a [2]catenane is other than 90°, the possibility for a rocking process also arises. This process involves rocking of one ring relative to the other, via a "rotation" about the mechanical bond, to effect the exchange between the two co-conformers. We have observed this rocking motion in a series of [2]catenanes and determined the rate of exchange by VT-NMR spectroscopy[17]. For the donor/acceptor [2]catenane, the structure of which is shown in Fig. 4a, the barrier at 215 K in CD_3COCD_3 was determined to be 9 kcal mol^{-1}. If the symmetry of the ring components is reduced or additional chiral elements are introduced into this [2]catenane, then the rocking process will[18] result in the interconversion of diastereoisomers.

In rotaxanes, which can alternatively be described as a catenane where one ring has been severed and stoppers placed on the ends, the equivalent of circumrotation is referred to as shuttling, a process in which the ring component undergoes translation along the rod-like component. An example of a molecular shuttle[19] was reported by Leigh et al.[20] in the form of a peptide-based [2]rotaxane (Fig. 5), in which hydrogen bonding between amides in the ring and in the rod-like component create two stable co-conformers. The ring shuttles back and forth between the two degenerate sites with a barrier of 11.2 kcal mol^{-1} in CD_2Cl_2 at 298 K, as observed by VT-NMR spectroscopy. A computational study was also performed[21] to shed light on the mechanism of shuttling in a series of related rotaxanes.

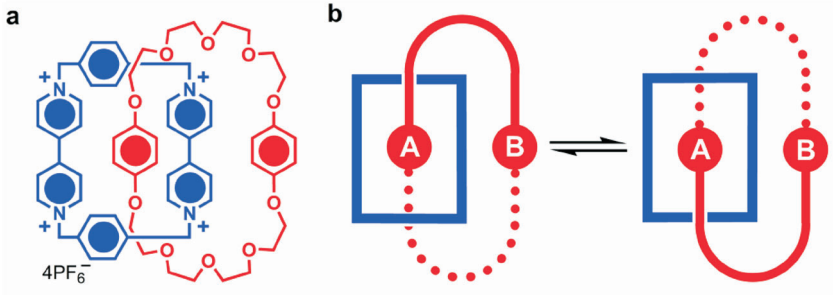

FIG. 4

a The structural formula of a donor–acceptor [2]catenane. **b** A schematic representation of rocking in a degenerate [2]catenane. If the angle between the planes of each ring is other than 90°, the rocking process interconverts between the two co-conformers shown

The previous three cases demonstrated examples of degenerate processes involving mechanical motion. Controlled mechanical motion as the result of an external stimulus, however, represents the true motivation for many of these studies. By designing catenanes and rotaxanes with nondegenerate co-conformers, where the energy levels can be shifted in some fashion by remote input, the dynamic processes involving mechanical motion can be controlled. Such control has been demonstrated using chemical[22], electrochemical[23], photochemical[24] and electromagnetic[25] inputs in a variety of bistable catenanes and rotaxanes. Here, a few examples of the different types of control processes and stimuli employed to switch states in these systems will be presented.

Controlled circumrotation in a [2]catenane can be achieved by creating two nondegenerate sites within one ring that will undergo some form of interaction with the other ring. Sauvage et al.[26] have demonstrated a controllable bistable [2]catenate[27] incorporating a copper ion that acts as a bridge between the two rings. In the Cu(I) form, a co-conformer is adopted that places two bidentate ligands in contact with the copper to give it the preferred tetrahedral coordination geometry. Upon chemical or electrochemical oxidation of the Cu(I) to Cu(II), the preferred coordination geometry changes to that of pentacoordinate, and so one of the rings undergoes

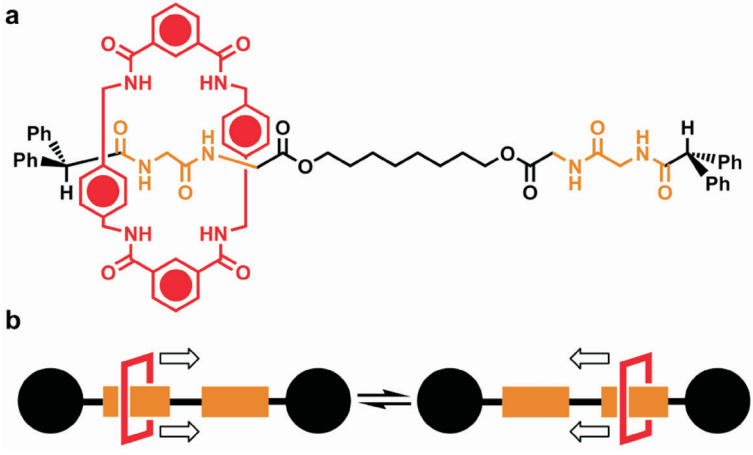

FIG. 5
a The structural formula of an amide-based [2]rotaxane. **b** A schematic representation of shuttling in a degenerate [2]rotaxane. The ring component undergoes translational motion along the dumbbell component, exchanging the two co-conformers

circumrotation to place the tridentate ligand in contact with the copper ion. This mechanical process can be reversed simply by reduction back to the Cu(I) species.

The shuttling process in [2]rotaxanes can also be harnessed by breaking the degeneracy of the recognition sites in the dumbbell component around which the ring resides. Leigh et al.[28] have incorporated two different hydrogen bonding sites, namely fumaramide and succinamide, into the dumbbell component to create a bistable [2]rotaxane. When the fumaramide unit is in its (*E*) configuration, the ring resides on that site because of the ability of the succinamide unit to form hydrogen bonds with itself, while the (*E*) isomer of fumaramide cannot. Upon irradiation with light at 254 nm, the fumaramide changes configuration to the (*Z*) form, which no longer allows for optimal hydrogen bonding with the ring component, and so the ring moves to the succinamide site. Heating the rotaxane results in reversal of the configuration change and the ring moves back to the fumaramide.

Many other methods of controlling shuttling in bistable rotaxanes have been explored. Another example involves the use of chemical control – namely pH. Two electron-deficient recognition sites for the electron-rich ring component, dibenzo[24]crown-8, were incorporated into a bistable [2]rotaxane by us[29]. One of these sites, a dialkylammonium one, can be deprotonated to "turn off" the hydrogen bonding interactions with the ring, leading to its shuttling to the other site, namely a bipyridinium unit, where favorable [π···π] stacking and [C–H···O] interactions can occur. Upon reprotonation of the amine, the ring component undergoes translational motion back to the more strongly favored dialkylammonium site.

Another controllable dynamic process in bistable [2]rotaxanes is pirouetting of the ring around the dumbbell component. Sauvage et al.[30] have demonstrated this motion in a rotaxane that can form a complex with Cu(I) or Cu(II). By analogy with the catenate (Fig. 6) described previously, electrons can be added or removed electrochemically or chemically to alter the oxidation state of the copper, and thereby change the preferred coordination number and co-conformation of the rotaxane (Figs 7, 8). By using variable scan rates in cyclic voltammetry experiments, they were able to show that pirouetting occurs (Fig. 9) with a time constant, τ, of ~200 ms after oxidation and <2 ms after reduction.

These selected examples are intended to demonstrate the variety and nature of the dynamic processes that occur in mechanically interlocked molecules as a direct result of the presence of a mechanical bond. More often than not when considering a bistable catenane or rotaxane, the characteristics of the dynamic processes which the molecules undergo are every

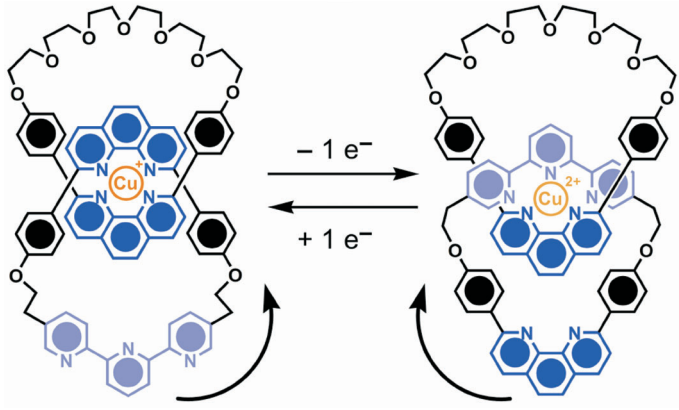

FIG. 6

A switchable bistable [2]catenate. Removal of an electron from Cu(I) results in circumrotation of one macrocycle to change the coordination from tetracoordinate to pentacoordinate. Adding an electron to Cu(II) in the wake of this process causes it to reverse

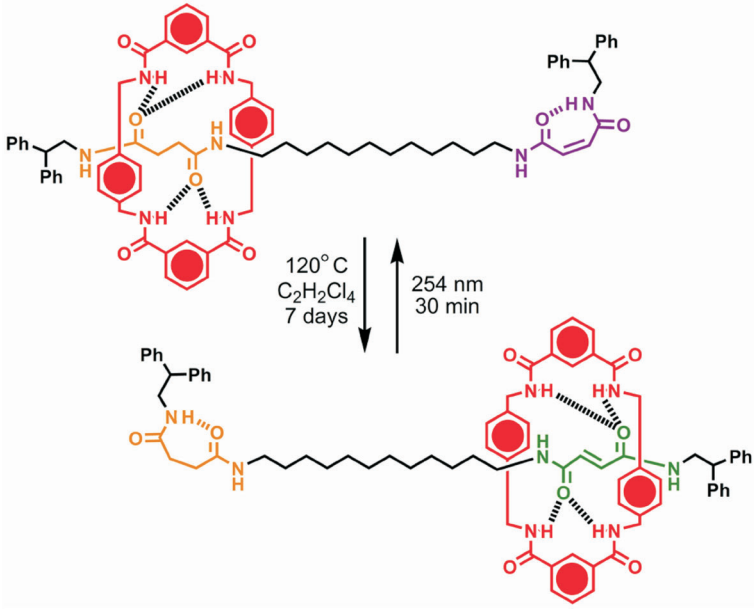

FIG. 7

A switchable bistable [2]rotaxane. Irradiation with light at 254 nm causes a configuration change of the fumaramide unit from *E* to *Z*, and translation of the ring component as a result of the disruption of the hydrogen bonding interactions. This process can be reversed by heating

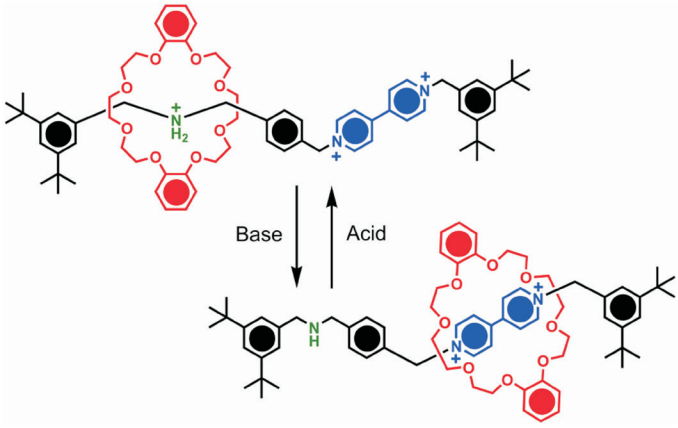

FIG. 8
A switchable bistable [2]rotaxane. Addition of base deprotonates the dialkyammonium center weakening the interactions with the ring component and causing shuttling of the ring to the bipyridinium site. Adding acid to protonate the amine reverses the process

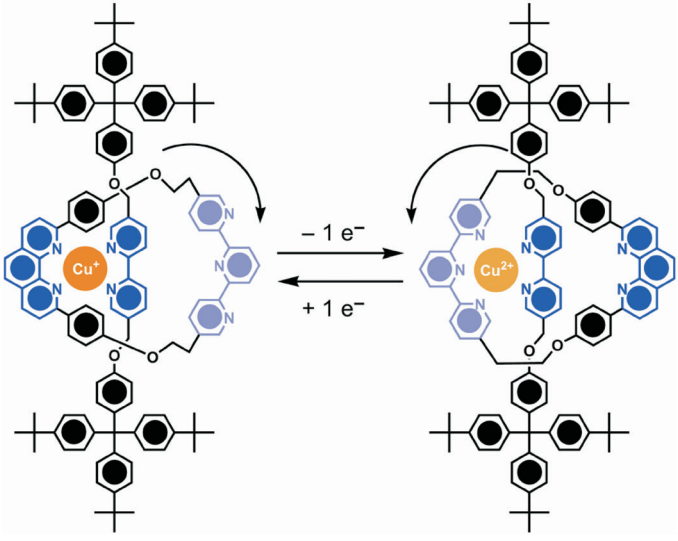

FIG. 9
A switchable bistable [2]rotaxane is shown. Removal of an electron from the Cu(I) results in pirouetting of the macrocycle around the dumbbell component to change the coordination from tetracoordinate to pentacoordinate. Adding an electron to the Cu(II) causes the process to be reversed

bit as important as their structural connectivities. Unique capabilities are created by incorporating mechanical bonds into molecules. Understanding the relative dynamics of the components is a prerequisite to taking advantage of these capabilities in potential applications.

1.3. Stereochemistry

Another aspect of growing importance in the area of mechanically-interlocked molecules is that of stereochemistry. Both Euclidian (classical) and topological chirality can be found in these molecules. While topological chirality is sometimes important in catenanes[31] and rotaxanes[32], for the purposes of this Review the discussion will be limited to the use and presence of classical chirality. In some cases, the chiral element is inserted as part of the covalently bonded components, while less frequently it can arise as a result of the orientation of the components around the mechanical bond.

One recent example where chiral elements were incorporated into the rings of a [2]catenate was reported by Sauvage et al.[33] An enantiomerically pure 1,1′-binaphthol was inserted into the glycol region of each macrocycle and the [2]catenate synthesized using metal templation. By performing circular dichroism (CD) spectroscopy on the metalated and demetalated catenate, the authors identified a chiral response from the absorption bands assigned to the 2,9-diphenyl-1,10-phenanthroline (dpp) units in the metalated catenate. This observation was attributed to chirality transfer from the binaphthol units to the metal complex, distorting as these units do, the coordination geometry into an asymmetric form.

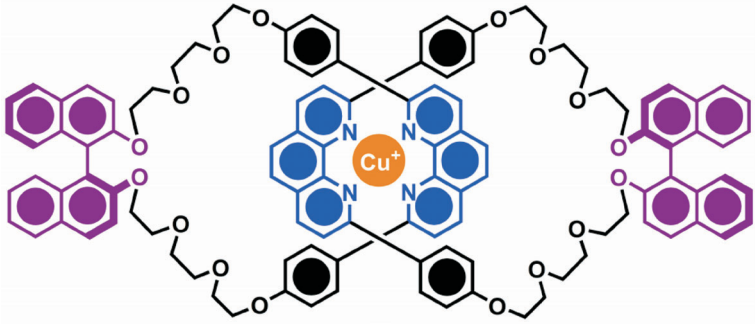

FIG. 10
The structural formula of a chiral [2]catenate. Transfer of chirality from the 1,1′-binaphthol units to the metal coordination site was observed by circular dichroism

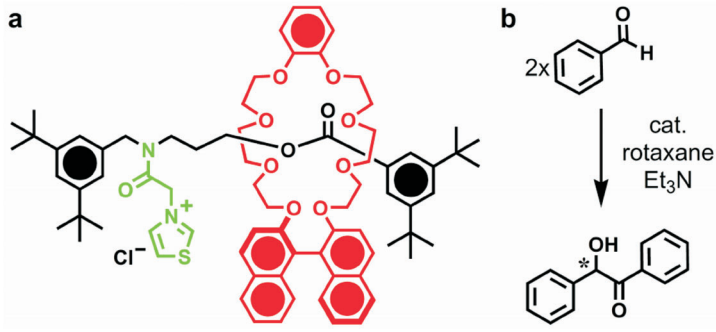

FIG. 11

a The structural formula of a chiral [2]rotaxane designed to act as a catalyst for the benzoin condensation is shown. **b** The benzoin condensation of benzaldehyde can be catalyzed using the chiral rotaxane to give an excess of one enantiomer. The chiral center is indicated with an asterisk (*)

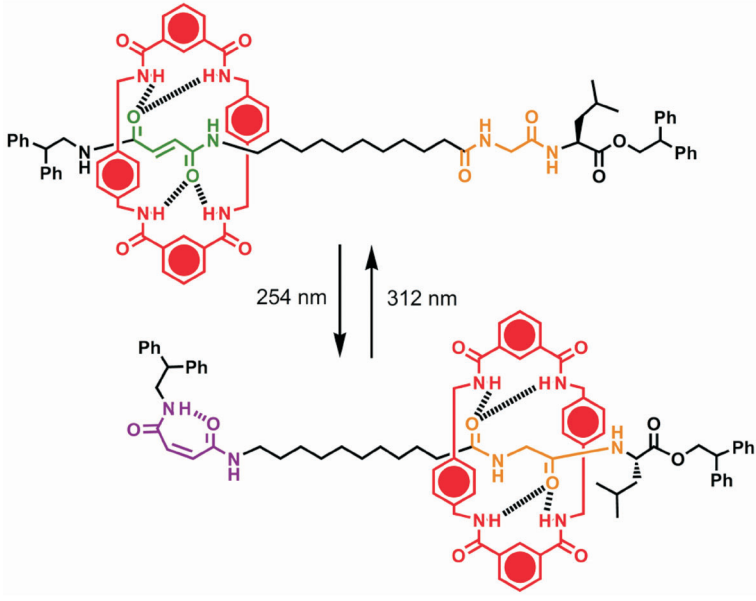

FIG. 12

The structural formula of a chiral bistable [2]rotaxane. Irradiation with light at 254 nm causes shuttling of the ring component to a site closer to the chiral center. Upon irradiation with 312 nm wavelength light, the ring moves back to the initial site

Once chirality has been incorporated into a mechanically interlocked system, it can be used for controlling the structure and dynamics or to perform a function, e.g., catalysis. For example, Takata et al.[34] have demonstrated the use of a chiral rotaxane as a catalyst for performing a benzoin condensation. A chiral crown ether was synthesized incorporating 1,1′-binaphthol and used as the ring component in a rotaxane (Fig. 11a) by threading it onto a dialkyammonium site, followed by stoppering. After formation of the rotaxane, the site was substituted with a thiazolium salt to act as the catalytic center. The authors were then able to perform the model reaction shown in Fig. 11b with 90% yield and 21% ee. Although significant improvement in selectivity is needed before this catalytic rotaxane may be useful, this result demonstrates a potential application of chiral mechanically interlocked molecules.

Incorporation of chiral centers into rotaxanes can also result in chirality transfer similar to the case of the catenate (Fig. 10) discussed previously. Leigh et al.[35] have reported a chiral switchable [2]rotaxane (Fig. 12) wherein induction of the chirality can be switched on and off. This no mean feat was accomplished by synthesizing a dumbbell component with a fumaramide and also a glycyl-L-leucine recognition site. Irradiation with light at 254 nm causes isomerization of the fumaramide from its (*E*) to its (*Z*) form, decreasing the interaction with the ring component and leading to its shuttling to the glycyl-L-leucine. When the ring resides near the chiral center of the L-leucine, a strong CD absorption band is observed at 246 nm. Irradiating at 312 nm reversed the isomerization, causing return of the ring to the fumaramide site and disappearance of the CD band.

As these examples demonstrate, stereochemistry provides an additional degree of complexity and control of the moving parts within mechanically interlocked molecules. The geometrical arrangement of the components in catenanes and rotaxanes can be influenced by chiral elements contained within any individual component. Alternatively, the geometrical arrangements of the components can give rise to chirality in the molecule. While the latter case is less common in terms of classical chirality, it can lead to a complex and interesting mix of dynamics and stereochemistry, as the research presented in this Review will demonstrate.

2. DYNAMICS AND STEREOCHEMISTRY OF DONOR–ACCEPTOR [2]CATENANES

2.1. Background

With the goal of producing a range of electrochemically controllable molecular switches in mind, a series of bistable [2]catenanes were synthesized[36]. Asymmetry was incorporated into the cyclobis(paraquat-*p*-phenylene) ($CBPQT^{4+}$) based cyclophane by replacing one of the bipyridinium units of the parent cyclophane with a bipicolinium unit. As a result, reduction of the bipyridinium unit, which is normally favored for encirclement by the crown ether component, should give rise to a circumrotation-based switching process (Fig. 13a) in which the bipicolinium unit becomes a more favorable site relative to the reduced bipyridinium unit. Three different bistable [2]catenanes, **1**–**3**·$4PF_6$, were synthesized incorporating different aromatic units in the crown ether component (Fig. 13b) in order to investigate the behaviors of these molecules.

X-ray crystal structures of all three bistable [2]catenanes were reported and show (Fig. 14) clear similarities in the conformations and co-conformations across the series. Three primary types of inter-ring interactions can be identified, namely [C–H···O], [C–H···π] and [π···π], which influence the preferred co-conformation. The [C–H···O] interactions occur between the alpha protons, H_α, of the bipyridinium unit and the central oxygen of each glycol chain in the crown ether component. The bipyridinium unit also

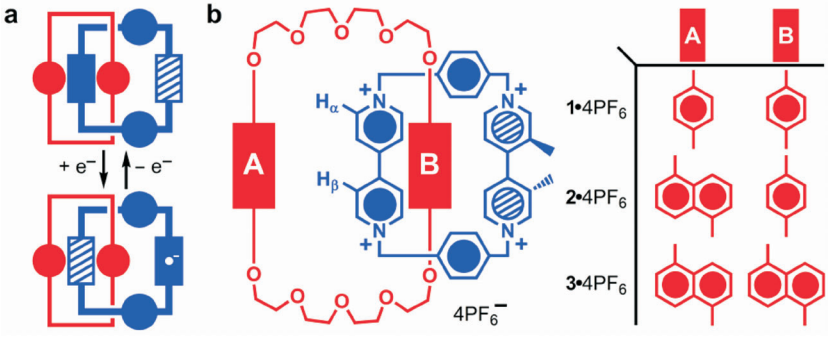

FIG. 13
a A schematic representation of a reduction-based electrochemical switching mechanism in a bistable [2]catenane. **b** The structures of three bistable [2]catenanes designed to undergo electrochemical switching are shown

participates in [π···π] interactions with the electron rich aromatic rings of the crown ether. Finally, the aromatic ring of the crown ether, which resides within the cavity of the tetracationic cyclophane, is involved in two [C–H···π] interactions with the *p*-phenylene units of the cyclophane. These interactions will be important in determining the types and rates of the various dynamic processes to be reported here for these bistable [2]catenanes.

2.2. Dynamics

A thorough spectroscopic investigation of the dynamic processes taking place in these bistable [2]catenanes was performed to obtain a better understanding prior to their evaluation as molecular switches. Variable-temperature (VT) ^{1}H NMR spectroscopy provided a means to probe the dynamics in solution and obtain kinetic and thermodynamic data. Two primary methods were used: (i) spin saturation transfer[37] (SST), where one of the two exchanging protons is saturated by a radio-frequency pulse and changes in the intensity and relaxation time for its exchange partner are observed, and (ii) partial line shape analysis[38] (PLSA), where calculated spectra are matched to experimental spectra using chemical shifts, line widths and exchange parameters as input.

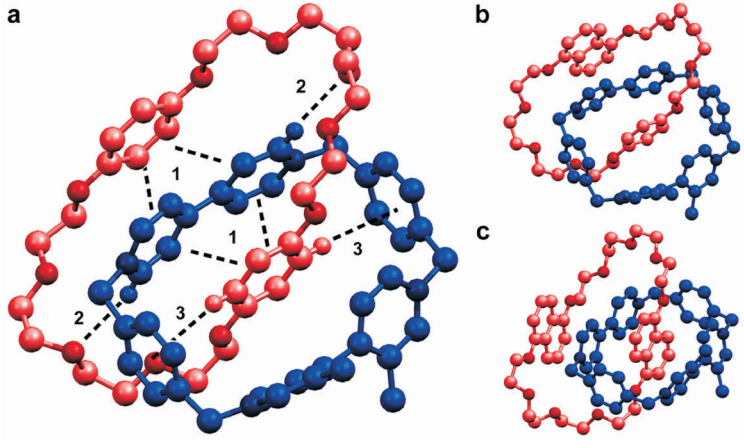

FIG. 14
a The X-ray crystal structure of $\mathbf{1}^{4+}$ is shown. Important inter-ring interactions are highlighted, namely (1) [π···π], (2) [C–H···O] and (3) [C–H···π]. The X-ray crystal structures of **b** $\mathbf{2}^{4+}$ and **c** $\mathbf{3}^{4+}$ are also shown

Qualitative examination of the ^{1}H NMR spectra of **1**–**3**·4PF$_6$ recorded in CD_3COCD_3 over a range of temperatures revealed four dynamic processes occurring in these catenanes. These processes are summarized in Fig. 15 – (1) phenylene rotation, (2) pyridinium rotation, (3) crown ether circumrotation and (4) ring rocking. The first two processes are degenerate ones in all three molecules. Circumrotation, however, is degenerate only in **1**·4PF$_6$ and **3**·4PF$_6$, while ring rocking is not degenerate in any of the three [2]catenanes. Another point of contrast is that the first two processes consist of simple covalent bond rotations, while the latter two processes involve mechanical motion. A more detailed analysis of each of these processes follows.

Under normal circumstances the aromatic ring rotations in the tetracationic cyclophane occur too rapidly to be observed by ^{1}H NMR spectroscopy. However, the unique environment presented by their incorporation into a [2]catenane slows down these rotational processes as a result of a combination of steric hindrance and intramolecular interactions. Thus, not only does probing these processes help to complete the overall dynamic picture of these molecules, but it also provides a means of studying the different structural properties across the series.

Phenylene rotation was investigated by observing the signals for the protons of the *p*-phenylene ring in the tetracationic cyclophane. On account of the methyl group present in the adjacent picolinium unit, the phenylene protons on one side of the plane containing the four nitrogen atoms of the

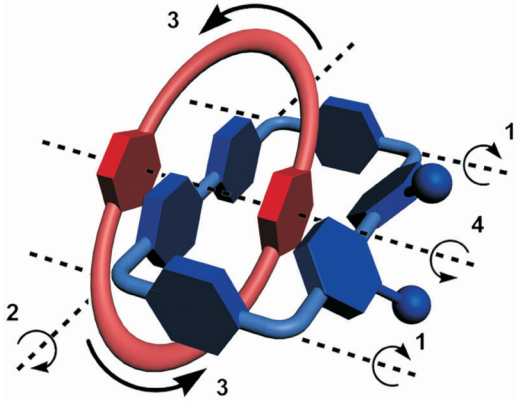

FIG. 15
A schematic representation of **1**·4PF$_6$ showing the four dynamic processes observed in this [2]catenane. These are (1) phenylene rotation, (2) pyridinium rotation, (3) crown ether circumrotation and (4) ring rocking

cyclophane are in a distinctly different chemical environment from those on the opposite side (Fig. 16a), giving rise to four signals in the ^{1}H NMR spectra (Fig. 16b–16d) for the four heterotopic protons. Rotation of the phenylene ring about its substitution axis exchanges the protons between these two environments. As the temperature is increased the rate becomes fast on the ^{1}H NMR timescale and only two average signals are observed, one for the pair of protons adjacent to the pyridinium ring and the other for those next to the picolinium ring.

Quantitative data for phenylene rotation was obtained (Table I) through SST experiments performed on the protons of the phenylene ring. Although the lack of data at a common temperature for the different

TABLE I
Phenylene rotation kinetic and thermodynamic data in CD_3COCD_3

	1·4PF$_6$ [a]			**2**·4PF$_6$ [b]					**3**·4PF$_6$ [c]		
T [d]	174	182	191	202	213	225	217	227	238	249	259
k_{ex} [c]	0.2	0.4	0.1	0.3	1.0	2.6	0.2	0.6	1.5	3.9	10.9
$\Delta G^{\ddagger}$ [f]	10.6	10.9	12.0	12.2	12.3	12.6	13.3	13.4	13.6	13.8	13.9

[a] Exchange observed between peaks corresponding to the protons on the phenylene ring of the tetracationic cyclophane at 8.45/7.92 and 8.25/7.68 ppm, [b] at 8.35/7.84 and 8.26/7.67 ppm, and [c] at 8.48/8.14 and 8.44/8.02 ppm; [d] K, calibrated using neat MeOH sample; [e] s^{-1}, measured using spin saturation transfer method (ref.[37]); [f] kcal mol^{-1}, ±0.1

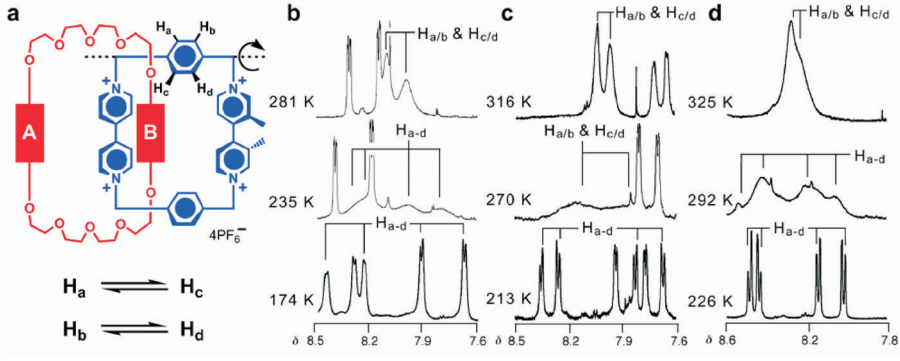

FIG. 16
a A schematic representation of phenylene rotation, where rotation about the substitution axis of the ring exchanges H_a with H_c and H_b with H_d. Also shown are partial 500 MHz ^{1}H NMR spectra recorded in CD_3COCD_3 of the signals for the phenylene ring protons in the tetracationic cyclophane for **b** **1**·4PF$_6$, **c** **2**·4PF$_6$ and **d** **3**·4PF$_6$ at varying temperatures

catenanes prohibits direct comparison of $\Delta G^{\ddagger}$ values, a qualitative trend of increasing barriers from **1**·4PF_6 to **2**·4PF_6 to **3**·4PF_6 can be identified, with a difference (increasing) of ~1 kcal mol^{-1} going from one catenane to the other. The increase in barrier height correlates with the number of 1,5-dioxynaphthalene (DNP) units present in the crown ether component of the [2]catenane, perhaps providing some clues to the mechanism. Increased steric hindrance arising from the larger DNP unit relative to the hydroquinone (HQ) unit within the cavity of the cyclophane is not likely to be the cause, as the first substitution from HQ to DNP occurs with the aromatic unit residing alongside the cyclophane. The X-ray crystal structures indicate that the contacts between the phenylene rings and glycol chains of the crown ether become shorter with increasing presence of DNP units, possibly causing hindrance to rotation of the phenylene ring. Further experiments are necessary to understand in detail the mechanism associated with this process.

The other set of aromatic ring rotations observed in these bistable [2]catenanes arises from the bipyridinium unit. Each pyridinium ring undergoes rotation about its substitution axis, exchanging (Fig. 17a) the corresponding protons between environments where they are either *syn* or *anti* with respect to the methyl group on the nearest picolinium unit in relation to the plane of the cyclophane containing its four nitrogens. As a result of this heterotopicity, the α- and β-pyridinium protons each appear as two sig-

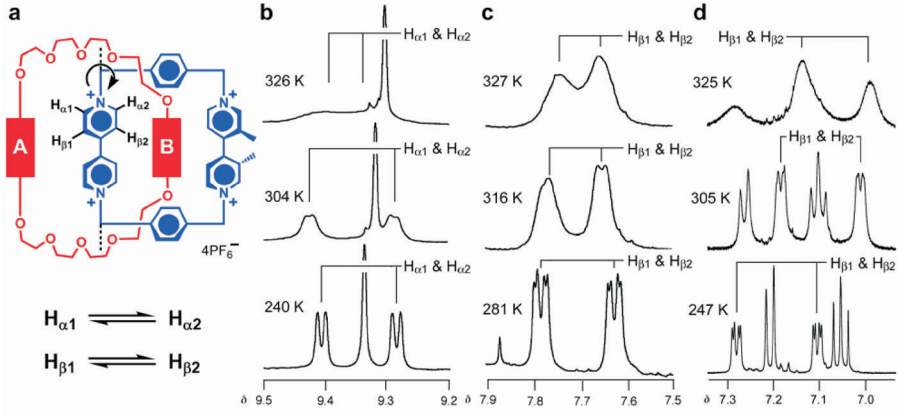

FIG. 17

a A schematic representation of pyridinium rotation, where rotation about the substitution axis of the ring exchanges $H_{\alpha1}$ with $H_{\alpha2}$ and $H_{\beta1}$ with $H_{\beta2}$. Also shown are partial 500 MHz ^1H NMR spectra recorded in CD_3COCD_3 of the signals for the pyridinium ring protons in the tetracationic cyclophane for **b** **1**·4PF_6, **c** **2**·4PF_6 and **d** **3**·4PF_6 at varying temperatures

nals – one pair for H_α and H_β *syn* to the methyl group, and another pair for the *anti* ones – in the ^{1}H NMR spectra (Fig. 17b–17d) at low temperatures. Upon increasing the temperature each pair of signals begins to coalesce into a single averaged signal because of the rapid interconversion relative to the ^{1}H NMR timescale of the proton chemical shift environments.

A combination of the SST and PLSA methods provided kinetic and thermodynamic data (Table II) for pyridinium rotation. At first glance, it is apparent that the barriers for this process are significantly higher – by ~3–4 kcal mol^{-1} – than those for phenylene rotation. Additionally, the availability of data at a common temperature, 293 K, for (nearly) all three [2]catenanes allows a comparison of $\Delta G^\ddagger$ values to be made across the series. Swapping the outside HQ ring for a DNP unit in going from **1**·4PF_6 to **2**·4PF_6 is observed to increase the barrier by 1.1 kcal mol^{-1}, while replacement of the inside HQ unit in **3**·4PF_6 appears to have little or no effect. As the pyridinium rings are involved in [π···π] interactions with the aromatic units of the crown ether, their effect on the barrier for rotation is not unexpected, but the lack of an effect by the inside aromatic unit is somewhat surprising.

A possible mechanism that explains these observations can be formulated. During rotation of the pyridinium ring the [π···π] interactions will be disrupted and the two electron-rich aromatic rings must dissociate and increase their distance from the pyridinium ring to provide space for the ring to rotate. As the inside aromatic unit has little room to move without leaving the cavity, which would lead to an even greater energetic penalty as a result of the loss of the remaining inter-ring interactions, the outside aromatic unit must make room by breaking contact with the side of the

TABLE II
Pyridinium rotation kinetic and thermodynamic data in CD_3COCD_3

	1·4PF_6 [a]								**2**·4PF_6 [b]			**3**·4PF_6 [c]	
T [d]	247	256	270	281	293	304	316	270	281	293	305	292	305
k_{ex} [e]	0.2 [f]	0.5 [f]	1.3 [f]	3.5 [f]	7.7 [g]	18 [g]	42 [g]	0.1 [f]	0.4 [f]	1.4 [f]	4.3 [f]	1.2 [f]	3.4 [f]
$\Delta G^\ddagger$ [h]	15.2	15.3	15.6	15.7	15.9	16.1	16.2	17.1	17.0	17.0	17.0	17.0	17.1

[a] Exchange observed between the $H_{\alpha1}$ and $H_{\alpha2}$ peaks of the pyridinium rings in the tetracationic cyclophane at 9.41 and 9.29 ppm, [b] the $H_{\beta1}$ and $H_{\beta2}$ peaks at 7.67 and 7.58 ppm, [c] the $H_{\beta1}$ and $H_{\beta2}$ peaks at 7.24 and 7.06 ppm; [d] K, calibrated using neat MeOH sample; [e] s^{-1}; [f] measured using spin saturation transfer method (ref.[37]); [g] measured using partial line shape analysis method; [h] kcal mol^{-1}, ±0.1

cyclophane. Thus, any remaining interactions with the other pyridinium ring are lost, explaining why the more strongly bound DNP unit leads to a greater energetic penalty. The inside aromatic unit has little or no effect because it is essentially remaining in place during the whole process. Computational studies are necessary to explore the mechanism of this process further.

The remaining aromatic ring rotation in the tetracationic cyclophane that could occur, picolinium rotation, was not observed at the temperatures studied in these ^{1}H NMR experiments. The barrier for such a process is expected to be relatively large as a result of the bulky methyl groups that would have to pass by one another or through the cavity of the cyclophane. Similarly substituted biphenyls are reported[39] to have large barriers for rotation. If this process is occurring at the temperatures accessed in this investigation, the rate is expected to be low enough as to not affect the other processes studied.

Beyond the covalent bond rotations in these catenanes, there is also motion between the two mechanically-interlocked components. One such process that was observed is circumrotation (Fig. 18) of the crown ether component through the cavity of the tetracationic cyclophane. The result is to exchange the inside and outside aromatic units. For **1**·4PF$_6$ and **3**·4PF$_6$ this process is degenerate because the two aromatic units are identical. In the case of **2**·4PF$_6$, however, the two units are different – namely HQ and DNP – leading to a nondegenerate exchange. As none of the minor isomer where

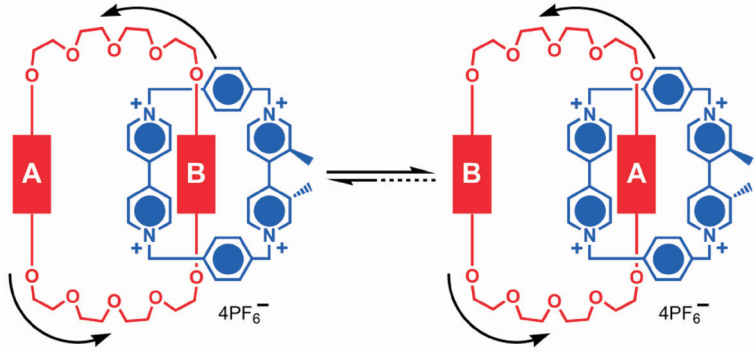

FIG. 18
A schematic representation of the circumrotation process is shown. The "inside" and "outside" aromatic units of the crown ether are exchanged by circumrotation through the cavity of the tetracationic cyclophane. Rotation of the ring is equally likely in either direction, i.e., clockwise or counter-clockwise

the DNP unit resides within the cavity of the cyclophane could be observed by ^{1}H NMR spectroscopy, investigation of circumrotation in **2**·4PF$_6$ was simply not possible. However, data for the two degenerate catenanes was obtained by PLSA of spectra acquired over a range of temperatures.

At 293 K, the barrier for circumrotation, $\Delta G^{\ddagger}$, was determined to be 15.4 and 16.6 kcal mol^{-1} for **1**·4PF$_6$ and **3**·4PF$_6$, respectively (Table III). During the circumrotation process all three sets of interactions – [C–H···O], [C–H···π] and [π···π] – are broken between the two rings, and so the catenane incorporating DNP units pays a greater price for circumrotation because of its stronger interactions with the cyclophane, relative to HQ. The larger π-surface and greater electron donating strength of DNP provide a stronger [π···π] interaction, while the size and geometry provide shorter and stronger [C–H···π] contacts. It is also interesting to note that, in contrast to the aromatic ring rotations, the magnitude of the barrier for circumrotation decreases with increasing temperature. This observation is indicative of a positive $\Delta S^{\ddagger}$ – i.e., an increase in entropy in the transition state – and can be explained by a combination of two factors. The loss of all interactions between the two rings presumably leads to a more flat potential energy surface near the transition state, allowing more conformations to be easily explored, and increased entropy from the release of solvent molecules previously organized around the glycol chains as they pass through the cavity of the cyclophane.

A quantitative comparison of the different contributions to the barriers for pyridinium rotation and circumrotation can be made for **1**·4PF$_6$, where data are available over a large temperature range (~70 degrees in both

TABLE III
Crown ether circumrotation kinetic and thermodynamic data in CD_3COCD_3

	1·4PF$_6$ [a]							**2**·4PF$_6$		**3**·4PF$_6$ [b]	
T [c]	256	270	281	293	304	316	326	N/A	271	282	293
k_{ex} [d]	0.2 [e]	1.2 [e]	5.6 [e]	21 [e]	60 [e]	180 [e]	450 [e]	N/A	0.13 [f]	0.57 [f]	2.6 [f]
$\Delta G^{\ddagger}$ [g]	15.7	15.6	15.5	15.4	15.4	15.3	15.2	N/A	16.9	16.8	16.6

[a] Exchange observed between the peaks corresponding to the outside (6.27 ppm) and inside (3.84 ppm) hydroquinone rings of the crown ether components, [b] exchange observed between peaks corresponding to the outside (7.28 ppm) and inside (2.70 ppm) 1,5-dioxynaphthalene rings of the crown ether component; [c] K, calibrated using neat MeOH sample; [d] s^{-1}; [e] measured using line shape analysis method; [f] measured using spin saturation transfer method (ref.[37]); [g] kcal mol^{-1}, ±0.1

cases). The $\Delta G^{\ddagger}$ values for these two processes at 270 K are the same, namely 15.6 kcal mol^{-1}. However, upon examination of the enthalpic, $\Delta H^{\ddagger}$, and entropic, $\Delta S^{\ddagger}$, contributions (Table IV), obtained from the corresponding Eyring plots, it is apparent that very different factors are contributing to these barriers. Circumrotation suffers from a large enthalpic penalty, most likely because of the large degree of disruption to the intramolecular interactions. Pyridinium rotation, on the other hand, causes only a small disruption in the [π···π] interactions and has a much smaller enthalpic contribution to the overall barrier. The entropic parameters tell a much different story. As mentioned before, circumrotation benefits from an entropy increase in the transition state, reflected by the positive $\Delta S^{\ddagger}$ value. The negative $\Delta S^{\ddagger}$ value for pyridinium rotation corresponds well with what appears to be a very sterically congested transition state. So although at first glance the barriers for these processes appear similar in magnitude, the components from which they are constructed provide insight into the very different nature of the two processes in a mechanistic sense.

TABLE IV
Activation parameters for select processes in **1**·4PF_6

Process	$\Delta G^{\ddagger}$ [a]	$\Delta H^{\ddagger}$ [b]	$\Delta S^{\ddagger}$ [c]
Pyridinium rotation	15.6	11.3	–15.5
Crown ether circumrotation	15.6	17.6	7.4

[a] 270 K, kcal mol^{-1}, ±0.1; [b] kcal mol^{-1}; [c] cal mol^{-1} K^{-1}.

2.3. Stereochemistry

A final dynamic process involving mechanical motion was observed in some of the bistable [2]catenanes studied, but probing this process requires an understanding of its stereochemistry first of all. Up to three different chiral elements are present in each catenane as shown in Fig. 19. The first only applies to those catenanes possessing DNP units, namely **2**·4PF_6 and **3**·4PF_6, and is a form of planar chirality[40] arising (Fig. 19a) from incorporation of a DNP unit into a macrocycle. The second chiral element, present in all three catenanes, is the bipicolinium unit, which exhibits (Fig. 19b) axial chirality[5]. Finally, the fundamental geometry of these donor–acceptor [2]catenanes, namely the ~45° angle[41] between them, gives rise (Fig. 19c) to a form of helical chirality.

Although the first two chiral elements have standard descriptors and appear in simple covalently bonded molecules, this form of helical chirality is unique to the presence of a mechanical bond and no standard rules for defining this chirality existed. As a result, a few simple rules for determining the chiral descriptors will be presented here. First, the molecule should be oriented as shown in Fig. 19c with the higher priority ring in front, where the priority is determined using standard atom priority rules. Here, the crown ether ring is determined to be higher priority as it contains oxygen atoms, whereas the tetracationic cyclophane's highest priority atom is nitrogen. Once properly oriented, an arrow drawn from the higher priority ring to the lower priority ring, following the shorter of the two possible pathways, determines the chirality. A clockwise arrow is given the descriptor (*P*) and a counter-clockwise arrow is described as (*M*).

As a result of the combination of these chiral elements present in the [2]catenanes, a number of different stereoisomers are possible. For **1**·4PF$_6$ there are four possible stereoisomers (Fig. 20), or two enantiomeric pairs of diastereoisomers, of which only one enantiomeric pair was observed in the X-ray crystal structure (Fig. 14a), namely the (*aR*)-(*P*)/(*aS*)-(*M*) one. The addition of another chiral element (DNP) in **2**·4PF$_6$ increases the number of possible stereoisomers by two-fold for a total of eight. Again, however, only one enantiomeric pair of diastereoisomers was observed (Fig. 14b) in the solid-state and corresponds to the (*aR*)-(*P*)-(*pS*)/(*aS*)-(*M*)-(*pR*) configuration. The final case, **3**·4PF$_6$, has the greatest complexity with 16 possible stereoisomers (Fig. 21), but once again there was only one observed form in the crystal, (*aR*)-(*P*)-(*pS*)-(*pS*)/(*aS*)-(*M*)-(*pR*)-(*pR*).

Although the X-ray crystal structures provide a static picture of presumably the most stable of these diastereoisomers, in solution the situation is much more dynamic. All of the chiral elements are capable of undergoing

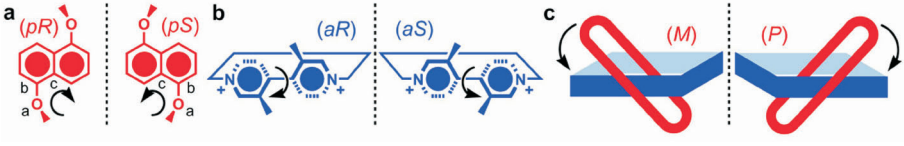

FIG. 19

The three different chiral elements present in **1**·4PF$_6$–**3**·4PF$_6$ are shown. **a** Planar chirality, denoted as (*pR*) or (*pS*), arises from the incorporation of a 1,5-dioxynaphthalene unit into a macrocycle. **b** Atropisomerism of the bipicolinium combined with the asymmetry induced by cyclophane formation creates an axially chiral center described as (*aR*) or (*aS*). c The tilted geometry of the rings in a [2]catenane creates the possibility for two helical enantiomers with either a clockwise (*P*) or counter-clockwise (*M*) twist

inversion via an appropriate dynamic process. For example, the axial chirality can be inverted through picolinium rotation, which although it was not observed to occur on the ^{1}H NMR timescale presumably occurs rapidly on the laboratory timescale, precluding any attempts to isolate the different enantiomers. Likewise, inversion of the planar chirality can occur by flipping of the DNP ring about the axis passing through the 1,5-substitution sites. Finally, a process dubbed ring rocking, to be discussed in more

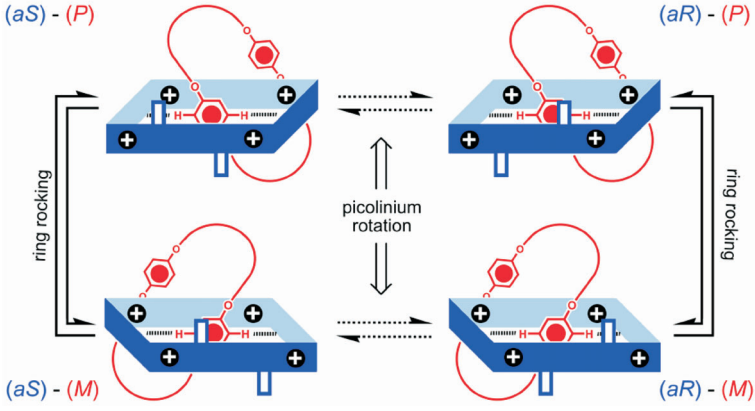

FIG. 20
The [2]catenane **1**·4PF$_6$ can exist as four different stereoisomers. The stereochemical descriptors are defined in Fig. 19. Two dynamic processes – picolinium rotation and ring rocking – allow interconversion between the stereoisomers

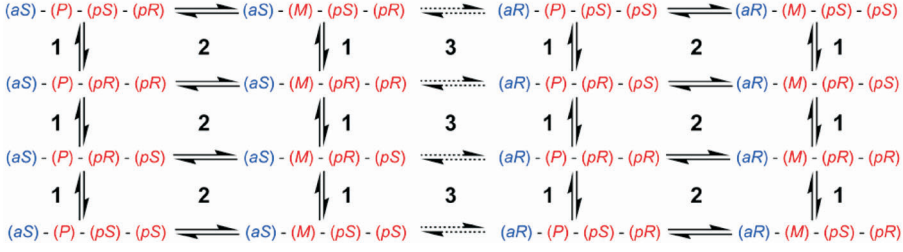

FIG. 21
The [2]catenane **3**·4PF$_6$ can exist as 16 different stereoisomers, i.e., eight diastereoisomers each with their enantiomeric pairs. The stereochemical descriptors are defined in Fig. 19. Three dynamic processes – (1) 1,5-dioxynaphthalene flipping, (2) ring rocking and (3) picolinium rotation – allow interconversion between the stereoisomers. Only some of the possible exchange pathways are shown

detail below, interconverts helical stereoisomers. The result of the combination of a large number of possible diastereoisomers and dynamic processes connecting them to one another is something akin to a dynamic combinatorial library, where the lowest energy enantiomeric pair of a mixture of rapidly equilibrating diastereoisomers dominates.

In the case of **1**·4PF_6 it was possible to identify a second diastereosiomer in solution in addition to the major one. This minor isomer appears as a second set of peaks (Fig. 22a) in the ^{1}H NMR spectrum at low temperature (182 K) with an integrated intensity corresponding to ~5% of that for the major set of signals. The major species present is presumably the same as that observed in the X-ray crystal structure, namely the (*aR*)-(*P*)/(*aS*)-(*M*) racemic modification, meaning that the minor species corresponds to the other enantiomeric pair (*aS*)-(*P*)/(*aR*)-(*M*) of diastereoisomers. This supposition was supported by molecular modeling of the two forms. The calculated[42] energy difference, ΔE, for the two diastereoisomers was 1.6 kcal mol^{-1}, which is in good agreement with the experimentally measured energy difference of ΔG = 1.1 kcal mol^{-1}, as calculated from the relative integrations for H_a at 182 K in the ^{1}H NMR spectrum.

Careful SST experiments also revealed that these two diastereoisomers are exchanging rapidly via a ring rocking process. The large difference in chemical shift between protons H_a and H_b (Fig. 22), which is caused by the shielding effect (Fig. 22b) of the aromatic rings of the tetracationic cyclophane, is what made observation of this rapid dynamic process possible[43] at accessible temperatures. Ring rocking consists of a mechanical motion between the two components of the catenane, more specifically a rotation

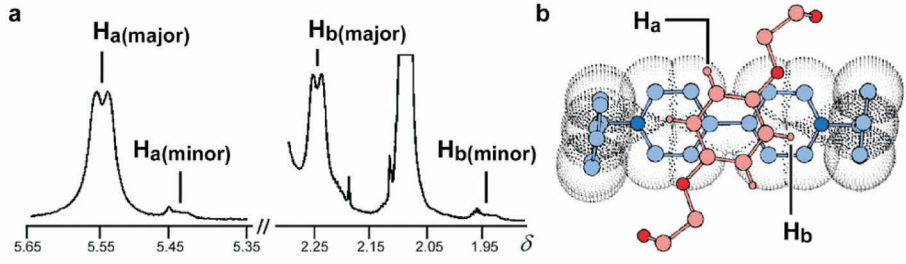

FIG. 22

a Partial 500 MHz ^{1}H NMR spectrum recorded in CD_3COCD_3 at 182 K of **1**·4PF_6 showing the proton signals for the inside hydroquinone unit. Major and minor indicate the presence of two different diastereoisomers. **b** A cut-away diagram showing the shielding effect of the tetracationic cyclophane on H_b that causes the large upfield shift observed for this proton

about the axis that passes through the centroids of the two aromatic units in the crown ether component. As a result, H_a and H_b are exchanged, and the helical chirality is also inverted.

Irradiation of either one of the H_a or H_b signals for the minor isomer caused a decrease in intensity of the signal corresponding to the other proton of the major isomer, i.e., if $H_{a(minor)}$ is irradiated then $H_{b(major)}$ decreases in intensity, and vice versa. Thus, the rate of interconversion between the two sets of diastereoisomers as a result of ring rocking could be measured (Table V) using SST. From these experiments the barrier to ring rocking, $\Delta G^{\ddagger}$, was determined to be 9.9 kcal mol^{-1} at 174 K upon going from the minor to major diastereoisomer of **1**·4PF$_6$. Similar experiments were carried out on **2**·4PF$_6$ and a barrier of 13.3 kcal mol^{-1} at 234 K was measured. The larger value in the latter case is presumably because of the need for inversion of the planar chirality associated with the outside DNP unit in addition to ring rocking. For **3**·4PF$_6$, only one diastereoisomer was observed, and so it was not possible to study ring rocking in this compound. The presence of DNP units in the catenanes seems to increase the selectivity for one of the two possible helical enantiomers, most likely as a result of their asymmetric geometry relative to the HQ rings. Thus, the different chiral elements do not act independently, but there is communication between them that allows the configuration of one element to influence the others.

This ring rocking process is not unique to these bipicolinium-containing catenanes and has been reported[44] previously in other donor–acceptor [2]catenanes. In order to determine if the helical chirality associated with this ring rocking process could be observed in the absence of other chiral elements present in the catenane, one of simplest donor–acceptor [2]catenanes[45] (Fig. 22a) was chosen to study. For **4**·4PF$_6$ the only chirality

TABLE V
Ring rocking kinetic and thermodynamic data in CD_3COCD_3

	1·4PF$_6$[a]		**2**·4PF$_6$[b]	**3**·4PF$_6$
T[c]	174	182	234	N/A
k_{ex}[d]	1.2	2.5	1.8	N/A
$\Delta G^{\ddagger}$[e]	9.9	10.2	13.3	N/A

[a] Exchange observed between the peaks corresponding to the protons of the inside hydroquinone ring of the crown ether component at 5.43 and 2.25 ppm, [b] at 5.26 and 2.18 ppm; [c] K, calibrated using neat MeOH sample; [d] s^{-1}, measured using spin saturation transfer method (ref.[37]); [e] kcal mol^{-1}, ±0.1

arises from the tilted geometry of the two rings (Fig. 23), and the ring rocking process interconverts (Fig. 22b) the two enantiomeric forms. By exposing this catenane to a chiral environment, such as a chiral shift reagent (CSR), it should be possible to observe the two enantiomers by ^{1}H NMR spectroscopy.

A chiral naphthalene derivative, (*S*)-**5**, was chosen (Fig. 24a) such that it would interact with the electron-deficient bipyridinium units of the cyclophane and influence the helical chirality of **4**·4PF$_6$. At low temperatures the exchange between helical enantiomers is slow on the ^{1}H NMR timescale (Fig. 24b), as can be deduced from the presence of two distinct peaks (Fig. 24c) for the protons on the inside HQ ring. Upon addition of 1.2

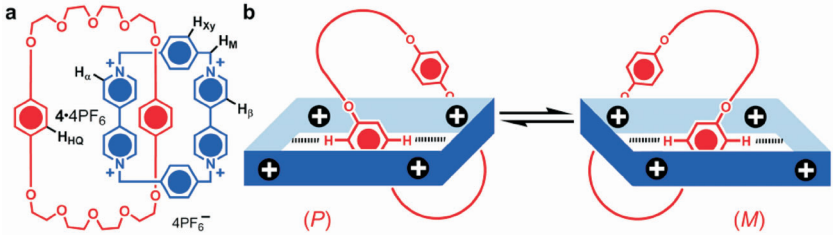

FIG. 23

a Structural formula for the donor–acceptor [2]catenane **4**·4PF$_6$. **b** The two helical enantiomers can be interconverted by ring rocking. The stereochemical descriptors are as described in Fig. 19

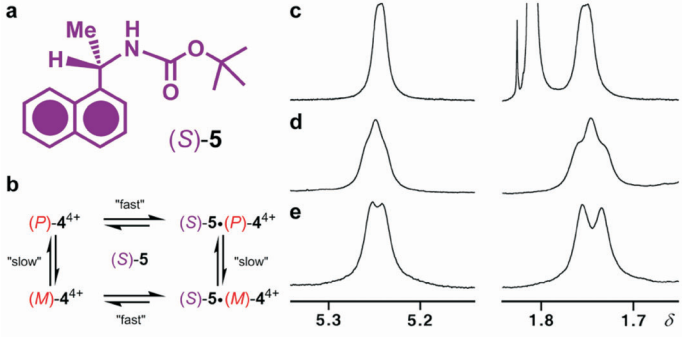

FIG. 24

a Structural formula for the chiral shift reagent (*S*)-**5**. **b** Exchange diagram showing the interconversion between helical enantiomers by ring rocking, which is slow on the ^{1}H NMR timescale at 197 K, and binding of (*S*)-**5**, which is fast on the ^{1}H NMR timescale at the same temperature. Partial 500 MHz ^{1}H NMR spectra recorded in CD_3COCD_3 at 197 K **c** of **4**·4PF$_6$, **d** of **4**·4PF$_6$ plus 1.2 equivalents of (*S*)-**5** and **e** the same solution as **d**, but with ^{1}H decoupling

equivalents of the CSR, the morphology of the signals changes and they now appear (Fig. 24d) as two overlapping doublets of nearly equivalent intensity. ^{1}H decoupling experiments were performed to confirm the presence of two distinct signals, which appear (Fig. 24e) as broad singlets upon decoupling. These two sets of signals correspond to the two diastereoisomeric complexes formed between the catenane and the CSR.

For the CSR (*S*)-**5**, no selectivity was shown for one helical enantiomer over the other, i.e., the diastereoisomeric complexes were present at equilibrium in a 1:1 ratio. This lack of selectivity could be a result of weak binding between the CSR and the catenane, or a relatively minor influence of the chiral group on the co-conformation. In order to attempt to remedy this situation and create some significant selectivity for one enantiomer, a CSR was identified that should interact more strongly with the catenane. The chiral anion (*S*)-**6**$^-$ (Fig. 25a) was selected in the hopes that it could replace (Fig. 25b) the PF_6^- counterions of the catenane and surround it with a chiral environment.

A solution of **4**·4PF_6 was prepared in CD_3COCD_3 and four equivalents of (*S*)-**6**·NH_2Me_2 were added. Attempts to isolate the ion-exchanged catenane were unsuccessful, so ^{1}H NMR experiments were performed on the solution immediately after addition of the CSR. At low temperature (197 K) the

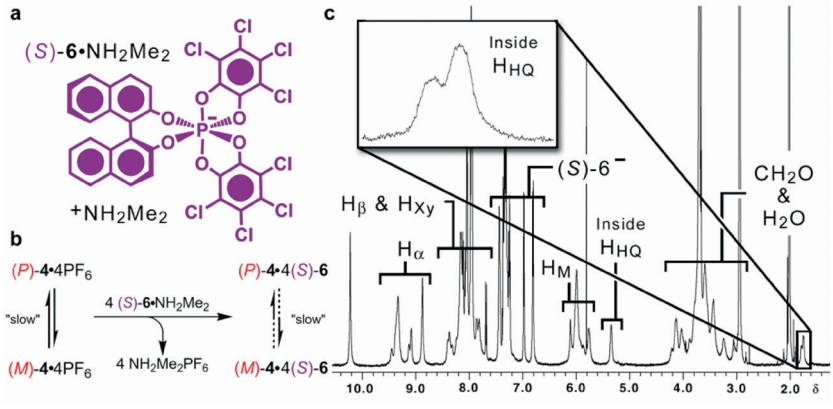

FIG. 25

a Structural formula for the chiral anion (*S*)-**6**·NH_2Me_2. **b** Exchange diagram showing exchange of the PF_6^- counterions for (*S*)-**6**$^-$. The equilibrium between helical enantiomers in the presence of the chiral anion is biased towards one of the two possible diastereoisomeric salts. **c** A 600 MHz ^{1}H NMR spectrum recorded in CD_3COCD_3 at 197 K of a solution containing **4**·PF_6 and four equivalents of **6**·NH_2Me_2. The inset shows an expanded view of the signals corresponding to the inside HQ protons that result from formation of diastereoisomeric salts

600 MHz ^{1}H NMR spectrum revealed the presence of two broad signals at 1.76 ppm, corresponding to the formation of two diastereoisomeric salts, (*P*)-(*S*) or (*M*)-(*S*). Unlike the previous CSR, the relative ratios in the presence of the chiral anion are now approximately 2:1, indicating a preference for one of the two possible helical enantiomers. It was not possible to determine which enantiomer was the preferred one.

2.4. Conclusions

A thorough investigation into the dynamic processes occurring within a series of donor–acceptor bistable [2]catenanes has been presented. The aromatic ring rotations and mechanical motions observed provide insight on the nature of the interactions present in these catenanes. Exploring these processes over a large range of temperatures in some cases also allowed the different enthalpic and entropic contributions to be determined, providing information about the mechanistic details. Such an understanding is important when the ultimate goal is to construct operating molecular switches and machines, and provides the knowledge necessary to tune these interactions for providing the properties desired in a particular device setting.

It was also shown that some of the dynamic processes occurring within these bistable catenanes have stereochemical implications. The presence of multiple chiral elements – planar, axial and helical – led to the possibility for a library of diastereoisomers that are interconverted dynamically as a result of these processes. The ability of the system to select the most stable of these forms, and the influence of each of the chiral elements on the others, bodes well for the use of chirality in controlling co-conformations in molecular machines. Isolation of the helical chirality in a catenane with no other chiral elements was also demonstrated with the possibility for external control over the preferred stereoisomer. The delicate intertwining of dynamics and stereochemistry in these bistable catenanes demonstrates remarkable possibilities for designing complex mechanically interlocked systems with a high degree of self-organization and controllability.

3. DYNAMICS AND SWITCHING OF TETRATHIAFULVALENE-CONTAINING CATENANES AND ROTAXANES

3.1. Background

One of the most prominent potential applications of mechanically-interlocked molecules is in the area of molecular electronics[46]. Bistable catenanes and rotaxanes have been incorporated[47] as the active components in molecular switch tunnel junctions (MSTJs), where they are sandwiched between a carbon or silicon bottom electrode and a titanium/aluminum top electrode. Application of sufficient bias (ca. ±2 V) across the MSTJ causes the device to switch from a low conductivity (high resistance) to a higher conductivity (lower resistance) state. This change can be reversed thermally over time (minutes to hours) or immediately by application of an opposite bias. Control experiments – i.e., degenerate mechanically interlocked molecules do not switch – and temperature studies – i.e., no switching occurs at low temperatures (e.g., 220 K) – provide evidence that the observed effect is a result of a molecular mechanism that is believed to be mechanical in nature.

The proposed mechanism of operation for tetrathiafulvane (TTF)/1,5-dioxynaphthalene (DNP)-containing bistable [2]catenanes or [2]rotaxanes (Fig. 26) is shown in Fig. 27. In its non-perturbed form, the catenane or rotaxane exists in equilibrium between two co-conformers[48], namely the "stable state" and "metastable state", which are interconverted by circumrotation or shuttling. This equilibrium is heavily biased towards the "stable state", until an electron is removed from the molecule. The now oxidized species also equilibrates between two co-conformers – the "oxidized state" and the "switched state" – where the "switched state" is greatly favored. Reinstating an electron into this isomer converts it into the "metastable state", leading to inversion of the equilibrium population rela-

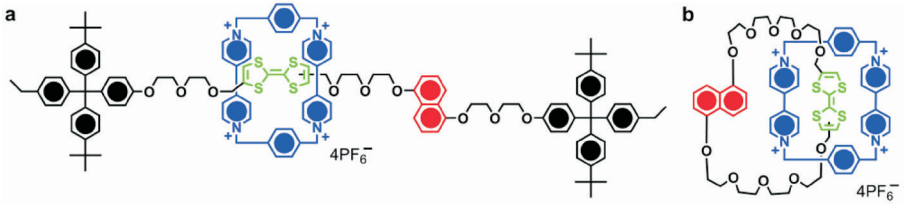

FIG. 26
Structural formulas that show examples of a TTF/DNP-containing bistable **a** [2]rotaxane and **b** [2]catenane

tive to the non-perturbed system. The inverted population has a certain lifetime[49] on account of the barrier for circumrotation/shuttling, which is dependent on the environment of the molecule and its constituent components (Fig. 28).

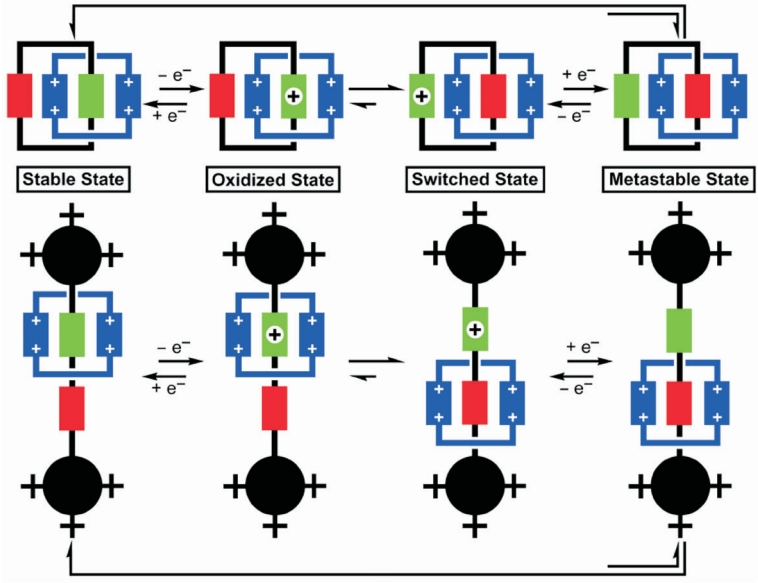

FIG. 27
Schematic diagram showing the switching cycle for TTF/DNP-containing bistable catenanes and rotaxanes

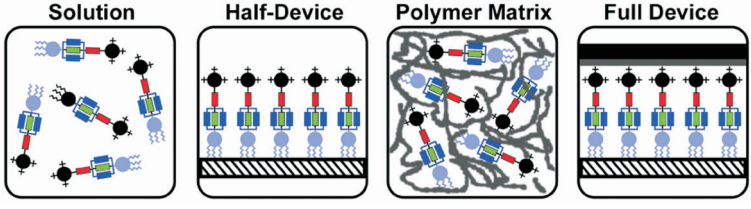

FIG. 28
Schematic representation of four different environments where the mechanism described in Fig. 27 has been demonstrated to operate. The barrier for circumrotation/shuttling increases on going from left to right as a result of the increasingly constricted nature of the environment

This mechanism has been observed[50] in solution for many bistable catenanes and rotaxanes by both UV/VIS spectroscopy and electrochemistry. Although the specific kinetic and thermodynamic parameters differ between the solution phase and device setting, the general mechanism is consistent and remains constant. As a result, characterization of these parameters for molecules in solution should allow a prediction of their device performance. By making modifications to the structure of the molecular switches, the kinetic and thermodynamic parameters of the switching mechanism can be tuned. More specifically, changing the recognition sites or altering the components linking them together allows manipulation of the equilibrium ratios and barriers for interconversion. The general relationship of these parameters to molecular structure across a range of environments – namely, solution phase, half-device, polymer matrix and full device – has been established[51] in numerous recent publications.

Thus, in order to provide improved molecular switches for the construction of future MSTJs and other devices, it could be helpful to obtain a complete understanding of their behavior in solution. Towards this end, an investigation of some solution phase dynamic processes related to relaxation of the "metastable state" to the "stable state" will be presented here. In addition, characterization of the "switched state" and the reversibility of the switching process in solution will be described for some bistable catenanes and rotaxanes, as well as for a few model compounds.

3.2. Dynamics

In solution, the kinetics of "metastable state" relaxation in bistable catenanes and rotaxanes are too rapid to be determined by ^{1}H NMR spectroscopy. Investigating circumrotation or shuttling in the non-perturbed "stable states" of the bistable compounds is also not possible as a result of the inability to detect the small amounts of the minor co-conformers where the CBPQT^{4+} rings encircle the DNP units. An alternate strategy for determining the energy barriers and the effects of structural changes upon these dynamic processes in bistable systems is to use structurally-related degenerate model compounds, where both recognition sites are identical such that exchange occurs between two isoenergetic co-conformers. Thus, a series of degenerate [2]rotaxanes (Fig. 29) containing three different spacer units – namely, a glycol chain (Fig. 29a), a terphenyl unit (Fig. 29b) and a diphenylether (Fig. 29c) – between two identical recognition sites, either DNP or TTF ones, were investigated[52].

The ring component of these [2]rotaxanes must pass over the spacer unit in order to move from one TTF or DNP unit to the other, suggesting that structural changes in the spacer should impact the rate of shuttling. To determine if this supposition is indeed the case, the interconversion between these two isoenergetic co-conformers was observed using variable-temperature (VT) ^{1}H NMR spectroscopy. In the absence of the ring, the dumbbell components of these rotaxanes possess an axis of symmetry normal to their long axis that bisects them affording two equivalent[53] halves. Localization of the CBPQT^{4+} ring on one of the two possible recognition sites breaks this symmetry, resulting in two non-equivalent halves. If the ring shuttles (Fig. 30) between the two sites rapidly on the timescale of observation (in this case, the ^{1}H NMR timescale), then it will appear as though the axial symmetry has been restored.

The first rotaxanes studied were the DNP-containing ones – **7**·4PF$_6$, **9**·4PF$_6$ and **11**·4PF$_6$. As a result of their symmetry properties, at low temperatures (226–236 K), where shuttling is slow on the ^{1}H NMR timescale, the protons on the two stoppers of the degenerate [2]rotaxanes give rise to two

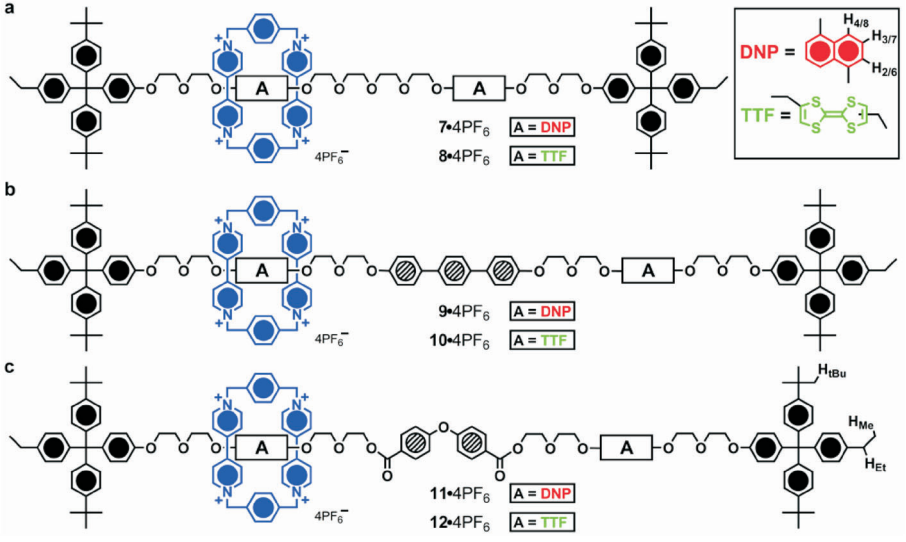

FIG. 29

Structural formulas for a series of degenerate [2]rotaxanes with **a** a glycol chain spacer and either two DNP, **7**·4PF$_6$, or two TTF, **8**·4PF$_6$, units and **b** a terphenyl spacer and either two DNP, **9**·4PF$_6$, or two TTF, **10**·4PF$_6$, units and **c** a diphenyl ether spacer and either two DNP, **11**·4PF$_6$, or two TTF, **12**·4PF$_6$ units

sets of equal intensity signals (Fig. 31). One set corresponds to the stopper close to the recognition site where the $CBPQT^{4+}$ resides, and the other for the more distant stopper. As the temperature is increased, the rate of shuttling becomes rapid on the ^1H NMR timescale and the symmetry of the rotaxane becomes averaged, leading to an effective axis of symmetry that is the same as the one in the dumbbell. As a result, the two sets of signals are observed to coalesce and then ultimately appear as a single set of averaged peaks.

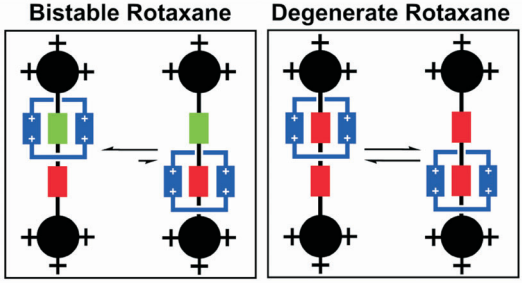

FIG. 30
Schematic representation of shuttling in a bistable [2]rotaxane, where the two co-conformers are nondegenerate, and a degenerate [2]rotaxane, where the two co-conformers and isoenergetic

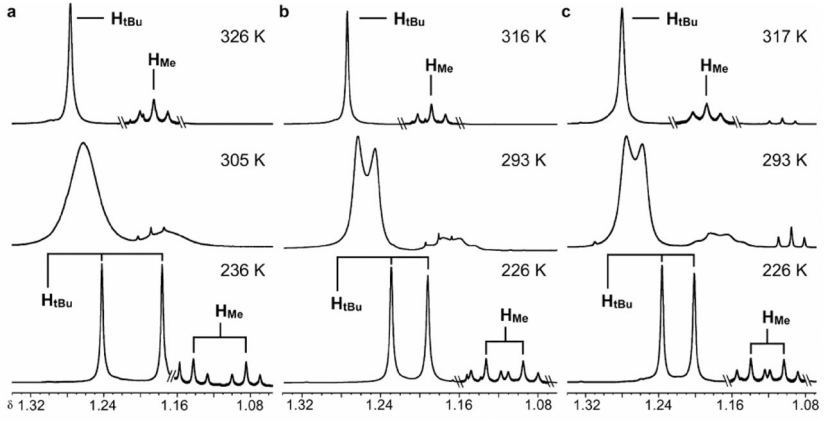

FIG. 31
Partial 500 MHz ^1H NMR spectra recorded in CD_3COCD_3 of **a** **7**·$4PF_6$ at 236, 305 and 326 K, **b** **9**·$4PF_6$ at 226, 293 and 316 K and **c** **11**·$4PF_6$ at 226, 293 and 317 K. The signals shown correspond to some of the alkyl protons on the hydrophobic stoppers. See Fig. 29 for structural assignments

Kinetic data was extracted from these spectra using two methods – namely, spin saturation transfer, for the slow exchange regime, and line shape analysis, over the whole range. A summary of the data is presented in Table VI. An initial appraisal of these data reveals that the barriers for shuttling ($\Delta G^{\ddagger}$) in all three of these DNP-containing [2]rotaxanes are very similar. Although the largest difference is 0.6 kcal mol^{-1} at 282 K between **9**·4PF$_6$ and **11**·4PF$_6$, the average difference is closer to 0.2–0.3 kcal mol^{-1} across the series. The magnitude of the barrier is slightly smaller (~1.5 kcal mol^{-1}) than that reported[54] (17.2 kcal mol^{-1} at 361 K) for a similar degenerate [2]catenane – composed of CBPQT^{4+} and a crown ether containing two DNP units. This difference presumably arises from the presence of an enforced alongside interaction between a bipyridinium unit of CBPQT^{4+} and the non-encircled DNP unit in the catenane, which is not present in the [2]rotaxanes[55].

TABLE VI
Kinetic and thermodynamic data for shuttling in the [2]rotaxanes **7**·4PF$_6$, **9**·4PF$_6$ and **11**·4PF$_6$ in CD_3COCD_3

7·4PF$_6$			**9**·4PF$_6$			**11**·4PF$_6$		
T [a]	k_{ex} [b]	$\Delta G^{\ddagger}$ [c]	T [a]	k_{ex} [b]	$\Delta G^{\ddagger}$ [c]	T [a]	k_{ex} [b]	$\Delta G^{\ddagger}$ [c]
247	0.2 [d]	15.2	236	0.1 [d]	14.8	248	0.2 [d]	15.3
255	0.7 [d]	15.3	247	0.4 [d]	14.9	259	0.7 [d]	15.3
259	0.8 [e]	15.2	247	0.4 [e]	14.8	270	1.8 [d]	15.4
271	3 [e]	15.2	258	1.4 [e]	14.9	270	2 [e]	15.4
282	8 [e]	15.3	259	1.5 [d]	14.9	282	4.7 [e]	15.6
293	20 [e]	15.4	270	4.4 [e]	15.0	282	6 [e]	15.5
305	47 [e]	15.5	282	13 [e]	15.0	294	19 [e]	15.5
			293	33 [e]	15.1	304	55 [e]	15.4
			305	85 [e]	15.2	317	120 [e]	15.6

[a] K, calibrated using neat MeOH sample; [b] s^{-1}; [c] kcal mol^{-1}, ±0.1; [d] measured using spin saturation transfer method (ref.[37]). For **7**·4PF$_6$ exchange was observed between the resonances of H_{Me} at 1.15/1.20 ppm, for **9**·4PF$_6$ the resonances of $H_{2/6}$ at 2.26/7.33 ppm and for **11**·4PF$_6$ the resonances of H_{tBu} at 1.27/1.30 ppm; [e] measured using partial line-shape analysis method. For **7**·4PF$_6$ the H_{Et} signals at 2.52/2.58 ppm, for **9**·4PF$_6$ the H_{Et} signals at 2.54/2.57 ppm and for **11**·4PF$_6$ the H_{Et} signals at 2.56/2.59 ppm were simulated.

The availability of data over wide temperature ranges in the case of all three [2]rotaxanes studied provides the opportunity to analyze the effect of changing the spacer units in more depth by examining the components of the free energy of activation ($\Delta G^{\ddagger}$). Eyring plots for **7**·4PF_6, **9**·4PF_6 and **11**·4PF_6 are shown in Fig. 32. Using these plots the enthalpic ($\Delta H^{\ddagger}$) and entropic ($\Delta S^{\ddagger}$) activation parameters (Table VII) can be obtained from the slopes and intercepts, respectively. Although the differences in $\Delta H^{\ddagger}$ and $\Delta S^{\ddagger}$ are small, it is apparent from these activation parameters that the spacers are more different than the free energies of activation alone would suggest. Unsurprisingly, the glycol chain spacer has the most negative entropic contribution as a result of its flexibility. It also has the smallest enthalpic contribution, possibly because of its relatively small size and favorable electrostatic interactions with the $CBPQT^{4+}$. The terphenyl and diphenyl ether spacers have very similar activation parameters, with the kinked nature of the latter possibly being represented by its slightly larger $\Delta H^{\ddagger}$.

TABLE VII
Activation parameters for shuttling in the [2]rotaxanes **7**·4PF_6, **9**·4PF_6 and **11**·4PF_6 in CD_3COCD_3

Compound	$\Delta H^{\ddagger}$, kcal mol^{-1}	$\Delta S^{\ddagger}$, cal mol^{-1} K^{-1}	$\Delta G^{\ddagger}$, kcal mol^{-1}
1·4PF_6	12.7	–9.3	15.3
3·4PF_6	14.5	–3.2	15.0
5·4PF_6	13.6	–4.8	15.6

[a] At 282 K. See Table VI for details.

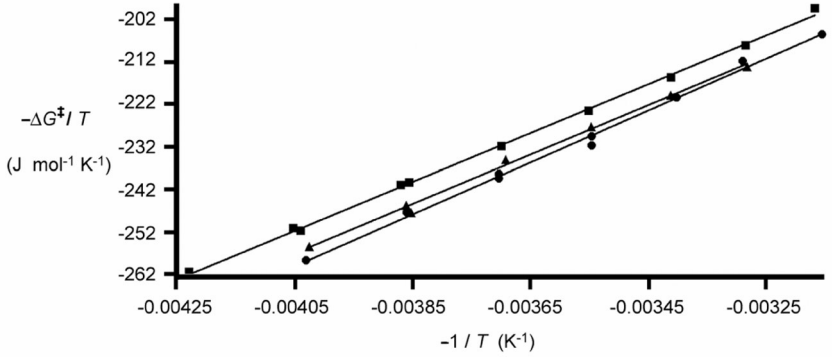

FIG. 32
Eyring plots for **7**·4PF_6 (▲), **9**·4PF_6 (■) and **11**·4PF_6 (●) based on the data in Table VI

A similar quantitative analysis of the degenerate TTF-containing [2]rotaxanes was complicated by the presence of many constitutional isomers. Disubstitution of the TTF unit can be such that the two connections are *cis* or *trans* relative to its central double bond. In the samples studied, a mixture of *cis* and *trans* TTF units in the rotaxanes leads to a complicated set of possible exchange pathways for shuttling, where the ring can move from *cis*-to-*cis*, *cis*-to-*trans*, *trans*-to-*cis* or *trans*-to-*trans*. While a thorough investigation of the different rates involved with these exchange pathways would be interesting, identification of the various isomers by ^{1}H NMR spectroscopy was not possible. Physical separation of the *cis* and *trans* isomers was also precluded by rapid rotation around the central bond of the TTF unit on the laboratory timescale.

It was possible, however, to estimate the rates of shuttling in the TTF-containing degenerate rotaxanes by using the coalescence method. The peak separation for H_{tBu} at low temperature ($\Delta\upsilon_{ex}$) was determined by taking an average value of the separations between the many signals observed. As the temperature was increased, the numerous peaks began to coalesce[56] and the so-called coalescence temperature, T_c, was estimated for each [2]rotaxane. The free energies of activation, $\Delta G^{\ddagger}$, could then be calculated[57]. The $\Delta G^{\ddagger}$ values fall in the range from 17–18 kcal mol^{-1}. The higher energy barriers for the TTF-containing rotaxanes relative to the DNP-containing ones – $\Delta\Delta G^{\ddagger} \sim 2$ kcal mol^{-1} – have their origin in the stronger interaction between TTF and CBPQT^{4+}, a property which is also reflected in the binding energies, ΔG^{o}_{298}, for the individual units with CBPQT^{4+} of –6 and –8 kcal mol^{-1} for DNP [58] and TTF [50b] in CD_3CN, respectively.

Another component of these catenanes and rotaxanes that can be modified and should have some effect on the rate of circumrotation/shuttling is the tetracationic cyclophane. A bistable [2]catenane with a modified cyclophane has been reported[47c]. In this catenane, the bipyridinium units of the tetracationic cyclophane have been replaced with diazapyrenium (DAP) units. They were chosen as acceptor units in order to assist in the attachment of a switchable [2]catenane to the surface of carbon nanotubes. The DAP units have a significantly larger π-surface in comparison with the bipyridinium ones and so the interactions between the cyclophane and crown ether macrocycle are expected to be considerably enhanced. The effect of this larger cyclophane on the rate of circumrotation in a degenerate [2]catenane will now be evaluated and discussed.

The degenerate [2]catenane **13**·4PF$_6$ (Fig. 33a) incorporating the DAP-cyclophane and a DNP-containing crown ether was synthesized[59] according to literature procedures. VT ^{1}H NMR spectroscopic studies on a solution

prepared in CD_3SOCD_3 revealed qualitatively that the circumrotations of the crown ether macrocycle in this catenane are slow on the ^1H NMR timescale, even at high temperature (403 K), i.e., no coalescence of the $H_{2/6}$, $H_{3/7}$ and $H_{4/8}$ signals for the free and encircled DNP units was observed over the range of accessible temperatures. Spin saturation transfer experiments (SST) on the $H_{3/7}$ signals at 5.13 ppm (encircled) and 6.57 ppm (free), however, allowed kinetic data to be accessed in the slow exchange regime for a sample of **7**·4PF_6 in CD_3SOCD_3. The results are summarized in Table VIII.

A comparison of these data with similar data for the analogous degenerate [2]catenane[54] containing the $CBPQT^{4+}$ cyclophane, **14**·4PF_6 (Fig. 33b), provides some insight into the effect of incorporating the DAP units on circumrotation (Fig. 33c). Although data at a common temperature for the two systems is not available, it is qualitatively apparent that the free energy of activation in **7**·4PF_6 is significantly higher (~6–7 kcal mol^{-1}) than it is in **14**·4PF_6. This difference reflects a stronger [π···π] stacking interaction between the DAP units and the DNP units of the crown ether, presumably as a result of the larger π-surface involved in the case of the [2]catenane **7**·4PF_6

TABLE VIII
Kinetic and thermodynamic data for circumrotation of the crown ether macrocycle in the [2]catenanes **13**·4PF_6 and **14**·4PF_6

Compound	T [a]	k_{ex} [b]	$\Delta G^{\ddagger}$ [c]
13·4PF_6 [d]	388	0.4	23.7
	403	1.1	23.8
14·4PF_6 [e]	361	240	17.2

[a] K, calibrated using neat MeOH sample; [b] s^{-1}, measured using spin saturation transfer method (ref.[37]); [c] kcal mol^{-1}, ±0.1; [d] in CD_3SOCD_3; [e] in 19:1 CD_3COCD_3/CD_3CN, see ref.[8]

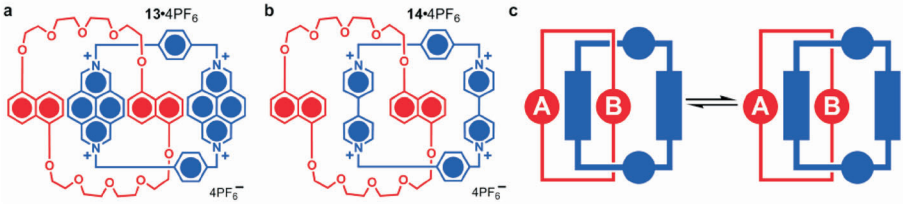

FIG. 33
Structural formulas for the degenerate [2]catenanes **a** **13**·4PF_6 and **b** **14**·4PF_6. **c** A schematic representation of circumrotation in a degenerate [2]catenane

incorporating the DAP-cyclophane. These results correlate well with previously reported studies[59] on a [2]catenane composed of a 1/5DNP38C10 macrocycle and an asymmetric cyclophane containing one bipyridinium and one DAP unit. In this case, the major co-conformer observed corresponded to the one where the DAP unit resides inside the macrocycle.

3.3. Switching

Although it is not possible to determine the kinetics of the switching cycle for TTF/DNP-containing bistable catenanes and rotaxanes in solution via ^{1}H NMR spectroscopy, some of the states can be observed. Characterization of the "ground state" and "switched state" in solution allows structural variants to be examined and so confirm or otherwise the complete relocation of the ring component after oxidation and the reversibility of the switching process before their incorporation into devices. Previous attempts[50] to observe the chemical or electrochemical switching in solution have relied primarily on UV/VIS spectroscopy and occasionally cyclic voltammetry. While these methods provide general structural information through charge transfer bands and oxidation/reduction potentials, they do not provide the fine structural detail that becomes available from NMR spectroscopy.

The first step towards NMR characterization of the switching cycle was to find an appropriate method for oxidizing the TTF unit to convert from the "ground state" into the "switched state." Because of the complexities inherent[60] with electrochemical NMR cells, a chemical oxidant was chosen as the preferred method. In this choice, the oxidant was required to meet three requirements: (i) It must possess a high enough potential to oxidize the TTF unit to its dicationic form since the monocation is paramagnetic[61]. (ii) It has to be soluble in the same solvents as the majority of TTF/DNP-containing bistable catenanes and rotaxanes, i.e., acetone and acetonitrile. (iii) It must not be paramagnetic after reacting with the TTF unit and should give rise to as small a number of signals in the ^{1}H NMR spectrum as possible. A survey of the literature with these desired characteristics in mind led to a potential candidate – namely, tris(*p*-bromophenyl)amminium hexafluoroantimonate[62] (TAH).

The next step was to test this oxidant on some model compounds[63] before attempting to oxidize a bistable derivative. Two model compounds were chosen, a single-station TTF-containing dumbbell **15** (Fig. 34a) and its corresponding [2]rotaxane **16**·4PF_6 (Fig. 34b). A solution of **15** in CD_3COCD_3 was prepared and its ^{1}H NMR spectrum (Fig. 34c) recorded at room temper-

ature. The two signals corresponding to the protons of the *cis* and *trans* TTF units, H_{TTF}, appear[64] at 6.47 and 6.50 ppm, with the adjacent $–CH_2–$ group protons, H_{CH2}, resonating at 4.30 and 4.31 ppm. Some of the alkyl protons of the hydrophobic stoppers also give rise to two nearly overlapping signals (Fig. 34c, inset) as a result of the *cis*/*trans* isomerism. Upon addition of 2.0–2.5 equivalents of the oxidant, a large downfield shift of ~2.3 ppm for H_{TTF} and ~1.1 ppm for H_{CH2} is observed in the ^{1}H NMR spectrum (Fig. 34e) of the oxidized species. The new spectrum also displays only a single set of signals for all the protons, indicating that only one isomer is present and thus providing further evidence[65] for formation of the non-planar TTF dication.

Oxidation of the [2]rotaxane **16**·4PF$_6$ was also performed in order to establish that the oxidant will operate with a CBPQT^{4+}-encircled TTF unit. In common with the case of the dumbbell **15**, the ^{1}H NMR spectrum (Fig. 34d) of a solution of **16**·4PF$_6$ in CD_3COCD_3 displays two sets of signals for H_{TTF}, at 6.29 and 6.43 ppm, and H_{CH2}, at 4.31 and 4.32 ppm, corresponding to the two isomers of the TTF unit. After oxidation with 2.0–2.5 equivalents of

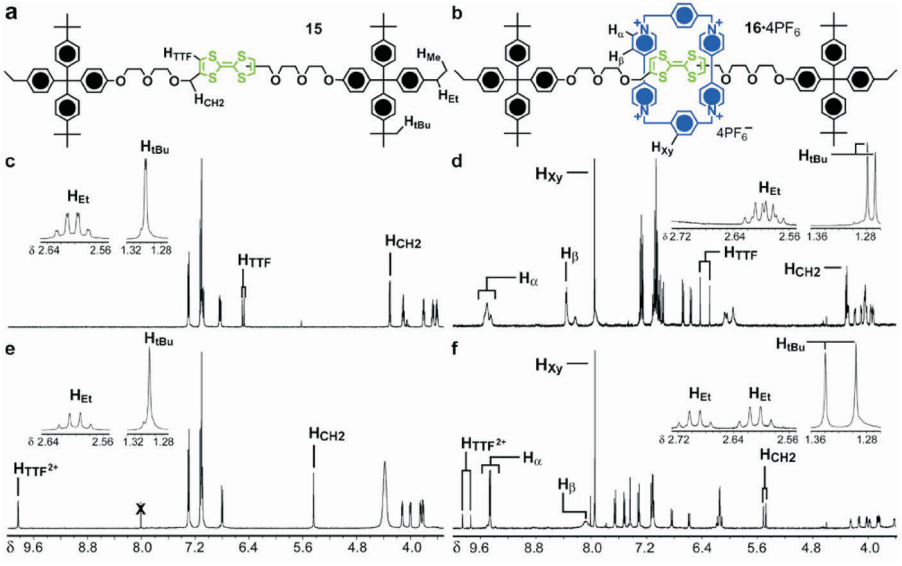

FIG. 34

Structural formulas for **a** the dumbbell **15** and **b** the single-station [2]rotaxane **16**·4PF$_6$. Partial 500 MHz ^{1}H NMR spectra in CD_3COCD_3 at room temperature of **c 15**, **d 16**·4PF$_6$, **e 15** after addition of 2.0–2.5 equivalents of oxidant and **f 16**·4PF$_6$ after addition of 2.0–2.5 equivalents of oxidant

TAH and recording the ^{1}H NMR spectrum (Fig. 34f) again, these signals exhibit a downfield shift of ~3.4 and ~1.2 ppm, for H_{TTF} and H_{CH2}, respectively. In contrast with the dumbbell compound **15**, two sets of signals are observed for both the oxidized and non-oxidized [2]rotaxane **16**·4PF$_6$. In addition, the separation between the two sets of signals for some of the alkyl protons in the stoppers increases significantly after oxidation, from 0.01 to 0.09 and 0.01 to 0.04, for H_{Et} and H_{tBu}, respectively. For the non-oxidized species, the two set of signals arise because of the *cis*/*trans* TTF isomerism. In the oxidized species, however, the TTF dication is non-planar and no longer exists in different isomers. The breaking of the dumbbell's axial symmetry in the oxidized species can be explained by the dislocation of the CBPQT^{4+} ring from the TTF^{2+} dication to one side of the dumbbell component.

Once the TTF oxidation had been established, a relatively simple bistable [2]rotaxane, **17**·4PF$_6$, containing both a TTF and DNP unit with a terphenyl spacer and two hydrophobic stoppers was chosen[66] for the first investigation of the switching cycle by ^{1}H NMR spectroscopy. The spectrum (Fig. 36a) was recorded of a solution containing **17**·4PF$_6$ in CD_3CN at room temperature and signals corresponding to the H_{TTF} protons of an encircled TTF unit were observed at 6.01, 6.10, 6.21 and 6.26 ppm (two signals for each isomer). Upon oxidation with 2.0–2.5 equivalents of TAH, the characteristic downfield shift of H_{TTF} to 9.03 and 9.15 ppm was observed in the re-

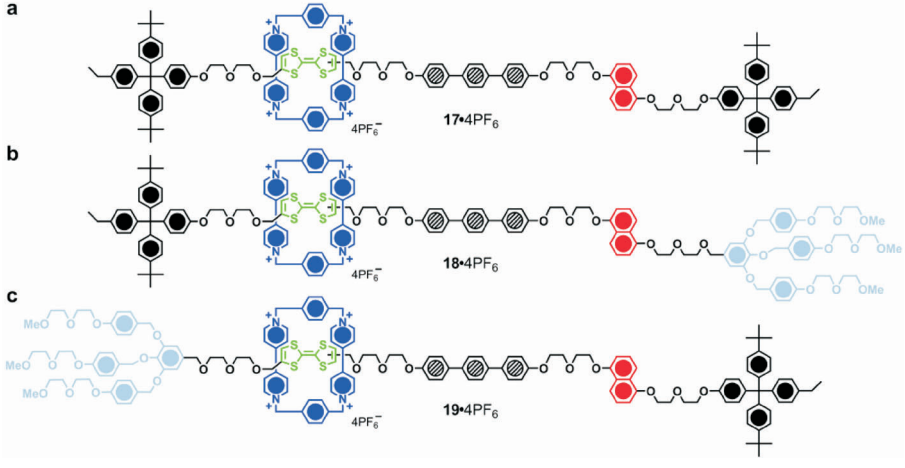

FIG. 35
Structural formulas of the TTF/DNP-containing bistable [2]rotaxanes **a** **17**·4PF$_6$, **b** **18**·4PF$_6$ and **c** **19**·4PF$_6$

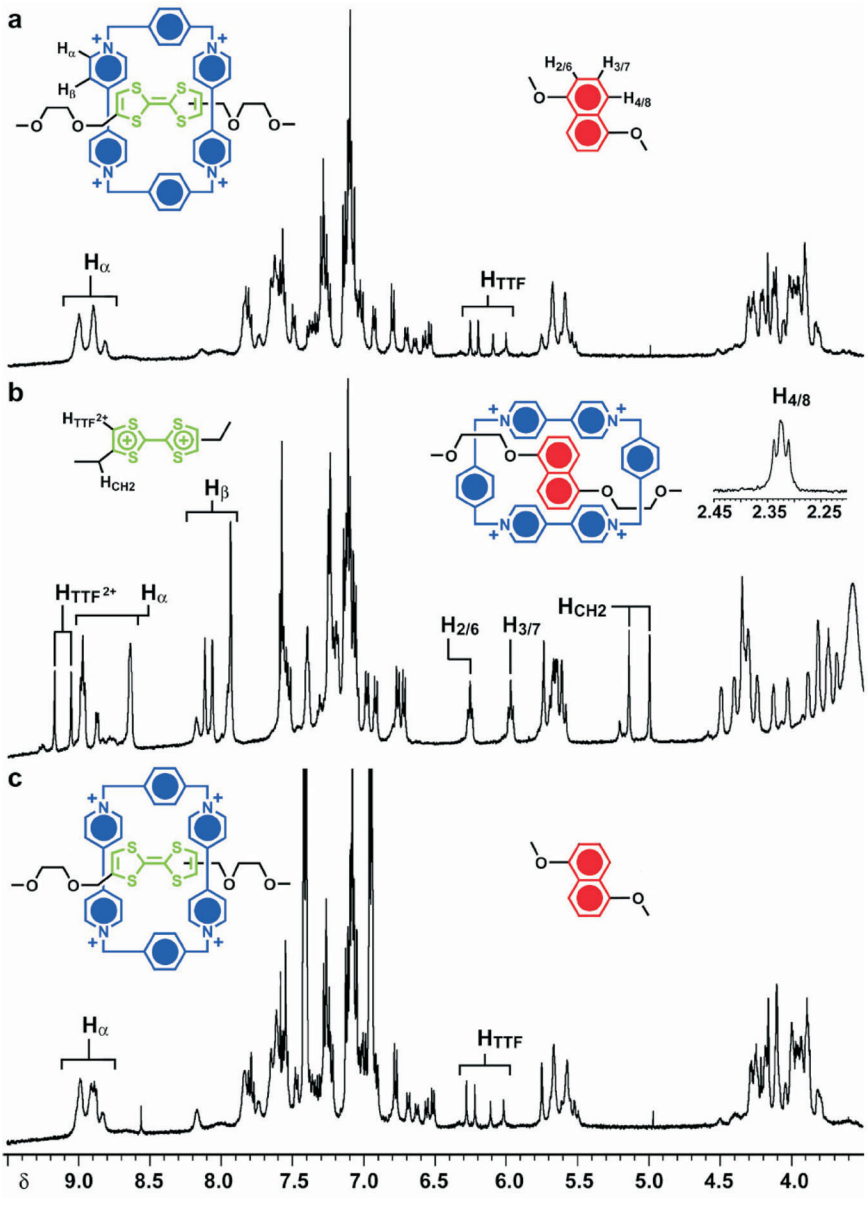

FIG. 36

Partial 500 MHz ^{1}H NMR spectra recorded in CD_3CN of **a** **17**·4PF_6 at room temperature, **b** after oxidation with 2.0–2.5 equivalents of TAH at 243 K and **c** after reduction with Zn powder at room temperature

corded spectrum (Fig. 36b). The adjacent methylene protons H_{CH2} were also observed to resonate at 4.98 and 5.12 ppm after oxidation, indicative of TTF^{2+} dication formation. Evidence for movement of the $CBPQT^{4+}$ ring to the DNP unit was also found in the shape of signals for $H_{4/8}$, $H_{3/7}$ and $H_{2/6}$ at 2.30, 5.95 and 6.23 ppm, respectively. The extreme upfield shift of $H_{4/8}$ arises from shielding effects of the aromatic rings in the encircling $CBPQT^{4+}$. No signals corresponding to a free DNP unit were observed, indicating complete translation of the ring to the DNP recognition site.

In order to reverse the switching process, it was necessary to find a reductant that would neutralize the TTF^{2+} dication without reducing the $CBPQT^{4+}$ ring. Zn powder was found to work well for this reductive process. Addition of a small amount to the solution, followed by vigorous shaking, returned the TTF^{2+} dication to its neutral form. The ^1H NMR spectrum (Fig. 36c) was then recorded and correlated well with the original spectrum (Fig. 36a) before oxidation. One notable difference was the presence of two large signals at 7.0 and 7.5 ppm corresponding to tris(*p*-bromophenyl)-amine, the reduced form of the oxidant. Thus, the chemically-induced switching of this bistable [2]rotaxane was shown to adopt completely the "switched state" upon oxidation and return fully to the "stable state" upon reduction.

One of the structural variants that has proved to be useful when incorporating a bistable [2]rotaxane into devices involves replacing one of the hydrophobic stoppers with a hydrophilic stopper to create amphiphilicity. The hydrophilic stopper can be placed either near the TTF or the DNP unit, resulting in two constitutionally different amphiphilic bistable [2]rotaxanes (Fig. 35b and 35c). The introduction of this hydrophilic stopper represents a significant structural change, and so to ensure that there is no detrimental effect on the switching cycle, the chemically-induced switching of **19**·$4PF_6$ was performed[67] and monitored by ^1H NMR spectroscopy.

A ^1H NMR spectrum of **19**·$4PF_6$ was recorded (Fig. 37a) in CD_3CN at 243 K and showed the usual four signals for the H_{TTF} protons of the TTF unit resonating at 5.91, 5.96, 6.17 and 6.20 ppm. Ring movement was induced by the addition of 2.0–2.5 equivalents of the oxidant TAH to oxidize the TTF unit to its dication. After recording the ^1H NMR spectrum (Fig. 37b) again, characteristic downfield shifts for the $H_{TTF^{2+}}$ protons, at 9.12 and 9.23 ppm, and for the H_{CH2} protons, at 5.03 and 5.19 ppm, occurred. Evidence for localization of the $CBPQT^{4+}$ ring on the DNP unit is found in the chemical shifts of the $H_{4/8}$, $H_{3/7}$ and $H_{2/6}$ protons at 2.30, 5.95 and 6.24 ppm, respectively. No signals corresponding to a free DNP unit were observed. From these data, it would appear the presence of a hydrophilic

stopper has no adverse effect on the ring movement induced by oxidation of the TTF unit.

In addition to their use as switches for molecular electronics, bistable molecules can be designed to act as molecular machines. One example of this application is the construction of a molecular muscle from a palindromic [3]rotaxane. Such a molecule has two ring components on a long dumbbell component. Upon oxidation, the ring components are expected to move closer to one another in a motion that is reminiscent of a muscle contraction. To determine the feasibility of such a design using the TTF/DNP recognition motif, a model [3]rotaxane **20**·8PF_6 (Fig. 38a) was investigated[68]. Two fundamental questions were posed regarding this system. To begin with, (i) would it be possible to bring two highly charged rings so

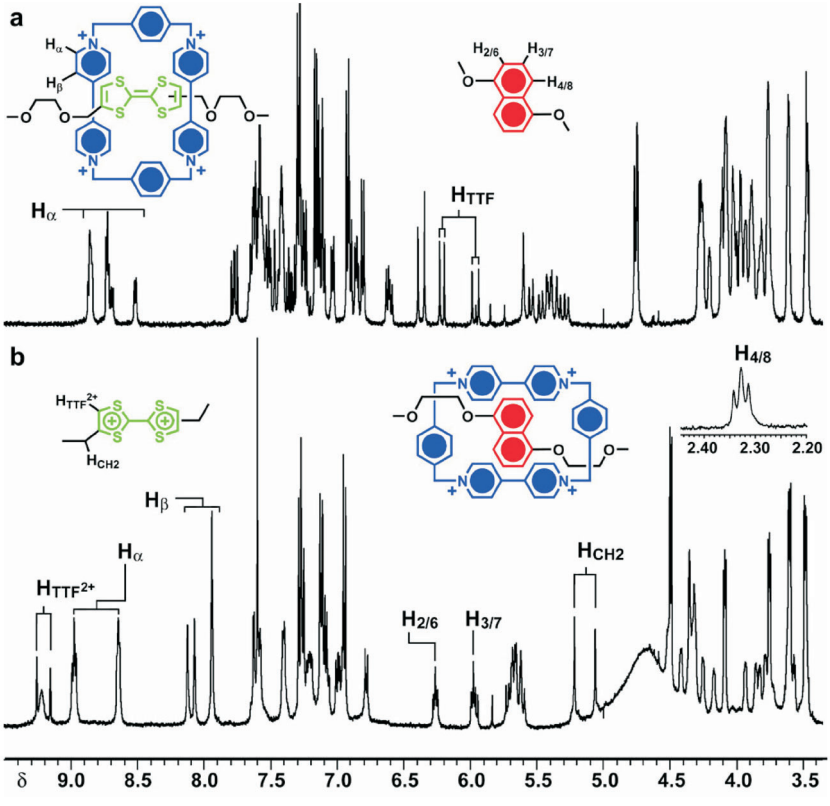

FIG. 37

Partial 500 MHz ^{1}H NMR spectra recorded in CD_3CN at 243 K of **19**·4PF_6 **a** before and **b** after addition of 2.0–2.5 equivalents of the oxidant

close together? And if so, (ii) would the contraction be reversed after neutralization of the TTF unit?

A solution of the [3]rotaxane **20**·8PF_6 was prepared in CD_3CN and its ^1H NMR spectrum (Fig. 38b) recorded at 243 K. The signals corresponding to the *cis* and *trans* isomers of the TTF units appear at 6.04, 6.05, 6.19 and 6.24 ppm, two[69] for each isomer. After addition of 2.0–2.5 equivalents of the oxidant TAH, a signal corresponding to the TTF^{2+} dication appeared at 9.31 ppm in the spectrum of the oxidized species (Fig. 38c). Six signals were observed for the encircled DNP units resonating at 2.77, 2.84, 5.92, 6.25, 6.30 and 7.28 ppm. The two upfield signals correspond to H_4 and H_8, which participate in [C–H···π] interactions with the $CBPQT^{4+}$ rings, and so are

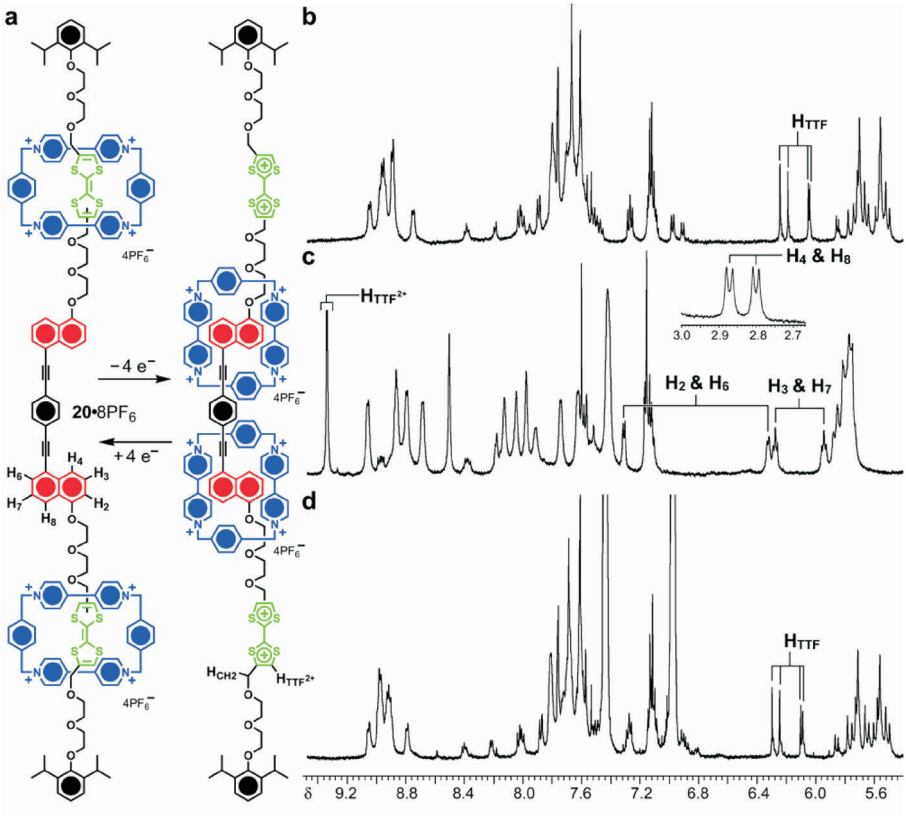

FIG. 38

a Structural formula for the bistable [3]rotaxane **20**·8PF_6 and the structure after four-electron oxidation. **b** Partial ^1H NMR spectra of **20**·8PF_6 recorded in CD_3CN at 243 K **c** after addition of 2.0–2.5 equivalents of oxidant and **d** after reduction with Zn powder

highly shielded. It was not possible, however, to assign which signal belongs to which proton. Reversibility of the switching process was confirmed by addition of Zn powder, followed by vigorous shaking and recording the spectrum (Fig. 38d) afresh. These experiments suggest that the model [3]rotaxane behaves as two essentially independent bistable [2]rotaxanes in relation to its switching cycle.

Previously, the effect on circumrotation of changing the bipyridinium units in $CBPQT^{4+}$ to diazapyrenium units in a degenerate [2]catenane was presented. Before incorporating this structural motif into a device, it was also important to determine if the DAP units interfered with oxidative switching[70] of the bistable TTF/DNP-containing [2]catenane **21**·4PF_6. Thus, the ^{1}H NMR spectrum (Fig. 39b) of a solution of **21**·4PF_6 in CD_3CN was recorded at room temperature. Two sets of signals with a ratio of 1.6:1 could be identified in the spectrum. The signals (H_{TTF}) for the TTF unit resonate at 5.55 and 5.60 ppm, with the more upfield one being the one of lower intensity. Interestingly, two sets of signals are also observed for the DNP unit, and the order of the signals differs between the two isomers. For the minor isomer, the signals appear at 6.63 ($H_{4/8}$), 7.16 ($H_{3/7}$) and 7.39 ($H_{2/6}$) ppm: in the major isomer, however, $H_{3/7}$ is the most downfield signal, resonating at 6.99 ppm, with the other two appearing at 6.36 ($H_{4/8}$) and 6.88 ($H_{2/6}$) ppm.

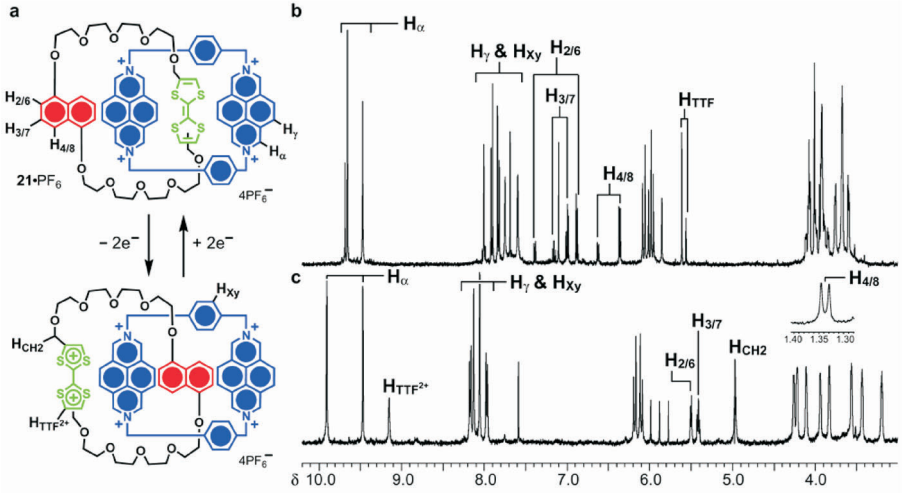

FIG. 39

a The structural formula for the bistable [2]catenane **21**·4PF_6 and its structure after two-electron oxidation. **b** Partial ^{1}H NMR spectra of **21**·4PF_6 recorded in CD_3CN at room temperature and **c** after addition of 2.0–2.5 equivalents of oxidant

The two sets of signals can be explained by the presence of *cis* and *trans* TTF isomers in unequal amounts. These constitutional isomers would be expected to have different effects on the co-conformers adopted. The orientation of the DNP unit relative to the DAP unit is most likely different in the two co-conformers resulting in differing shielding effects for $H_{2/6}$, $H_{4/8}$ and $H_{3/7}$, and thus causing the change in ordering of the respective signals for the two isomers.

Oxidation of **21**·4PF_6 to the "switched state" was accomplished by addition of 2.0–2.5 equivalents of TAH, followed by recording the ^{1}H NMR spectrum (Fig. 39c). On oxidation, only a single set of peaks is observed for the catenane. The characteristic peaks for formation of the TTF^{2+} dication were observed at 9.15 (H_{TTF}) and 4.97 (H_{CH2}) ppm. Evidence for circumrotation of the crown ether in order to place the DNP unit inside the cavity of the cyclophane is found in the upfield shift of the corresponding signals, i.e., $H_{4/8}$, $H_{3/7}$ and $H_{2/6}$ appear at 1.34, 5.41 and 5.50 ppm, respectively. The larger DAP units seem to have a greater shielding effect relative to the bipyridinium units observed previously, accounting for the ~0.5–1.0 ppm greater upfield shift of the DNP unit signals. Reversal of the switching process by using Zn powder to reduce the TTF^{2+} dication was precluded by the irreversible reduction apparently of the DAP units, leading to broad uninterpretable spectra.

A summary of chemical shift data for all of the TTF-containing compounds discussed here is presented in Table IX. From these data, it is apparent that the chemical shifts for the protons (H_{TTF}) on the TTF unit remain

TABLE IX
Chemical shift data for compounds containing a neutral or oxidized TTF unit

Compd [a]	Neutral TTF		Oxidized TTF				
	T	H_{TTF}	*T*	H_{TTF}	$H_{2/6}$	$H_{3/7}$	$H_{4/8}$
15 [b]	RT	6.47, 6.50	RT	9.83	–	–	–
16·4PF_6 [b]	RT	6.29, 6.43	RT	9.74, 9.86	–	–	–
17·4PF_6 [c]	RT	6.01, 6.10, 6.21, 6.26	243	9.03, 9.15	6.23	5.95	2.30
19·4PF_6 [c]	243	5.91, 5.96, 6.17, 6.20	243	9.12, 9.23	6.24	5.95	2.30
20·8PF_6 [c]	243	6.04, 6.05, 6.19, 6.24	243	9.31	6.30, 7.28	5.92, 6.25	2.77, 2.84
21·4PF_6 [c]	RT	5.55, 5.60	RT	9.15	5.50	5.41	1.34

[a] See Figs 34, 35, 38 and 39 for structural formulas; [b] in CD_3COCD_3; [c] in CD_3CN.

relatively consistent across all the structural variants, granted the changes in temperature and solvent. A notable exception is **21**·4PF_6, wherein the neutral TTF unit experiences a stronger shielding effect from the DAP-containing cyclophane, such that its signals are shifted upfield ~0.5–1.0 ppm. This difference disappears in the oxidized species as a result of translocation of the cyclophane to the DNP unit. The TTF^{2+} dication, however, does appear to be somewhat affected by solvent changes. The chemical shifts for $H_{TTF^{2+}}$ in the oxidized species are ~0.5 ppm higher in CD_3COCD_3 than they are in CD_3CN possibly because of differences in polarity, leading to ion-pairing to different extents.

The signals corresponding to the DNP unit in these bistable catenanes and rotaxanes are diagnostic of the presence of the "switched state". In general, all of the protons on the DNP unit experience significant upfield shifts because of the shielding effects of the highly-aromatic tetracationic cyclophanes. The $H_{4/8}$ protons, however, experience the strongest effect, with shifts on the order of 5 ppm, as a result of their participation in [C–H···π] interactions with the bridging *p*-xylylene units. All three sets of protons exhibit similar chemical shifts in the compounds studied with two exceptions. The first is a result of modification of the DNP unit in **20**·8PF_6 wherein one of the glycol chains is replaced by an ethynylene rod, substantially altering the chemical shifts for one half of the 1,5-disubstituted naphthalene unit. The other exception is in **21**·4PF_6 where the protons on the DNP unit, as well as the TTF unit, experience increased shielding effects as a result of the larger DAP units in the cyclophane. These minor differences, however, do not diminish the usefulness of the extremely large chemical shift for $H_{4/8}$ in the "switched state" as a diagnostic probe for this state.

3.4. Conclusions

Solution-phase characterization of bistable catenanes and rotaxanes, as well as of the corresponding model compounds, allows structural variants to be tuned and tested before their incorporation into devices[47]. Here, the study of shuttling in a series of degenerate [2]rotaxanes, incorporating different spacer units, provided insight into the effects of the spacer unit on the kinetics of ring movement. It is also apparent, from the range of spacers investigated that substantial structural changes are necessary for these spacers to have a significant impact on the rate of shuttling. In addition, it was shown that the DAP-containing tetracationic cyclophane is effective in slowing down circumrotation in a degenerate catenane, relative to that observed with the parent cyclophane $CBPQT^{4+}$. Detailed investigations of

the dynamics exhibited in these systems will be crucial to providing the knowledge-base necessary for the directed design of future molecular switches and machines.

The nature of the switching cycle in a number of TTF/DNP-containing bistable catenanes and rotaxanes has also been discussed in this Section. NMR Spectroscopy provides access to the fine structural detail and quantitative information that would be difficult to obtain using other methods. A chemical oxidant, which was tested on TTF-containing model compounds, was shown to oxidize the TTF units and thus cause switching to occur in a number of structurally diverse compounds. The characteristics of the "stable state" and "switched state" remain remarkably consistent across all the compounds investigated, an observation which provides further evidence for the robust nature of the TTF/DNP switching mechanism in a range of different environments. As new switches and machines are developed with increasingly complex molecular structures, it will become more and more important, if not essential, to have tools for characterizing their desired functions in solution. Thus far, NMR spectroscopy has proven to be an extremely useful method for evaluating these TTF/DNP-containing systems.

4. DYNAMICS AND SWITCHING OF DONOR–ACCEPTOR NEUTRAL ROTAXANES

4.1. Background

Molecular switch tunnel junctions (MSTJs) incorporating TTF/DNP-containing bistable [2]catenanes and [2]rotaxanes (**22**$^{4+}$ in Fig. 40a) take advantage of the donor–acceptor interactions between the electron-rich TTF and DNP units and an electron-deficient tetracationic cyclophane, CBPQT^{4+}, to create two different switchable states. See Section 3 for details. An unavoidable consequence of the four positive charges carried by the cyclophane, however, is the presence of a sufficient number of anions to counterbalance the charge. Although the detailed role of these anions in a device setting has not been elucidated yet, in the case of an amphiphilic bistable [2]rotaxane, they must serve to induce some drag on the ring component during its translational motion. They also complicate any structural analysis and may exchange partially or wholly with ions contained in the sub-phase during Langmuir–Blodgett monolayer[71] formation – a prerequisite step to their use in a device – leading to a degree of uncertainty regarding the actual composition of the molecular monolayer[72].

Perhaps the most important ramification of counterions is their role in influencing the co-conformation adopted in mechanically-interlocked mo-

lecular systems. Recent work has shown[73] that changing the counterions in a bispyrrolotetrathiafulvalene (BPTTF)/DNP-containing bistable [2]rotaxane (**22**$^{4+}$ in Fig. 40a) can have a dramatic effect on the equilibrium co-conformer distribution in solution. The PF_6^- salt (Fig. 40b) of **23**$^{4+}$ exists in CD_3COCD_3 at room temperature as roughly a 1:1 mixture of the two co-conformers, where the CBPQT^{4+} ring resides half the time on the BPTTF site and the other half on the DNP site. After exchanging (Fig. 40b) the four PF_6^- counterions for TRISPHAT$^-$ ones, the equilibrium ratio shifts to 95:5 in favor of the co-conformer where the ring encircles the BPTTF unit. From the result of this experiment, it is apparent that the role of the counterions in bistable [2]rotaxanes is much more important than simply that of counterbalancing charge.

Although the presence of counterions in mechanically-interlocked compounds can be viewed as providing an additional degree of control, it may also be desirable for many reasons – not the least of which is to simplify the system – to have access to neutral bistable catenanes and rotaxanes where there is no need for external[74] charge balancing. Consequently, the recognition system developed by Sanders et al.[75] was investigated for its potential application in the creation of molecular switches and machines. This recognition motif (Fig. 41a) is defined by two electron-poor aromatic units – pyromellitic diimide (PmI) and 1,4,5,8-naphthalenetetracarboxylate diimide (NpI) – to act as recognition sites for an electron-rich crown ether macryocycle, namely 1,5-dinaphtho[38]crown-10 (1/5DNP38C10). Two control mechanisms have been demonstrated using this motif by the

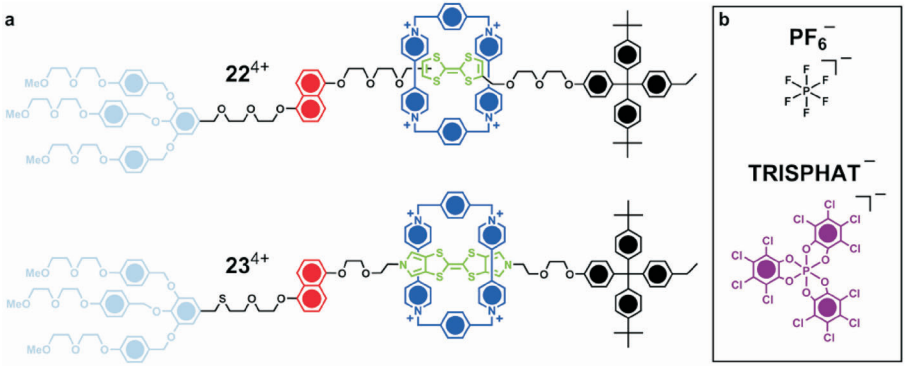

FIG. 40

Structural formulas for **a** two bistable [2]rotaxanes composed of a tetracationic cyclophane and a dumbbell component containing a DNP unit and either a TTF unit (**22**$^{4+}$) or a bispyrrolotetrathiafulvalene unit (**23**$^{4+}$) and **b** two counterions that have been paired with **23**$^{4+}$.

Sanders group. Chemical control was demonstrated[76] by the use of lithium cations to influence pseudorotaxane formation, which occurs preferentially for 1/5DNP38C10 with the NpI unit, as opposed to the PmI one. Upon addition of at least two equivalents of Li^+ ions, however, this preference is reversed (Fig. 41b). Electrochemical control (Fig. 41c) was also demonstrated[77] in a bistable [2]catenane using cyclic voltammetry (CV). The first reduction occurs at –0.76 V (relative to SCE) and was assigned[78] to a one-electron reduction of the NpI unit. Relative to the NpI anion, the PmI unit is a better acceptor and circumrotation occurs, placing the PmI unit inside the electron-rich crown ether. This supposition is supported by observation of a second peak in the CV at –1.14 V that was assigned to one-electron reduction of an encircled PmI unit.

Using the Sanders recognition motif, an amphiphilic bistable neutral [2]rotaxane, **25**, was designed (Fig. 42a) using features similar to those of the TTF/DNP-containing equivalents, e.g., with a hydrophobic stopper and a hydrophilic one. The proposed electrochemical switching mechanism (Fig. 42b) for this neutral bistable rotaxane is similar to the one demonstrated for the TTF/DNP-based systems, with the main difference being that

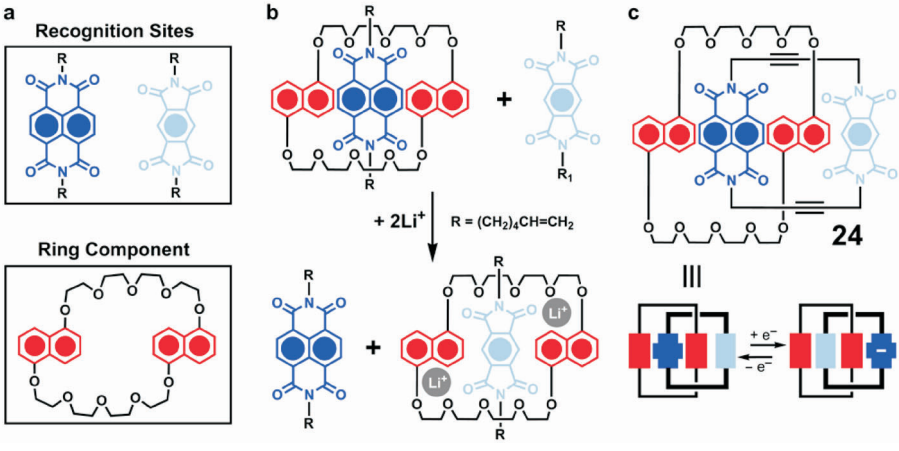

FIG. 41

a The constituent components of a neutral recognition motif. The two electron-poor aromatic units associate separately with the electron-rich crown ether macrocycle 1/5DNP38C10. **b** The 1,4,5,8-naphthalenetetracarboxylate diimide (NpI) unit binds more strongly to 1/5DNP38C10, but upon addition of Li^+ ions it is displaced by the pyromellitic diimide (PmI) unit, which forms a co-complex with the 1/5DNP38C10 and two Li^+ ions. **c** The structural formula for a bistable neutral [2]catenane **24** based on this recognition motif is shown and a schematic representation of its electrochemical switching

the neutral system switches as a result of a reduction instead of oxidation. At equilibrium, the neutral rotaxane exists primarily as the co-conformer where the crown ether encircles the NpI unit. The lower reduction potentials[76] for the NpI unit (–0.83 and –1.11 V vs SCE for free and encircled, respectively) relative to the PmI unit (–1.07 and –1.21 vs SCE for free and encircled, respectively) in related compounds suggest that it should be reduced first. Upon reduction of the NpI unit the co-conformer where the crown ether encircles the PmI unit will become the much more favored one. Once the rotaxane has been returned to its neutral form, the initial equilibrium will be reestablished with a time constant dependent upon the barrier for shuttling.

The lack of counterions in this neutral bistable [2]rotaxane should simplify any investigation of its shuttling behavior, particularly in condensed phases, and potentially increase the accessible switching speeds. Two factors could contribute to the latter property. The first is the reduction in drag on the ring component that will occur as a result of the absence of associated counterions. Secondly, there is considerable evidence in the literature[79] to suggest that larger and more flexible ring components undergo translational motion more rapidly than the rigid cyclophane rings. Before the required amphiphilic compounds were identified as primary goals in synthesis and prior to their use in devices, several model compounds were prepared in order to obtain a better understanding of the shuttling behavior of degenerate and bistable [2]rotaxanes based on this recognition motif.

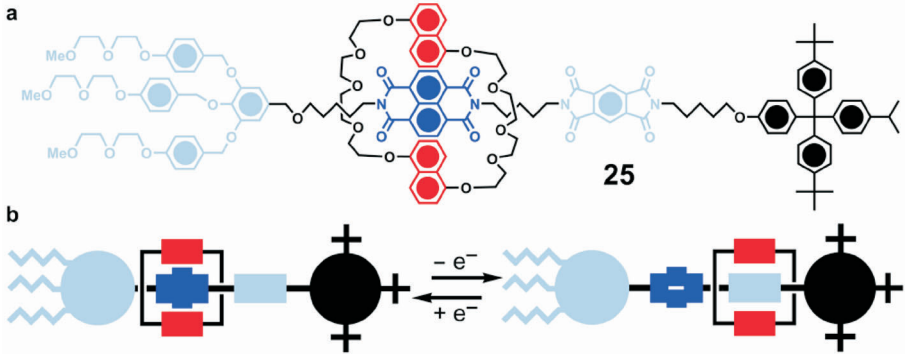

FIG. 42

a The structural formula for a proposed amphiphilic bistable neutral [2]rotaxane **25**. **b** A schematic representation of the proposed electrochemical switching mechanism for this [2]rotaxane. Only the major co-conformers for each oxidative state are shown.

4.2. Dynamics

A series of model compounds was investigated[80] in order to probe the dynamic processes inherent to NpI/PmI-containing [2]rotaxanes and determine the kinetic and thermodynamic parameters associated with them. The compounds studied (Fig. 43) included two degenerate [2]rotaxanes – where both recognition sites are equivalent, i.e., either PmI/PmI (**26**) or NpI/NpI (**27**) – and one bistable compound (**28**) – incorporating one NpI unit and one PmI one. In all three cases, the dumbbells in the rotaxanes were terminated by two identical hydrophobic stoppers composed of a tetraarylmethane core, substituted in the *para* positions of its aryl rings with *t*-butyl groups in two cases, and with an isopropyl group in the third case. A short five-carbon alkyl chain links the two recognition sites to one another and so should provide little or no obstruction to the movement of the 1/5DNP38C10 macrocycle from one site to the other. Here, the details of two dynamic processes observed in these systems will be presented and discussed.

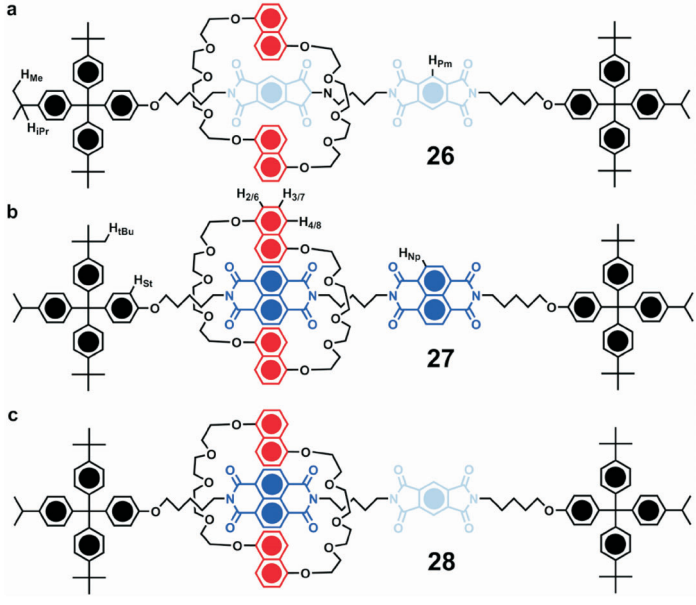

FIG. 43
Structural formulas for three neutral [2]rotaxanes composed of a 1/5DNP38C10 macrocycle, two hydrophobic stoppers and two recognition sites. Two are degenerate and contain **a** two PmI units (**26**) or **b** two NpI units (**27**). **c** The third is a nondegenerate [2]rotaxane containing one PmI and one NpI unit (**28**)

The first dynamic process observed was shuttling of the macrocyclic component between two identical recognition sites – either PmI or NpI – in the degenerate [2]rotaxanes **26** and **27**, respectively. At low temperature (202 K) in $CDCl_3$, shuttling in **26** is slow on the ^1H NMR timescale and the two halves of the dumbbell component give rise to different sets of signals in the spectrum (Fig. 44c). A signal for H_{Pm} of the free PmI unit was observed at 8.32 ppm, but the signal corresponding to the encircled PmI unit is obscured in the region 6.8–7.2 ppm. As the temperature is increased to 266 K, the two signals are observed to coalesce (Fig. 44b) at 7.62 ppm, and ultimately sharpen up (Fig. 44a) into a single peak at 332 K. Partial line shape analysis of the coalescence of these two signals over a range of temperatures provided kinetic data for shuttling in **26**. The $\Delta G^{\ddagger}$ values range from 10.7 to 11.4 kcal mol^{-1} and are summarized in Table X.

Similar observations were made for the other degenerate rotaxane, **27**, containing two NpI units. The ^1H NMR spectrum (Fig. 44f) at low temperature (202 K) revealed three signals corresponding to H_{Np}. The signal at 8.80 ppm correlates with that for a free NpI unit. Two other broad signals were observed at 8.09 and 8.20 ppm, which were assigned to an encircled

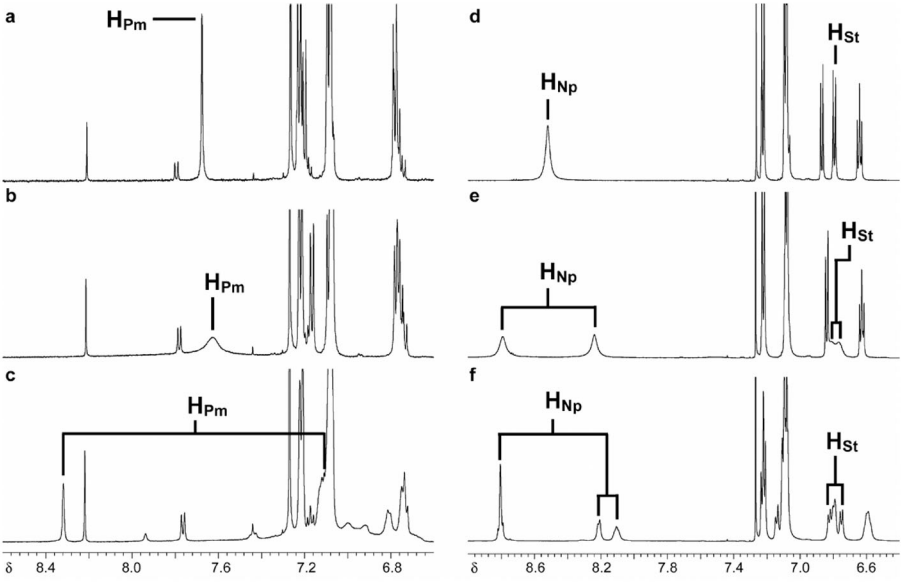

FIG. 44
Partial 600 MHz ^1H NMR spectra recorded in $CDCl_3$ of **26** at **a** 332 K, **b** 266 K, **c** 202 K and **27** at **d** 332 K, **e** 277 K **f** 202 K. See Fig. 43 for structural assignments

NpI unit. It was also possible in the case of **27** to observe (Table XI) the presence of two sets of signals for several of the protons in the hydrophobic stoppers. For example, the H_{St} protons appear as two doublets at 6.74 and 6.82 ppm – one for the stopper near the encircled NpI unit and one for the far off one. As the temperature is increased, both of these sets of signals are observed to broaden (Fig. 44e) and finally they appear (Fig. 44d) as averaged signals at high temperature. Partial line shape analysis of these signals

TABLE X
Kinetic and thermodynamic data for shuttling of **26** and **27** in $CDCl_3$

[2]Rotaxane **26**			[2]Rotaxane **27**		
T, K [a]	k_{ex}, s^{-1} [b]	$\Delta G^{\ddagger}$, kcal mol^{-1} [c]	T, K [a]	k_{ex}, s^{-1} [d]	$\Delta G^{\ddagger}$, kcal mol^{-1} [c]
226	45	11.4	266	10	14.3
239	300	11.2	277	60	13.9
248	1050	11.0	294	300	13.9
277	14500	10.9	305	1000	13.7
294	50000	10.9	277	60	13.9
305	140000	10.7	294	350	13.8
			305	1000	13.7
			319	4000	13.5
			332	13000	13.3

[a] Calibrated using neat MeOH sample; [b] measured using the partial line shape analysis method on the signals for H_{Pm}; [c] ±0.1; [d] measured using the partial line shape analysis method on the signals for H_{St}.

TABLE XI
Selected chemical shift values for the degenerate [2]rotaxanes **26** and **27** in $CDCl_3$

Rotaxane	Assigment [a]	Low temperature δ [b]	High temperature δ [c]
26	H_{Pm}	8.32/(6.8–7.2)	7.62
	H_{Np}	8.80/(8.09/8.20)	8.52
	H_{St}	6.82/6.74	6.80
27	H_{iPr}	2.86/2.84	2.88
	H_{tBu}	1.26/1.25	1.31
	H_{Me}	1.19/1.20	1.25

[a] See Fig. 43 for structural assignments; [b] 202 K; [c] 322 K.

provided the data summarized in Table X. For the NpI-containing [2]rotaxane, the $\Delta G^{\ddagger}$ values for shuttling range from 13.3 to 14.3 kcal mol^{-1}.

A comparison of the $\Delta G^{\ddagger}$ values for shuttling in **26** and **27** reveals a higher barrier to shuttling by ~3 kcal mol^{-1} for the degenerate NpI-containing [2]rotaxane. This result is not totally unexpected based on ground state effects. The free energy of binding (ΔG^{o}) for 1/5DNP38C10 with a PmI and NpI unit is, respectively, –1.8 and –2.8 kcal mol^{-1}. Thus, the more strongly bound NpI unit pays a larger penalty during translation of the ring component. The significantly greater difference in $\Delta G^{\ddagger}$ values compared with the ΔG^{o} ones, however, suggests that there is possibly more than a ground-state effect at work. Other possibilities include some form of secondary interaction between the free recognition site and the ring component, e.g., formation of a folded superstructure[55]. The larger NpI unit may also present a greater steric barrier to escape of the 1/5DNP38C10 macrocycle relative to that of the smaller PmI unit.

Further information was extracted from the shuttling data by creating Eyring plots (Fig. 45) based on the data presented in Table X. Linear fits of the data were used to obtain the $\Delta H^{\ddagger}$ and $\Delta S^{\ddagger}$ values (Table XII) from the slope and intercept, respectively. Rotaxane **27** has a significantly larger enthalpic contribution ($\Delta H^{\ddagger}$) to the free energy of activation for shuttling relative to **26** (17.8 and 13.0 kcal mol^{-1}, respectively), a difference which is presumably caused by the stronger interactions between 1/5DNP38C10 and the NpI unit as a result of its larger π-surface. It is also interesting to note that both rotaxanes have a positive entropy of activation ($\Delta S^{\ddagger}$), indicating an increase in entropy for the transition state. This observation can be explained in terms of an increase in the conformational freedom for the

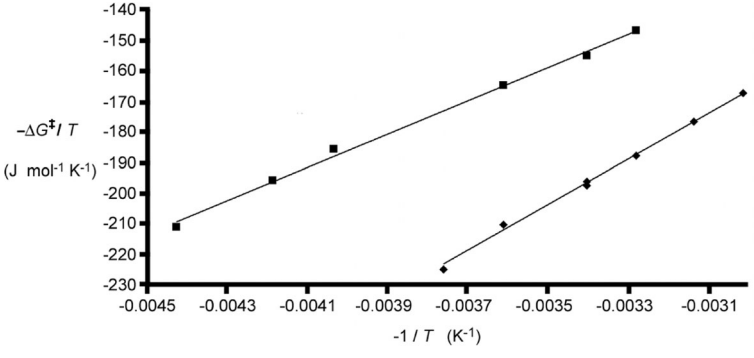

FIG. 45
Eyring plots for **26** (■) and **27** (◆) based on the data in Table X

1/5DNP38C10 ring after it is removed from the recognition site. The positive $\Delta S^{\ddagger}$ for these neutral rotaxanes is in contrast with the data (Table VII) for shuttling in DNP/DNP-containing charged [2]rotaxanes, where there is an entropic penalty to pay for translation of the ring component.

Another dynamic process was observed in the two rotaxanes – i.e., **27** and **28** – containing NpI units. As the temperature is lowered, the ^{1}H NMR signals for the H_{Np} protons of an encircled NpI unit in these two rotaxanes were observed (Fig. 46a and 46b) to change from broad singlets into two sets of broad signals. This phenomenon arises from the influence of the local C_{2v} symmetry (Fig. 46c) of the 1/5DNP38C10 encircling these NpI units. Even in the absence of the ring component, the two substituted ends of the NpI unit are nonequivalent and thus one would expect to see two signals

TABLE XII
Activation parameters for shuttling in the [2]rotaxanes **26** and **27** in $CDCl_3$

Compound	$\Delta H^{\ddagger}$, kcal mol^{-1}	$\Delta S^{\ddagger}$, cal mol^{-1} K^{-1}
26	13.0	7.6
27	17.8	13.6

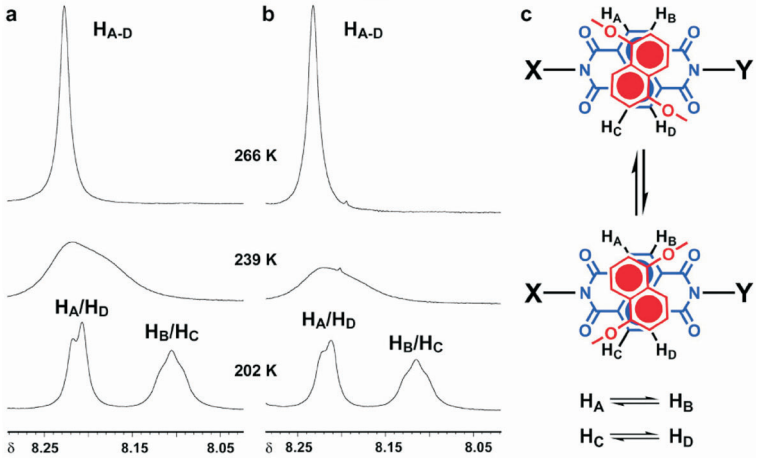

FIG. 46
Partial 600 MHz ^{1}H NMR spectra recorded in $CDCl_3$ of **a** **27** and **b** **28**. **c** The asymmetry induced by the presence of the 1/5DNP38C10 macrocycle around the NpI unit is shown. A dynamic process occurs that exchanges H_A with H_B and H_C with H_D. See text for details

for the H_{Np} protons. It is evident, however, from the signal for the free NpI unit, which appears as a broad singlet, that this separation is too small to be resolved on the basis of constitutional asymmetry alone. When the 1/5DNP38C10 ring encircles the NpI unit, it imposes its own local symmetry (C_{2v}) upon the four H_{Np} protons, resulting in all four (H_A, H_B, H_C and H_D) being (Fig. 46c) heterotopic. In contrast with the constitutional asymmetry arising from the substitution of the NpI unit, the further two-fold reduction in symmetry introduced by the crown ether results in a larger separation (~0.11 ppm) between the two sets of signals which can be more easily observed. As the temperature is raised, these multiple signals coalesce into a single broad peak, suggesting that a dynamic process is occurring that increases the effective symmetry at the NpI unit.

There are at least two dynamic processes that can account for the apparent increase in symmetry around the NpI unit (Fig. 46c). The first involves flipping of the 1,5-dioxynaphthalene (DNP) units of the crown ether by rotation about the axis that passes through the two oxygen atoms. This process has been observed[81] in other donor–acceptor [2]catenanes and [2]rotaxanes previously. In order to accomplish the degenerate exchange observed, both DNP units would have to undergo this reorientation. An alternative process that would also accomplish the degenerate exchange of the protons on the NpI unit is pirouetting[30] of the crown ether about the dumbbell component. This process would involve breaking the interactions between the 1/5DNP38C10 and the NpI unit, followed by mutual exchange of the DNP units on either side of the NpI unit. Because the first process requires two independent exchanges to occur – and would also pass through a nondegenerate intermediate that was not observed – the pirouetting process seems to be the more likely one of the two.

An estimate of the barrier for this symmetry-averaging process can be made by using the coalescence method[82] and a summary of the resulting data is presented in Table XIII. The $\Delta G_c^{\ddagger}$ values for both [2]rotaxanes are

TABLE XIII
Kinetic and thermodynamic data for reorientation of the DNP units about the NpI unit in $CDCl_3$

Rotaxane	$\Delta\nu$, s^{-1}	k_{ex}, s^{-1}	T_c, K [a]	$\Delta G_c^{\ddagger}$, kcal mol^{-1} [b]
27	66	147	239	11.5
28	63	140	239	11.5

[a] Calibrated using neat MeOH sample; [b] ±0.1

the same within experimental error, i.e., 11.5 kcal mol^{-1}. The fact that the kinetic and thermodynamic parameters for this process are virtually identical in the two rotaxanes studied suggests that only the encircled NpI unit and the 1/5DNP38C10 macrocycle are involved, and the identity of the second recognition site has no effect on the rate with which this process occurs.

4.3. Switching

At least two possible mechanisms exist (Fig. 41) for the switching of a bistable PmI/NpI-containing [2]rotaxane. Observation of the first mechanism – namely, electrochemically-induced switching – by NMR spectroscopy was precluded by the paramagnetic nature of the reduced NpI unit. Cyclic voltammetry and differential pulse voltammetry have been used[77] to investigate this mechanism. These two techniques have revealed that the crown ether moves to the PmI unit upon disruption of its interactions with the NpI unit following reduction. The second mechanism – namely, chemical switching using Li^+ ions – was observable[83] using ^{1}H NMR spectroscopy and the details of the switching cycle will now be reported and discussed here.

The first step in investigating the switching cycle for the bistable [2]rotaxane **28** was to determine the nature of the co-conformer(s) present in solution under equilibrium conditions. Thus, a series of ^{1}H NMR spectra (Fig. 47) were recorded at low temperature (202 K) for the three rotaxanes **26**–**28**. At this temperature, shuttling in the degenerate rotaxanes is slow on the ^{1}H NMR timescale and signals corresponding to protons for the free and encircled recognition sites can be observed. Comparing these signals with those observed for the nondegenerate rotaxane **28**, the co-conformer present in solution can be assigned unequivocally to the one where the crown ether encircles the NpI unit. Specifically, the signal observed in the spectrum of **28** (Fig. 47b) at 8.30 ppm correlates with the one at 8.32 ppm in the spectrum of **26** (Fig. 47a) for a free PmI unit. Likewise, the two broad signals at 8.11 and 8.21 ppm for **28** match those at 8.09 and 8.20 ppm in the spectrum of **27** (Fig. 47c) as signals which were assigned to an encircled NpI unit. No signals were observed in the spectrum of **28** which correspond to the presence of an encircled PmI unit or a free NpI unit. These results indicate that, within the limits of detection by ^{1}H NMR spectroscopy at least, only a single co-conformer is present in a solution of **28** – namely, the one in which the crown ether encircles the NpI unit.

The major co-conformer observed in solution for **28** was the expected one based on previous results[75] which contrasted the propensity for

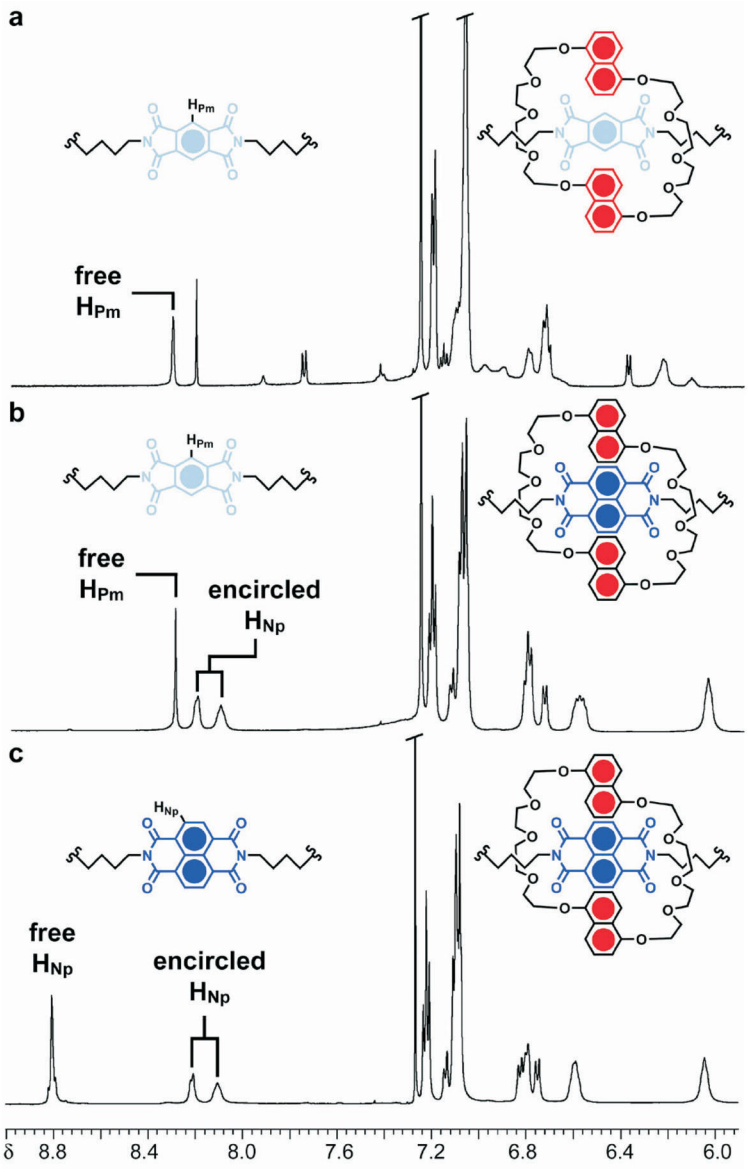

FIG. 47

Partial 600 MHz ^{1}H NMR spectra recorded in $CDCl_3$ at 202 K of **a 26**, **b 28** and **c 27**. The insets show partial structures for the three [2]rotaxanes. A comparison of the signals corresponding to the protons on the NpI and PmI units allows the translational isomer present in **28** to be assigned to the one with the ring encircling the NpI unit

pseudorotaxane formation by similar compounds. The equilibrium for 1/5DNP38C10 binding to either PmI or NpI units is highly biased towards the NpI unit. It is expected, however, that, upon addition of two equivalents or more of Li^+ ions, this equilibrium situation (Fig. 48) will be reversed totally. This reversal arises as a result of formation of a co-complex between the 1/5DNP38C10, a PmI unit and two Li^+ ions. Formation of this co-complex is more favorable than the corresponding one involving an NpI unit. It was also predicted that it should be possible to restore the original equilibrium situation by removing the Li^+ ions. One way of accomplishing this goal would be to add a sequestering agent, such as [12]crown-4, to bind strongly[84] with all of the Li^+ ions. With these ideas and procedures in mind, the chemical switching of **28** was attempted.

The ^1H NMR spectrum (Fig. 49a) for **28** was recorded in CD_2Cl_2 at room temperature. The signals corresponding to an encircled NpI unit and free PmI unit appear at 8.19 and 8.24 ppm, respectively. A solution containing an excess of $LiClO_4$ dissolved in ~200 µl of CD_3COCD_3 was then added, followed by vigorous shaking to ensure complete mixing. After addition of the Li^+ ion source, the ^1H NMR spectrum (Fig. 49b) was recorded again. Several changes were observed in the new spectrum, most noticeably the disappearance of the signals corresponding to the encircled NpI unit and free PmI unit. A pair of doublets appears at 8.62 and 8.66 ppm, and these two signals were assigned to the H_{Np} protons of a free NpI unit in the **28**·$2Li^+$ species. Unfortunately, the signals for the encircled PmI unit are obscured in the region of 6.8–7.2 ppm. It is interesting to note that the presence of the Li^+

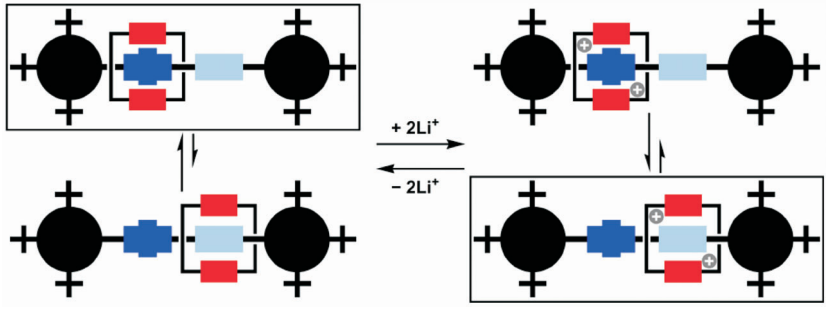

FIG. 48
A schematic representation of the chemical switching of **28** is shown. The neutral bistable [2]rotaxane exists in equilibrium between two co-conformers, where the one with the ring encircling the NpI unit is highly preferred. Upon addition of two equivalents of Li^+ ions, a new equilibrium is established that greatly favors the co-conformer where the ring encircles the PmI unit, which forms a co-complex with two Li^+ ions

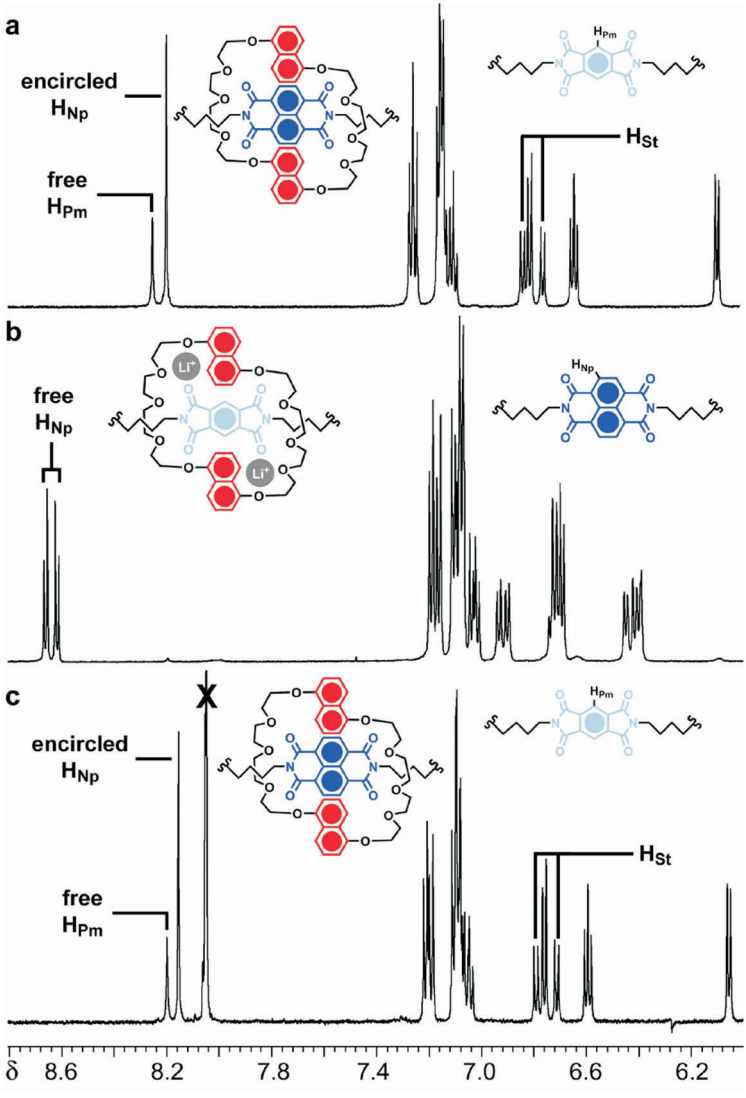

FIG. 49

Partial 600 MHz ^{1}H NMR spectra recorded in CD_2Cl_2 at room temperature of **28 a** before and **b** after addition of excess of $LiClO_4$ (200 μl, CD_3COCD_3 solution). The insets show the partial structures of the [2]rotaxanes indicating switching has occurred after addition of the Li^+ ions. **c** Addition of excess of [12]crown-4 sequesters all of the Li^+ ions and returns the rotaxane to its original state

ions in the complex with the rotaxane enhances the constitutional heterotopicity of the two ends of the NpI unit in **28**·2Li$^+$, resulting in the appearance of the H_{Np} protons as two signals, as opposed to one broad signal for the free NpI unit in **27**.

The bistable rotaxane **28** was returned to its original state by addition of an excess of [12]crown-4 (12C4) to the solution of **28**·2Li$^+$. After the Li$^+$ ions had been sequestered by 12C4, the ^{1}H NMR spectrum (Fig. 49c) was recorded again. A comparison of the spectra before (Fig. 49a) addition of the Li$^+$ ions and after (Fig. 49c) their removal shows that they are nearly identical, with a slight shift relative to the CH_2Cl_2 solvent peak in the latter presumably as a result of the change in solvent polarity. The signal at 8.05 ppm arises from an impurity present in the commercial sample of 12C4. At all three stages of the switching cycle – (i) before addition of Li$^+$, (ii) after its addition and (iii) after its removal with 12C4 – only a single co-conformer was observed for **28**. No indication of irreversibility or degradation was observed, at least within the limits of detection afforded by ^{1}H NMR spectroscopy.

4.4. Conclusions

Counterions associated with charged mechanically-interlocked molecules provide an additional degree of complexity and, in some cases, control. It is sometimes desirable, however, for the sake of simplicity or function to remove external counterions from the scene. Thus, a neutral recognition system has been investigated for its potential use in the construction of molecular switches and machines. The dynamic processes occurring in a series of model [2]rotaxanes were investigated using VT-NMR spectroscopy. In comparison to previously studied charged TTF/DNP-containing rotaxanes, the barriers to shuttling in these neutral systems are substantially lower (by ~4–5 kcal mol^{-1}), suggesting switching and relaxation of the metastable state back to the ground state would occur more rapidly for the neutral rotaxanes when they are incorporated into MSTJs. Access to this data will be useful in understanding the performance of related molecules in a device setting, as well as in predicting the effects of structural modifications on the molecular properties.

The switching of a neutral bistable [2]rotaxane has also been reported in this Section. Although it was not possible to investigate electrochemically controlled switching using ^{1}H NMR spectroscopy, an alternative switching mechanism using chemical control was established. The addition of two equivalents of Li$^+$ ions to a solution of a PmI/NpI-containing rotaxane in-

duced shuttling of the ring component from the NpI unit to the PmI one, a phenomenon which was reversed upon addition of [12]crown-4 to sequester the Li^+ ions. The existence of this chemically controlled process, while probably not applicable in a device setting, bodes well for the potential use of these systems as the molecular component of novel sensors. The demonstration of two orthogonal means – namely, chemical and electrochemical – of accomplishing the same mechanical motion in a single bistable [2]rotaxane may also provide opportunities for creating more flexible hybrid artificial molecular machines in the future.

5. DYNAMICS AND SWITCHING IN SELF-COMPLEXES AND PRETZELANES

5.1. Background

The defining feature of [2]catenanes and [2]rotaxanes is that their two components are connected only by a mechanical bond, i.e., there are no covalent bonds joining them. If a covalent connection is made between their two components, then a pretzelane[85] and a self-complex[86] result (Fig. 50) from a [2]catenane and a [2]rotaxane, respectively. These hybrid compounds, which nonetheless each still contain a mechanical bond, can be considered as analogues of the corresponding mechanically-interlocked compounds. The covalent tether, connecting what were originally two components, provides an additional means of control since it will inevitably influence the dynamic processes and stereochemical properties of these exotic compounds.

Several self-complexes (**29**·4PF_6–**31**·4PF_6 in Fig. 51) have been synthesized[87] based on the donor–acceptor recognition motif, involving the electron-poor tetracationic cyclophane $CBPQT^{4+}$ and electron-rich π-sys-

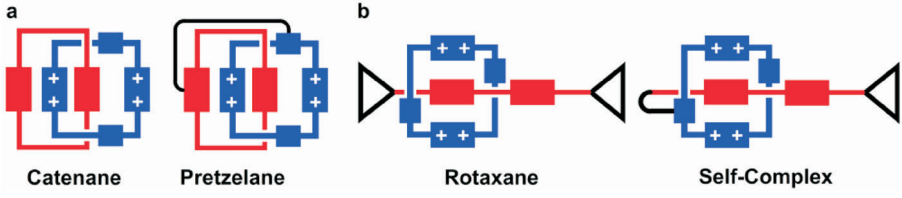

FIG. 50
Schematic representations of **a** a [2]catenane and pretzelane and **b** a [2]rotaxane and a self-complex. These species are related by the presence or absence of a covalent tether between the two components

tems – e.g., hydroquinone (HQ), 1,5-dioxynaphthalene (DNP) and tetrathiafulvalene (TTF). The covalent tether was introduced by fusion of a five-membered cyclic diimide linkage to the cyclophane, such that some of the symmetry problems encountered in previous research[88] were alleviated, simplifying the spectroscopy. Variable temperature ^{1}H NMR and UV/VIS experiments were used[87] to investigate the thermochromic properties of the HQ and DNP-containing self-complexes that arise as a result of decomplexation of the arm component from the cyclophane at higher temperatures. For **31**·4PF$_6$, this decomplexation could be induced either by chemical oxidation – using tris(*p*-bromophenyl)amminium hexachloroantimonate – or by electrochemical oxidation – at +0.53 and +0.73 V versus SCE – of the TTF unit to its dication, as observed by ^{1}H NMR spectroscopy and cyclic voltammetry, respectively. Here, some dynamic processes occurring in **29**·4PF$_6$ and also the chemical switching of a TTF/DNP-containing self-complex will be discussed.

Some pretzelanes based on the same recognition motif as these self-complexes have also been reported[89]. In the recent work, a series of DNP-containing pretzelanes were synthesized and investigated to determine the effect of tether length on formation of the pretzelane as opposed to the formation of a cyclic bis[2]catenane[90]. It was found that shorter tether lengths promoted formation of the cyclic bis[2]catenane structure, while longer and more flexible tethers led to formation of pretzelanes. The crystal structure of one (**32**·4PF$_6$) of these pretzelanes is shown in Fig. 52. The intramolecular interactions present in the solid-state for this pretzelane are similar to those described previously for related [2]catenanes (see Section 2) and

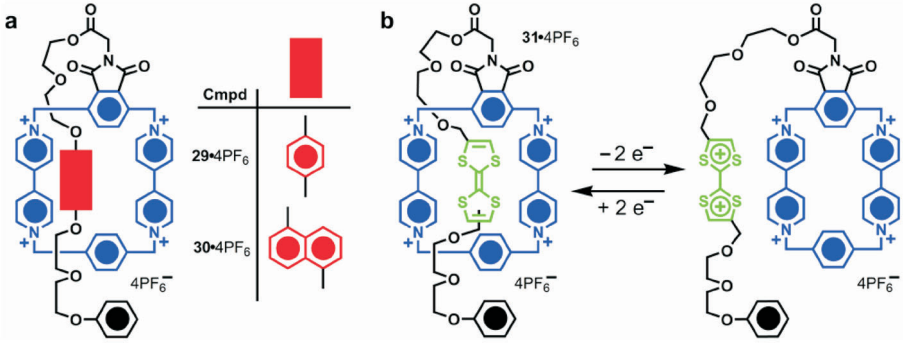

FIG. 51

a Structural formula for the self-complexes **29**·4PF$_6$ and **30**·4PF$_6$. **b** The structural formula for **31**·4PF$_6$ and its oxidatively-induced decomplexation

consist of [C–H···O], [C–H···π] and [π···π] interactions. In this Section, the dynamics and stereochemistry of these and related pretzelanes will be examined.

5.2. Dynamics

The dynamic processes occurring in donor–acceptor self-complexes are generally the same ones as those that occur in [2]rotaxanes – namely, aromatic ring rotations and exchange of the recognition sites between encircled and free environments. The presence of the tether in these self-complexes, however, introduces a multitude of perturbations into these dynamic processes. At a fundamental level, the symmetry properties are altered: at a quantitative level, the barrier heights associated with the dynamic processes are influenced. For example, the C_2 axis that bisects the bipyridinium units in the free tetracationic cyclophane is no longer present in the substituted one. As a result, the self-complexing compounds have two pairs of nonequivalent pyridinium rings. These two sets of rings will participate in different exchange processes (II and III in Fig. 53) with distinct kinetic and thermodynamic parameters. In order to investigate the dynamic processes occurring in self-complexes and determine what, if any, effect the tether has on them, a variable temperature ^{1}H NMR study was carried out[63] on **29**·4PF$_6$.

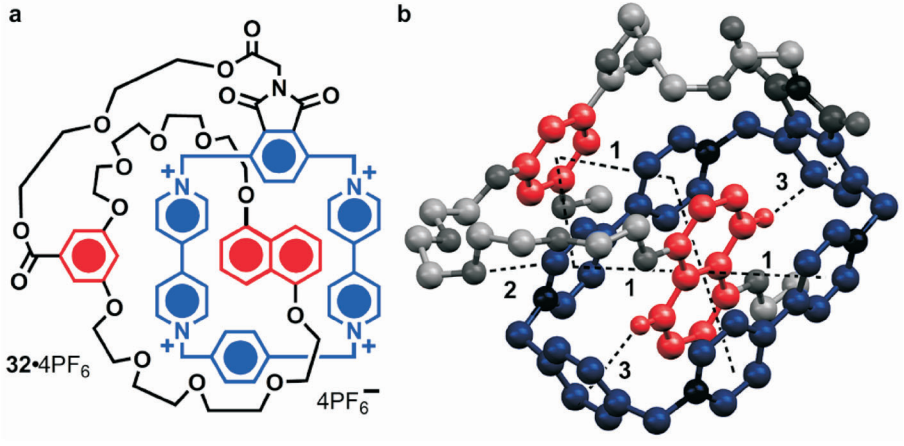

FIG. 52

a Structural formula for the donor–acceptor pretzelane **32**·4PF$_6$. **b** The X-ray crystal structure of **32**·4PF$_6$ is shown. Important intramolecular interactions are highlighted, namely (1) [π···π], (2) [C–H···O] and (3) [C–H···π]

The ^{1}H NMR spectrum (Fig. 54) of **29**·4PF$_6$ was recorded in CD_3COCD_3 at 207 K. At this temperature, all of the processes (i.e., I, II and III) shown in Fig. 53 are slow on the ^{1}H NMR timescale, as confirmed by the observation of four signals for the H_α protons – at 9.07, 9.40, 9.51 and 9.63 ppm – and two signals for the H_a/H_b protons – at 8.38 and 8.58 ppm. Although when the temperature was increased all the signals began to broaden as a result of exchange processes, the observation of coalescence behavior was precluded by decomplexation occurring at increased temperatures. Thus, in order to determine the kinetic and thermodynamic data, spin saturation transfer (SST) experiments were performed on exchanging proton pairs in the slow

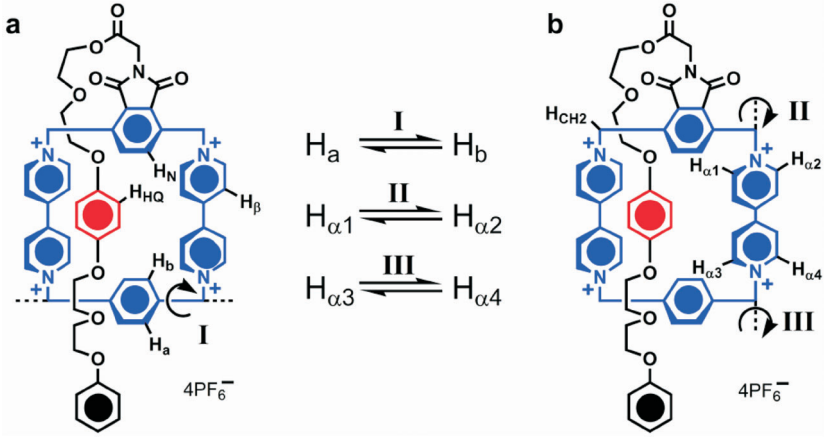

FIG. 53
Some of the dynamic processes occurring in **29**·4PF$_6$ are shown, namely **a** phenylene rotation (I) and **b** pyridinium rotation (II and III)

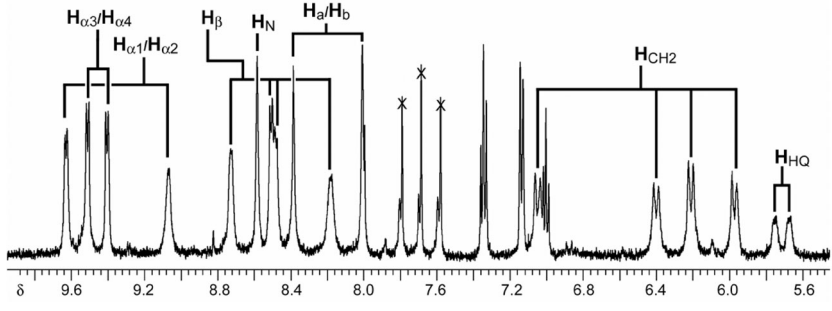

FIG. 54
The 500 MHz ^{1}H NMR spectrum recorded in CD_3COCD_3 at 207 K of **29**·4PF$_6$. See Fig. 53 for proton assignments

exchange regime. The exchange partners for the H_α protons were determined by irradiating one signal and observing the other three to determine which one showed a decreased intensity. As a result, the exchanging pairs were identified as 9.07 and 9.63 ppm, and 9.40 and 9.51 ppm. Assignment of these pairs, however, to $H_{\alpha1}/H_{\alpha2}$ and $H_{\alpha3}/H_{\alpha4}$ was not possible using this data by itself.

In order to assign the pairs of H_α proton signals to either the pair of pyridinium rings close to the benzodiimide or the pair of further away ones, a series of 1D-ROESY experiments was performed. In the first experiment, the H_α signal at 9.63 ppm was irradiated and the spectrum recorded (Fig. 55a). The signals with positive intensity – at 8.72, 8.57 and 6.39 ppm – indicate a close spatial relationship between their corresponding protons – H_β, H_N and H_{CH2}, respectively – and the proton irradiated. As a result, the exchanging pair of H_α protons at 9.07/9.63 ppm can be assigned to the pyridinium rings close to the benzodiimide. The analogous experiment was performed by irradiating the exchanging pair of H_α protons at 9.40/9.51 ppm. From this spectrum (Fig. 55b), the signals at 8.49, 8.38, 8.01 and

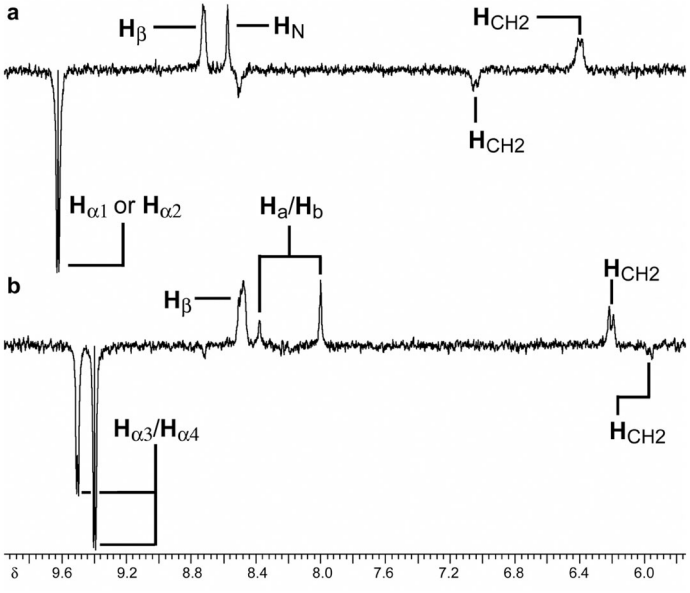

FIG. 55

The 1D-ROESY spectra recorded in CD_3COCD_3 at 207 K of **29**·4PF_6 with irradiation of the H_α protons at **a** 9.63 and **b** 9.40/9.51 ppm. Signals with a positive intensity indicate a close spatial relationship with the irradiated proton

6.21 ppm were assigned as H_β, H_a, H_b and H_{CH2}, respectively. These data allow the pyridinium rings whose H_α protons resonate at 9.40/9.51 ppm to be assigned as the ones closer to the *p*-xylylene ring.

A summary of the kinetic and thermodynamic data for the aromatic ring rotations (processes I–III in Fig. 53) in **29**·4PF_6 is given in Table XIV. From these data it is clear that the barriers for all three processes are very similar (~13–14 kcal mol^{-1}) and lie within roughly 1 kcal mol^{-1} of one another. The similarity of these values to the barrier for shuttling, $\Delta G^\ddagger$, in a degenerate HQ-containing [2]rotaxane[19] of ~13 kcal mol^{-1} in CD_3COCD_3 suggests that the HQ unit may move wholly or partially out of the cavity of the tetracationic cyclophane to allow the ring rotations to occur. It is also interesting to note that the barrier for the rotation of the pyridinium rings adjacent to the benzodiimide is higher ($\Delta G^\ddagger$ = 13.8 kcal mol^{-1} at 217 K) than for the far ones ($\Delta G^\ddagger$ = 13.0 kcal mol^{-1} at 217 K), suggesting that perhaps the tethered glycol chain interferes with the rotation more than the free glycol chain.

From the analyses of the self-complexes, it is evident that the tether can influence the dynamic processes occurring in these compounds. In order to examine these influences further, a variable temperature ^1H NMR investiga-

TABLE XIV
Kinetic and thermodynamic data for **29**·4PF_6 in CD_3COCD_3

Process	T, K [a]	k_{ex}, s^{-1} [b]	$\Delta G^\ddagger$, kcal mol^{-1} [c]
Phenylene rotation (I) [d]	239	1.5	13.7
	228	0.6	13.5
	217	0.2	13.3
	207	0.1	12.9
Pyridinium rotation (II) [e]	228	0.8	13.3
	217	0.4	13.0
Pyridinium rotation (III) [f]	249	1.1	14.4
	239	0.5	14.2
	228	0.2	14.1
	217	0.1	13.8

[a] Calibrated using neat MeOH sample; [b] measured using spin saturation transfer method (ref.[37]); [c] ±0.1 kcal mol^{-1}; [d] exchange observed between the signals at 8.38 and 8.58 ppm, [e] at 9.40 and 9.51 ppm, [f] at 9.07 and 9.63 ppm.

tion was also carried out[89] on a donor–acceptor pretzelane composed of an electron-poor tetracationic cyclophane connected by a glycol tether to an electron-rich crown ether containing a 1,5-dioxynaphthalene unit (**32**·$4PF_6$). We have already come to appreciate in Section 2 that [2]catenanes have some unique and interesting stereochemistry associated with their (co-)conformations and dynamic processes. Pretzelanes, being close relatives of [2]catenanes, are thus also expected to exhibit a degree of stereochemical complexity.

Introduction of the benzodiimide function as an anchor site for the covalent tether creates an additional stereochemical element (Fig. 57a) for pretzelanes based on this structural motif. This chirality is maintained even in the absence of the tether, i.e., the two co-conformations of the [2]catenane shown schematically are enantiomers of one another. We have chosen to identify this chirality as helical, in analogy with, but not strictly comparable to, the helical chirality described previously for donor–acceptor [2]catenanes with a different symmetry (see Section 2). Priority rules[89] for determining the appropriate descriptor – either (*P*) or (*M*) – have also been established, but will not be discussed in any detail here.

The pretzelane **32**·$4PF_6$ (Fig. 56) possesses two stereochemical elements – the helical chirality as described in Fig. 57a and the planar chirality (Fig. 57b) arising from the DNP unit. Thus, the pretzelane can exist (Fig. 58) as two enantiomeric pairs of diastereoisomers, (*pR*)-(*P*)/(*pS*)-(*M*) or (*pS*)-(*P*)/(*pR*)-(*M*). Both in solution and the solid-state (Fig. 52b), however,

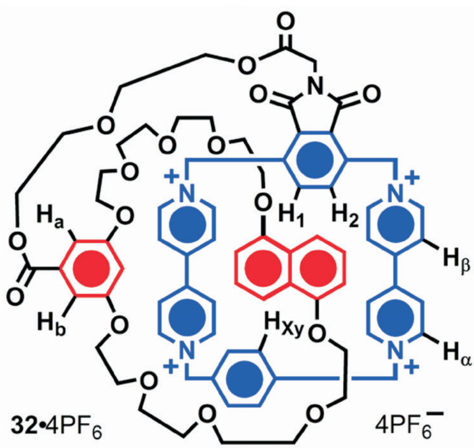

FIG. 56
Structural formula for the donor–acceptor pretzelane **32**·$4PF_6$

only one pair, namely (*pR*)-(*P*)/(*pS*)-(*M*), was observed[89] as the more favored one. As the minor diastereoisomer was present in far too small of an amount to be observed, it was not possible to investigate the dynamic interconversion of these stereoisomers directly. Resolution of the two enantiomeric pairs of the diastereoisomers present in solution, however, has been reported[89] using a chiral shift reagent.

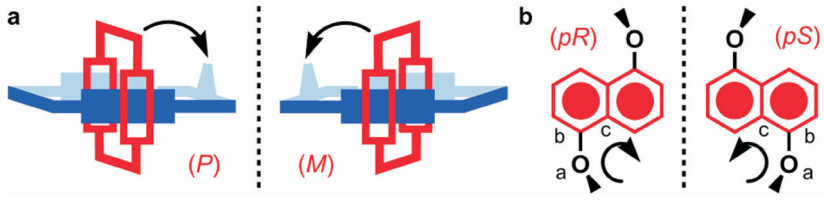

FIG. 57
Schematic representations of the two stereochemical elements present in **32**·4PF$_6$ – namely, **a** helical chirality and **b** planar chirality. See ref.[89] for the rules on assigning stereochemical descriptors for a

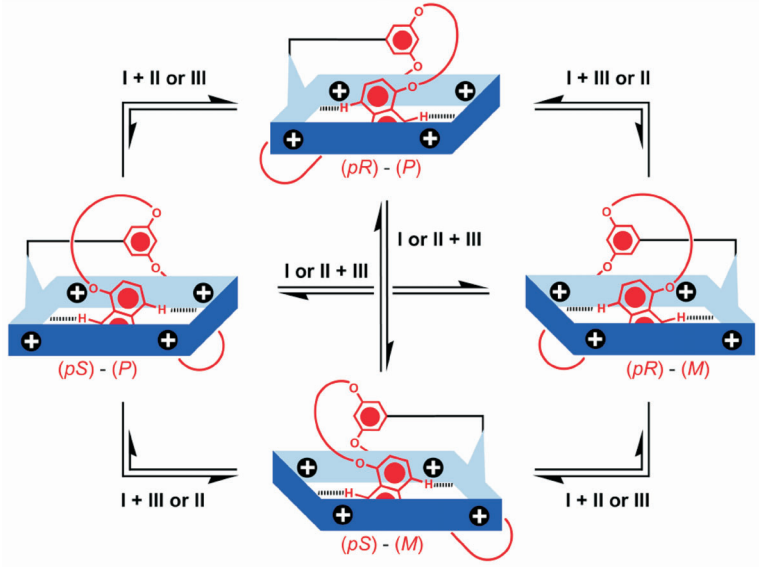

FIG. 58
Schematic representations of the four different stereoisomers of the pretzelane **32**·4PF$_6$ and the dynamic processes that interconvert them. See Fig. 59 for processes **I** and **II**. Process **III** is flipping of the DNP unit about its substitution axis

Two of the potential dynamic processes responsible for inverting the stereochemical elements of **32**·4PF_6 are shown in Fig. 59. Process I involves a "pirouetting" of the crown ether around the outside of the tetracationic cyclophane. The result of this process is to invert both the elements of helical and planar chirality. An alternative process – process II – which involves flipping of the benzodiimide unit only inverts the helical chirality, leaving the planar chirality of the DNP unit intact. A third process – process III – which is not shown is flipping of the DNP unit about its substitution axis, leading to inversion of its planar chirality. In order for degenerate exchange to occur, the process must interconvert between the two enantiomeric forms of the major diastereoisomer observed. Thus, either process I or a combination of processes II and III could be responsible for degenerate exchange of the protons in **32**·4PF_6, in addition to the processes such as aromatic ring rotations that have no stereochemical implications. In order to investigate if these processes occur, and their relative rates, pairs of proton signals must be identified that are only exchanged by one or other of these two combinations of processes.

The ^{1}H NMR spectrum of **32**·4PF_6 was recorded (Fig. 60b) in CD_3SOCD_3 at 301 K, conditions at which all the exchange processes become slow on the ^{1}H NMR timescale. Hence, each of the aromatic protons gives rise to its own signal – eight each for H_α and H_β, four for H_{Xy}, and two each for H_1/H_2 and H_a/H_b – indicating that they are all heterotopic. As the temperature is increased, the signals begin to broaden and coalesce into a small number of averaged signals. In particular, the ^{1}H NMR spectrum at 378 K shows (Fig. 60a) a single peak each for H_1/H_2 and H_a/H_b. A close examination of the structure of **32**·4PF_6 reveals that H_1/H_2 can only be exchanged via process I, while H_a and H_b only exchange by using processes II and III. These processes could be observed by a combination of spin saturation transfer and partial line-shape analysis performed on the relevant signals.

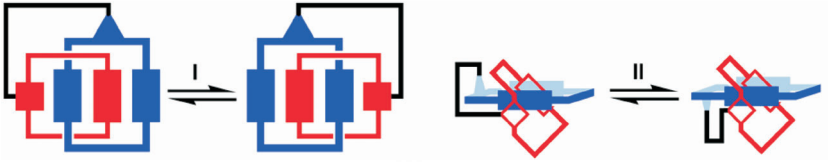

FIG. 59
Schematic representations of two possible dynamic processes for the pretzelane **32**·4PF_6, pirouetting of the crown ether component (**I**) and flipping of the benzodiimide unit (**II**)

The resulting data for **32**·4PF_6 is summarized in Table XV. The first thing to note is the nearly identical barriers – $\Delta G^{\ddagger}$ = 17.6 and 17.5 kcal mol^{-1} at 301 K for processes I and II, respectively – for the "two" processes, suggesting that, in fact, there is one common process or intermediate responsible for the observed interconversion of the protons. The most likely intermedi-

TABLE XV
Kinetic and thermodynamic data for **32**·4PF_6 in CD_3SOCD_3

Process I [c]			Process II [d]		
T, K [a]	k_{ex}, s^{-1}	$\Delta G^{\ddagger}$, kcal mol^{-1} [b]	*T*, K [a]	k_{ex}, s^{-1}	$\Delta G^{\ddagger}$, kcal mol^{-1} [b]
301	1.0 [e]	17.6	301	1.2 [e]	17.5
314	6 [f]	17.3	314	8 [f]	17.1
338	85 [f]	16.9	338	80 [f]	16.9
355	550 [f]	16.5	355	500 [f]	16.5
378	2800 [f]	16.3	378	2500 [f]	16.4
392	10000 [f]	16.0	392	9000 [f]	16.1

[a] Calibrated using neat MeOH sample; [b] ±0.1 kcal mol^{-1}; [c] exchange observed between the signals for H_1/H_2, [d] for H_a/H_b. See Fig. 56. [e] Measured using spin saturation transfer method (ref.[37]); [f] measured using partial line shape analysis.

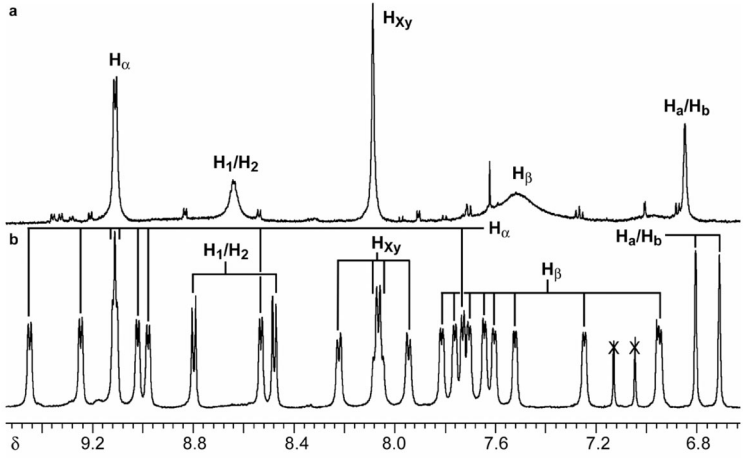

FIG. 60
The 600 MHz ^1H NMR spectra recorded in CD_3SOCD_3 of **32**·4PF_6 at **a** 378 K and **b** 301 K. See Fig. 56 for the structural assignments

ate is one where the DNP unit is removed from the cavity of the tetracationic cyclophane to allow the benzodiimide ring to rotate and/or the resorcinol ring to move around the outside of the cyclophane. This hypothesis is supported by the close correspondence of the barrier to that for circumrotation in a DNP-containing [2]catenane – namely, $\Delta G^{\ddagger} = 17.2$ kcal mol^{-1} (Table VIII) – where similar interactions are broken during the course of exchange. Further investigations will be necessary to determine the details of the dynamic stereochemistry properties of these pretzelanes.

5.3. Switching

A self-complexing compound presents the opportunity of being able to create a more compact molecular switch when compared with a bistable [2]rotaxane. In order to determine if tethering the components of such a rotaxane together covalently has any effect on the switching, a bistable TTF/DNP-containing self-complex **33**·4PF_6 (Fig. 61) was investigated[63]. This self-complexing compound is composed of a tetracationic cyclophane connected to the arm by a glycol tether. Two recognition sites – a TTF unit and a DNP one – are present in the arm component, which is terminated by a bulky aromatic ring to act as a stopper and prevent decomplexation. In the unperturbed state, the conformation where the TTF unit resides within the tetracationic cyclophane is expected to be the preferred one. Upon oxidation of the TTF unit to the TTF^{2+} dication, the preference should be for the DNP unit to reside exclusively within the cyclophane.

The ^{1}H NMR spectrum (Fig. 62a) of **33**·4PF_6 was recorded in CD_3COCD_3. As a result of the complex array of signals observed, it was not an easy matter to assign the spectrum. One reason for its complexity is the presence of

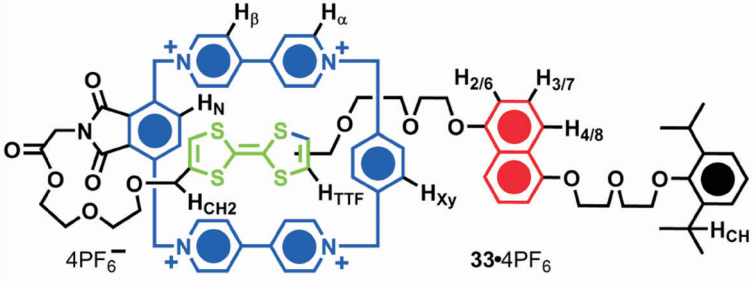

FIG. 61
Structural formula of the bistable TTF/DNP-containing self-complex **33**·4PF_6

cis and *trans* isomers associated with the TTF unit, leading to multiple conformations for the self-complex. Each of these isomers can exist in at least two different conformations, which arise because of the different possible orientations of the glycol chains relative to the benzodiimide. Thus, the unperturbed self-complex may exist in four or more conformations in different amounts, leading to the complicated spectrum observed. It is possible, however, to simplify this situation significantly by oxidizing the TTF unit and so remove the complexity caused by *cis*/*trans* isomerism.

A slight excess (2.0–2.5 equivalents) of the oxidant, tris(*p*-bromophenyl)-amminium hexafluoroantimonate, was added to a CD_3COCD_3 solution of **33**·4PF_6 and the ^{1}H NMR spectrum (Fig. 62b) was recorded. This spectrum, which was found to be greatly simplified with respect to the number of signals present in the starting spectrum (Fig. 62a), could be completely assigned. The two signals at 9.86 and 9.94 ppm were assigned to the H_{TTF} protons of the dication. Evidence for location of the DNP unit within the

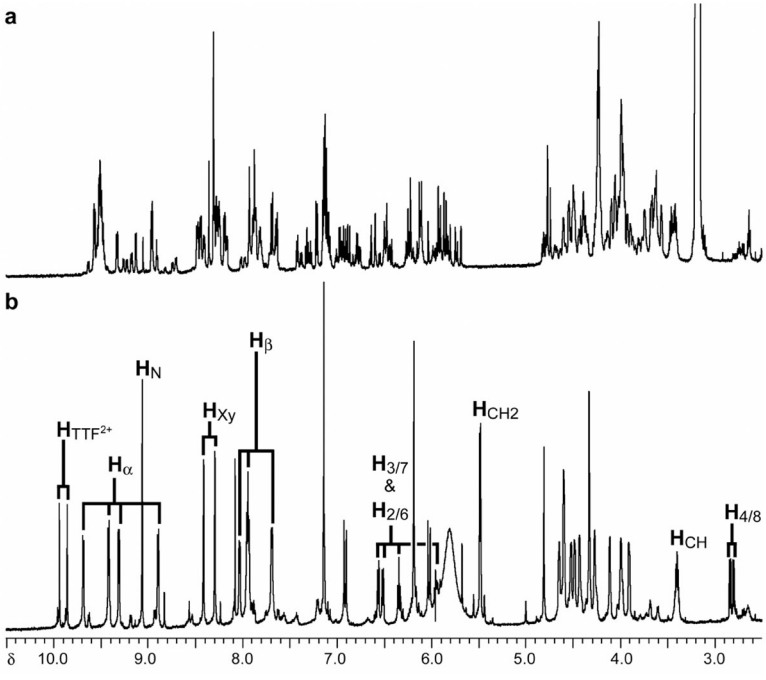

FIG. 62

The 600 MHz ^{1}H NMR spectrum recorded in CD_3COCD_3 at 273 K of **33**·4PF_6 **a** before and **b** after addition of 2.0–2.5 equivalents of the oxidant tris(*p*-bromophenyl)amminium hexafluoroantimonate

tetracationic cyclophane appears as signals at 2.80, 2.84, 5.95, 6.34, 6.51 and 6.56 ppm, corresponding to two signals each for $H_{4/8}$, $H_{3/7}$ and $H_{2/6}$, respectively. These values are not too dissimilar to those observed (Table IX) for bistable TTF/DNP-containing [2]rotaxanes upon oxidation. Although it was not possible to determine the identity of the species responsible for the small peaks observed in the spectrum (Fig. 62b) of the oxidized compound, one possibility is the presence of a small amount of decomplexed **33**·4PF_6.

5.4. Conclusions

Many of the interesting dynamic and stereochemical properties present in [2]catenanes and [2]rotaxanes are also present in their covalently tethered relatives – namely, pretzelanes and self-complexes, respectively. One of the primary effects of the tether is to lower the molecular symmetry, thereby removing the degeneracies associated with some of the dynamic processes. While there is far from sufficient data available on the effect of changing the tether's constitution, it is already apparent that the tether can be used to influence the barriers of these dynamic processes. Pretzelanes, in particular, also exhibit more complicated dynamic stereochemistry in comparison with the corresponding [2]catenanes as a result of the covalent tether connecting the two rings. Further investigations in this area will be necessary to appreciate fully the properties these compounds can afford.

The chemical switching exhibited by a bistable self-complex, suggests that these compounds may be suited to the provision of more compact molecular switches for use in molecular devices. Changing the constitution of the tether should provide another means of tuning the switching speed and lifetime of the metastable state in these particular bistable systems. Bistable pretzelanes may also prove to be useful compounds for constructing molecular switches. Not only does the tether slow down the pirouetting process enough to make it useful in a device setting, but it also opens up the possibility of creating metastable diastereoisomers. Although self-complexes and pretzelanes are not mechanically-interlocked compounds in the true sense of their definition, they do contain mechanical bonds and so share many of the same properties and applications of catenanes and rotaxanes. It follows that they should be given serious consideration when designing and constructing the next generation of molecular machines.

S. A. Vignon would like to thank P. C. Celestre, T. Iijima, J. O. Jeppesen, S. Kang, Y. Liu, H.-R. Tseng, J. Wong and T. Yamamoto for supplying compounds, and for their support and advice over the past four years. The work presented in this Review was supported by the Defense Advanced Research

Projects Agency (DARPA), the Office of Naval Research (ONR), the Microelectronics Advanced Research Corporation (MARCO) and the National Science Foundation (NSF grants DGE-0114443, CHE-9974928, CHE-0092036).

REFERENCES AND NOTES

1. Wasserman E.: *J. Am. Chem. Soc.* **1960**, *82*, 4433.
2. Frisch H. L., Wasserman E.: *J. Am. Chem. Soc.* **1961**, *83*, 3789.
3. a) Amabilino D. B., Ashton P. R., Reder A. S., Spencer N., Stoddart J. F.: *Angew. Chem., Int. Ed. Engl.* **1994**, *33*, 1286; b) Amabilino D. B., Ashton P. R., Balzani V., Boyd S. E., Credi A., Lee J. Y., Menzer S., Stoddart J. F., Venturi M., Williams D. J.: *J. Am. Chem. Soc.* **1998**, *120*, 4295; c) Wang L., Vysotsky M. O., Bogdan A., Bolte M., Böhmer V.: *Science* **2004**, *304*, 1312.
4. a) Walba D. M.: *Tetrahedron* **1985**, *41*, 3161; b) Dietrich-Buchecker C. O., Sauvage J.-P.: *Angew. Chem., Int. Ed. Engl.* **1989**, *28*, 189; c) Dietrich-Buchecker C., Rapenne G., Sauvage J.-P., Cian A. D., Fischer J.: *Chem. Eur. J.* **1999**, *5*, 1432; d) Vögtle F., Hünten A., Vogel E., Buschbeck S., Safarowsky O., Recker J., Parham A.-H., Knott M., Müller W. M., Müller U., Okamoto Y., Kudota T., Lindner W., Francotte E., Grimme S.: *Angew. Chem., Int. Ed.* **2001**, *40*, 2468.
5. Chichak K. S., Cantrill S. J., Pease A. R., Chiu S.-H., Cave G. W. V., Atwood J. L., Stoddart J. F.: *Science* **2004**, *304*, 1308.
6. Schill G., Lüttringhaus A.: *Angew. Chem., Int. Ed. Engl.* **1964**, *3*, 546.
7. a) *Templated Organic Synthesis* (F. Diederich and P. J. Stang, Eds). Wiley-VCH, Weinheim 1999; b) *Molecular Catenanes, Rotaxanes and Knots* (J.-P. Sauvage and C. O. Dietrich-Buchecker, Eds). Wiley-VCH, Weinheim 1999; c) *Self-Assembly in Supramolecular Systems*: Lindoy L. F., Atkinson I. M. in: *Monographs in Supramolecular Chemistry* (J. F. Stoddart, Ed.). Royal Society of Chemistry, Cambridge 2000; d) Philp D., Stoddart J. F.: *Synlett* **1991**, 445; e) Chambron J.-C., Dietrich-Buchecker C. O., Sauvage J.-P.: *Top. Curr. Chem.* **1993**, *165*, 131; f) Gibson H. W., Maraud H.: *Adv. Mater.* **1993**, *5*, 11; g) Amabilino D. B., Stoddart J. F.: *Chem. Rev.* **1995**, *95*, 2725; h) Fujita M., Ogura K.: *Coord. Chem. Rev.* **1996**, *148*, 249; i) Glink P. T., Schiavo C., Stoddart J. F., Williams D. J.: *Chem. Commun.* **1996**, 1483; j) Jäger R., Vögtle F.: *Angew. Chem., Int. Ed. Engl.* **1997**, *36*, 930; k) Breault G. A., Hunter C. A., Mayers P. C.: *Tetrahedron* **1999**, *55*, 5265; l) Hubin T. J., Busch D. H.: *Coord. Chem. Rev.* **2000**, *200*, 5; m) Raehm L., Hamilton D. G., Sanders J. K. M.: *Synlett* **2002**, 1743; n) Ancó F., Badjic J. D., Cantvill S. J., Flood A. H., Leung K. C. F., Liu Y., Stoddart J. F.: *Top. Curr. Chem.* **2005**, *249*, 203.
8. a) Philp D., Stoddart J. F.: *Angew. Chem., Int. Ed. Engl.* **1996**, *35*, 1154; b) Stoddart J. F., Tseng H.-R.: *Proc. Natl. Acad. Sci. U.S.A.* **2002**, *99*, 4797.
9. Raymo F. M., Stoddart J. F.: *Chem. Rev.* **1999**, *99*, 1643.
10. Co-conformation is used to describe the relative three-dimensional arrangement of the components of a mechanically-interlocked molecule with respect to one another. See: a) Fyfe M. C. T., Stoddart J. F.: *Acc. Chem. Res.* **1997**, *30*, 393; b) Fyfe M. C. T., Glink P. T., Menzer S., Stoddart J. F., White A. J. P., Williams D. J.: *Angew. Chem., Int. Ed. Engl.* **1997**, *36*, 2068.
11. a) Balzani V., Gómez-López M., Stoddart J. F.: *Acc. Chem. Res.* **1998**, *31*, 405; b) Stoddart J. F.: *Acc. Chem. Res.* **2001**, *34*, 410; c) Pease A. R., Jeppesen J. O., Stoddart J. F., Luo Y.,

Collier C. P., Heath J. R.: *Acc. Chem. Res.* **2001**, *34*, 433; d) Flood A. H., Ramirez R. J. A., Deng W.-Q., Muller R. P., Goddard III W. A., Stoddart J. F.: *Aust. J. Chem.* **2004**, *57*, 301; e) Flood A. H., Stoddart J. F., Steuerman D. W., Heath J. R.: *Science* **2004**, *306*, 2055.

12. Circumrotation is commonly used to describe the rotation of one ring in a [2]catenane through the other, while pirouetting pertains to the spinning of one ring around the outside of the other. Because the difference between these two processes is fundamentally just the frame of reference, we will consider them the same for the purposes of this Review.
13. Johnston A. G., Leigh D. A., Nezhat L., Smart J. P., Deegan M. D.: *Angew. Chem. Int. Ed. Engl.* **1995**, *34*, 1212.
14. Calculated from Fig. 3 in ref.[13] by using $\Delta\nu$ = 108 Hz and the equation $k_c = (\pi\Delta\nu)/\sqrt{2}$ to obtain the rate constant at coalescence, k_c, of 240 s^{-1} at 377 K. These values were then substituted into the Eyring equation, $\Delta G_c^{\ddagger} = -RT \ln (k_c h/k_B T)$, to determine $\Delta G_c^{\ddagger}$(377 K) = 18.1 kcal mol^{-1}.
15. Leigh D. A., Moody K., Smart J. P., Watson K. J., Slawin A. M. Z.: *Angew. Chem., Int. Ed. Engl.* **1996**, *35*, 306.
16. Deleuze M. S., Leigh D. A., Zerbetto F.: *J. Am. Chem. Soc.* **1999**, *121*, 2364.
17. Ashton P. R., Preece J. A., Stoddart J. F., Tolley M. S., White A. J. P., Williams D. J.: *Synthesis* **1994**, 1344.
18. See Section 2 for a detailed investigation into the dynamic stereochemistry of donor–acceptor [2]catenanes that arises partially as a result of this ring rocking process.
19. The term "molecular shuttle" was first used in 1991. See: Anelli P.-L., Spencer N., Stoddart J. F.: *J. Am. Chem. Soc.* **1991**, *113*, 5131.
20. Lane A. S., Leigh D. A., Murphy A.: *J. Am. Chem. Soc.* **1997**, *119*, 11092.
21. Leigh D. A., Troisi A., Zerbetto F.: *Angew. Chem., Int. Ed.* **2000**, *39*, 350.
22. a) Ashton P. R., Bissell R. A., Spencer N., Stoddart J. F., Tolley M. S.: *Synlett* **1992**, 923; b) Córdova E., Bissell R. A., Spencer N., Ashton P. R., Kaifer A. E., Stoddart J. F.: *J. Org. Chem.* **1993**, *58*, 6550; c) Devonport W., Blower M. A., Bryce M. R., Goldenberg L. M.: *J. Org. Chem.* **1997**, *62*, 885; d) Ashton P. R., Ballardini R., Balzani V., Gómez-López M., Lawrence S. E., Martínez-Díaz M.-V., Montalti M., Piersanti A., Prodi L., Stoddart J. F., Williams D. J.: *J. Am. Chem. Soc.* **1997**, *119*, 10641; e) Elizarov A. M., Chiu H.-S., Stoddart J. F.: *J. Org. Chem.* **2002**, *67*, 9175.
23. a) Bissell R. A., Córdova E., Kaifer A. E., Stoddart J. F.: *Nature* **1994**, *369*, 133; b) Raehm L., Kern J.-M., Sauvage J.-P.: *Chem. Eur. J.* **1999**, *5*, 3310; c) Ballardini R., Balzani V., Dehaen W., Dell'Erba A. E., Raymo F. M., Stoddart J. F., Venturi M.: *Eur. J. Org. Chem.* **2000**, 591; d) Collin J.-P., Kern J.-M., Raehm L., Sauvage J.-P. in: *Molecular Switches* (B. L. Feringa, Ed.), p. 249. Wiley-VCH, Weinheim 2000; e) Colasson B. X., Dietrich-Buchecker C., Jimenez-Molero M. C., Sauvage J.-P.: *J. Phys. Org. Chem.* **2002**, *15*, 476.
24. a) Ashton P. R., Ballardini R., Balzani V., Credi A., Dress R., Ishow E., Kocian O., Preece J. A., Spencer N., Stoddart J. F., Venturi M., Wenger S.: *Chem. Eur. J.* **2000**, *6*, 3558; b) Brouwer A. M., Frochot C., Gatti F. G., Leigh D. A., Mottier L., Paolucci F., Roffia S., Wurpel G. W. H.: *Science* **2001**, *291*, 2124; c) Gatti F. G., Len S., Wong J. K. Y., Bottari G., Altieri A., Morales M. A. F., Teat S. J., Frochot C., Leigh D. A., Brouwer A. M., Zerbetto F.: *Proc. Natl. Acad. Sci. U.S.A.* **2003**, *100*, 10.
25. Bermudez V., Capron N., Gase T., Gatti F. G., Kajzar F., Leigh D. A., Zerbetto F., Zhang S.: *Nature* **2000**, *406*, 608.

26. Livoreil A., Sauvage J.-P., Armaroli N., Balzani V., Flamigni L., Ventura B.: *J. Am. Chem. Soc.* **1997**, *119*, 12114.
27. Metal-containing catenanes have been dubbed catenates by Sauvage and co-workers. See: Livoreil A., Dietrich-Buchecker C. O., Sauvage J. P.: *J. Am. Chem. Soc.* **1994**, *116*, 9399.
28. Altieri A., Bottari G., Dehez F., Leigh D. A., Wong J. K. Y., Zerbetto F.: *Angew. Chem., Int. Ed.* **2003**, 42, 2296.
29. Ashton P. R., Ballardini R., Balzani V., Baxter I., Credi A., Fyfe M. C. T., Gandolfi M. T., Gómez-López M., Martínez-Díaz M.-V., Piersanti A., Spencer N., Stoddart J. F., Venturi M., White A. J. P., Williams D. J.: *J. Am. Chem. Soc.* **1998**, *120*, 11932.
30. Poleschak I., Kern J.-M., Sauvage J.-P.: *Chem. Commun.* **2004**, 474.
31. a) Mitchell D. K., Sauvage J.-P.: *Angew. Chem., Int. Ed. Engl.* **1988**, *27*, 930; b) Chambron J.-C., Mitchell D. K., Sauvage J.-P.: *J. Am. Chem. Soc.* **1992**, *114*, 4625; c) Reuter C., Pawlitzki G., Wörsdörfer U., Plevoets M., Mohry A., Kubota T., Okamoto Y., Vögtle F.: *Eur. J. Org. Chem.* **2000**, 3059.
32. Rotaxanes are not technically topological isomers of their components because it is possible to separate the components by distorting the ring component and sliding it over one of the stoppers of the dumbbell component. However, in some cases pseudo-topological chirality in rotaxanes has been reported. See: a) Yamamoto C., Okamoto Y., Schmidt T., Jäger R., Vögtle F.: *J. Am. Chem. Soc.* **1997**, *119*, 10547; b) Reuter C., Mohry A., Sobanski A., Vögtle F.: *Chem. Eur. J.* **2000**, *6*, 1674.
33. Koizumi M., Dietrich-Buchecker C., Sauvage J.-P.: *Eur. J. Org. Chem.* **2004**, 770.
34. Tachibana Y., Kihara N., Takata T.: *J. Am. Chem. Soc.* **2004**, *126*, 3438.
35. Bottari G., Leigh D. A., Pérez E. M.: *J. Am. Chem. Soc.* **2003**, *125*, 13360.
36. Tseng H.-R., Vignon S. A., Celestre P. C., Stoddart J. F., White A. J. P., Williams D. J.: *Chem. Eur. J.* **2003**, *9*, 543.
37. a) Mann B. E.: *J. Magn. Reson.* **1976**, *21*, 17; b) Mann B. E.: *J. Magn. Reson.* **1977**, *25*, 91; c) Mann B. E.: *Prog. Nucl. Magn. Spectrosc.* **1977**, *11*, 95; d) Perrin C. L., Johnston E. R.: *J. Magn. Reson.* **1979**, *33*, 619; e) Perrin C. L., Johnston E. R.: *J. Am. Chem. Soc.* **1979**, *101*, 4753.
38. Binsch G., Kessler H.: *Angew. Chem., Int. Ed. Engl.* **1980**, *19*, 411.
39. The barrier for racemization in 2,2′-dimethyl-6,6′–diethylbiphenyl was reported to be 56 kcal mol^{-1}. See: Zimmerman H. E., Crumrine D. S.: *J. Am. Chem. Soc.* **1972**, *94*, 498.
40. Eliel E. L., Wilen S. H.: *Stereochemistry of Organic Compounds*, Chap. 14. Wiley, New York 1994.
41. This chirality arises from the break in symmetry caused by the non-90° angle between the two rings. If the two rings were exactly perpendicular to one another, the geometry would be achiral.
42. Computational investigations were carried out using Macromodel 5.0. See: Mohamadi F., Richards N. G. J., Liskamp R., Lipton M., Caulfield C., Chang G., Hendrickson T., Still W. C.: *J. Comput. Chem.* **1990**, *11*, 440. The starting geometries were constructed from the X-ray crystal structure and then subjected to Monte Carlo conformational searches of 400 conformers. Energy minimization followed using the AMBER* force field as it is implemented in Macromodel 5.0 and a GB/SA $CHCl_3$ solvent model.
43. The rate at which two NMR signals exchanging by some dynamic process will coalesce is given by the equation $k_{ex} = (\pi\Delta\upsilon)/\sqrt{2}$, where $\Delta\upsilon$ is the limiting peak separation in Hz at low temperature. Thus, a larger separation between the two signals requires a higher rate constant before coalescence is observed. Although the ring rocking process is a relatively

rapid one, the large chemical shift difference between the proton environments for the inside HQ unit that it exchanges between allows it to be observed.

44. Anelli P.-L., Ashton P. R., Ballardini R., Balzani V., Delgado M., Gandolfi M. T., Goodnow T. T., Kaifer A. E., Philp D., Pietraszkiewicz M., Prodi L., Reddington M. V., Slawin A. M. Z., Spencer N., Stoddart J. F., Vicent C., Williams D. J.: *J. Am. Chem. Soc.* **1992**, *114*, 193.
45. Ashton P. R., Goodnow T. T., Kaifer A. E., Reddington M. V., Slawin A. M. Z., Spencer N., Stoddart J. F., Vicent C., Williams D. J.: *Angew. Chem., Int. Ed. Engl.* **1989**, *28*, 1396.
46. a) Aviram A., Ratner M. A.: *Chem. Phys. Lett.* **1974**, *29*, 277; b) Park J., Pasupathy A. N., Goldsmith J. I., Chang C., Yaish Y., Petta J. R., Rinkoski M., Sethna J. P., Abruña H. D., McEuen P. L., Ralph D. C.: *Nature* **2002**, *417*, 722; c) Liang W., Shores M. P., Brockrath M., Long J. R., Park H.: *Nature* **2002**, *417*, 725; d) Metzger R. M., Baldwin J. W., Shumate W. J., Peterson I. R., Mani P., Mankey C. J., Morris T., Szulczewski G., Bosi S., Prato M., Comito A., Rubin Y.: *J. Phys. Chem. B* **2003**, *107*, 1021; e) Heath J. R., Ratner M. A.: *Phys. Today* **2003**, *56*, 43; f) Wassel R. A., Gorman C. B.: *Angew. Chem., Int. Ed.* **2004**, *43*, 5120.
47. a) Collier C. P., Mattersteig G., Wong E. W., Luo Y., Beverly K., Sampaio J., Raymo F. M., Stoddart J. F., Heath J. R.: *Science* **2000**, *289*, 1172; b) Luo Y., Collier C. P., Jeppesen J. O., Nielsen K. A., DeIonno E., Ho G., Perkins J., Tseng H.-R., Yamamoto T., Stoddart J. F., Heath J. R.: *ChemPhysChem* **2002**, *3*, 519; c) Diehl M. R., Steuerman D. W., Tseng H.-R., Vignon S. A., Star A., Celestre P. C., Stoddart J. F., Heath J. R.: *ChemPhysChem* **2003**, *4*, 1335; d) Mendes P. M., Flood A. H., Stoddart J. F.: *Appl. Phys. A* **2005**, *80*, 1197.
48. Ab initio calculations have been performed on a bistable rotaxane. They suggest that the high conductivity state corresponds to the "metastable state", while the low conductivity one equates with the "stable state." See: a) Jang Y. H., Hwang S., Kim Y.-H., Jang S. S., Goddard W. A.: *J. Am. Chem. Soc.* **2004**, *126*, 12636; b) Deng W.-Q., Muller R. P., Goddard W. A.: *J. Am. Chem. Soc.* **2004**, *126*, 13562; c) Kim Y.-H., Jang S. S., Jang Y. H., Goddard W. A.: *Phys. Rev. Lett.* **2005**, *94*, 156801.
49. This process can be accelerated by two-electron reduction of the catenane, which turns off the noncovalent bonding interactions between the two rings, allowing rapid equilibration. It is believed that this mechanism also operates in the device and explains the ability to switch from the high to the low conductivity state by applying a bias opposite to that of the initial switching bias.
50. a) Asakawa M., Ashton P. R., Balzani V., Credi A., Hamers C., Mattersteig G., Montalti M., Shipway A. N., Spencer N., Stoddart J. F., Tolley M. S., Venturi M., White A. J. P., Williams D. J.: *Angew. Chem., Int. Ed. Engl.* **1998**, *37*, 333; b) Balzani V., Credi A., Mattersteig G., Matthews O. A., Raymo F. M., Stoddart J. F., Venturi M., White A. J. P., Williams D. J.: *J. Org. Chem.* **2000**, *65*, 1924.
51. a) Tseng H.-R., Wu D., Fang N. X., Zhang X., Stoddart J. F.: *ChemPhysChem* **2004**, *5*, 111; b) Flood A. H., Peters A. J., Vignon S. A., Steuerman D. W., Tseng H.-R., Kang S., Heath J. R., Stoddart J. F.: *Chem. Eur. J.* **2004**, *10*, 6558; c) Steuerman D. W., Tseng H.-R., Peters A. J., Flood A. H., Jeppesen J. O., Nielsen K. A., Stoddart J. F., Heath J. R.: *Angew. Chem., Int. Ed.* **2004**, *43*, 6486.
52. Kang S., Vignon S. A., Tseng H.-R., Stoddart J. F.: *Chem. Eur. J.* **2004**, *10*, 2555.
53. Mislow K., Raban M.: *Top. Stereochem.* **1967**, *1*, 1.

54. Ashton P. R., Brown C. L., Chrystal E. J. T., Goodnow T. T., Kaifer A. E., Parry K. P., Philp D., Slawin A. M. Z., Spencer N., Stoddart J. F., Williams D. J.: *J. Chem. Soc., Chem. Commun.* **1991**, 634.
55. These alongside interactions can occur fleetingly in rotaxanes in the form of a folded conformation. For precedents, see: a) Ashton P. R., Philp D., Spencer N., Stoddart J. F., Williams D. J.: *J. Chem. Soc., Chem. Commun.* **1994**, 181; b) Amabilino D. B., Anelli P.-L., Ashton P. R., Brown G. R., Córdova E., Godínez L. A., Hayes W., Kaifer A. E., Philp D., Slawin A. M. Z., Spencer N., Stoddart J. F., Tolley M. S., Williams D. J.: *J. Am. Chem. Soc.* **1995**, *117*, 11142.
56. a) Sutherland I. O.: *Annu. Rep. NMR Spectrosc.* **1971**, *4*, 71; b) *Dynamic NMR Spectroscopy* (J. Sandstrom, Ed.), Chap. 6. Academic Press, New York 1982.
57. The rate constant was determined using the equation $k_c = (\pi^* \Delta\upsilon_{ex})/\sqrt{2}$ and then inserted into the Eyring equation, $\Delta G^{\ddagger} = -RT_c \ln (k_c h/k_B T_c)$, where R is the gas constant, h is Planck constant, and k_B is Boltzmann constant.
58. Castro R., Nixon K. R., Evenseck J. D., Kaifer A. E.: *J. Org. Chem.* **1996**, *61*, 7298.
59. Ashton P. R., Boyd S. E., Brindle A., Langford S. J., Menzer S., Pérez-Garcia L., Preece J. A., Raymo F. M., Spencer N., Stoddart J. F., White A. J. P., Williams D. J.: *New J. Chem.* **1999**, *23*, 587.
60. a) Day J. B., Vuissoz P.-A., Oldfield E., Wieckowski A., Ansermet J.-P.: *J. Am. Chem. Soc.* **1996**, *118*, 13046; b) Tong Y., Rice C., Wieckowski A., Oldfield E.: *J. Am. Chem. Soc.* **2000**, *122*, 1123; c) Prenzler P. D., Bramley R., Downing S. R., Heath G. A.: *Electrochem. Commun.* 2 **2000**, 516; d) Webster R. D.: *Anal. Chem.* **2004**, *76*, 1603.
61. Coffen D. L., Chambers J. Q., Williams D. R., Garrett P. E., Canfield N. D.: *J. Am. Chem. Soc.* **1971**, *93*, 2258.
62. a) Steckhan E.: *Top. Curr. Chem.* **1987**, *142*, 1; b) Connelly N. G., Geiger W. E.: *Chem. Rev.* **1996**, *96*, 877.
63. Vignon S. A.: *Ph.D. Thesis*. University of California, Los Angeles 2005.
64. It was not possible to assign the two signals for the TTF unit to the specific isomer, *cis* or *trans*, that gives rise to them.
65. The TTF dication is known to have a twisted geometry with a 90° dihedral angle about the central bond connecting the two five-membered rings, removing the possibility for *cis*/*trans* isomerism. See: a) Ratner M. A., Sabin J. R., Ball E. E.: *Chem. Phys. Lett.* **1974**, *28*, 393; b) Ashton P. R., Balzani V., Becher J., Credi A., Fyfe M. C. T., Mattersteig G., Menzer S., Nielsen M. B., Raymo F. M., Stoddart J. F., Venturi M., Williams D. J.: *J. Am. Chem. Soc.* **1999**, *121*, 3951.
66. Tseng H.-R., Vignon S. A., Stoddart J. F.: *Angew. Chem., Int. Ed.* **2003**, *42*, 1491.
67. Tseng H.-R., Vignon S. A., Celestre P. C., Perkins J., Jeppesen J. O., Di Fabio A., Ballardini R., Gandolfi M. T., Venturi M., Balzani V., Stoddart J. F.: *Chem. Eur. J.* **2004**, *10*, 155.
68. Liu Y., Flood A. H., Bonvallet P. A., Vignon S. A., Northrop B. H., Tseng H.-R., Jeppesen J. O., Huang T. J., Brough B., Baller M., Magonov S., Solares S. D., Goddard W. A., Ho C.-M., Stoddart J. F.: *J. Am. Chem. Soc.* **2005**, *127*, 9745.
69. Technically there are four possible isomers, of which three are chemically distinct, namely *cis-cis*, *cis-trans* and *trans-trans*. However, only four signals, instead of the possible eight are observed, indicating that the TTF units are too far apart to influence the magnetic environment of each other and the conformational changes induced by the isomerism only affect the local protons.

70. The observation of the chemical switching of a bistable TTF/DNP-containing [2]catenane by UV/VIS spectroscopy has been reported previously. An initial communication also reported erroneously the observation of oxidative switching by ^{1}H NMR spectroscopy using *o*-chloranil. Later evidence, however, indicated that the switching in this case occurs as a result of adduct formation between the TTF unit and *o*-chloranil. See: ref.[9] and Shen C. K.-F., Duong H. M., Sonmez G., Wudl F.: *J. Am. Chem. Soc.* **2003**, *125*, 16206.
71. a) Brown C. L., Jonas U., Preece J. A., Ringsdorf H., Seitz M., Stoddart J. F.: *Langmuir* **2000** *16*, 1924; b) Asakawa M., Higuchi M., Mattersteig G., Nakamura T., Pease A. R., Raymo F. M., Shimizu T., Stoddart J. F.: *Adv. Mater.* **2000**, *12*, 1099; c) Collier C. P., Jeppesen J. O., Luo Y., Perkins J., Wong E. W., Heath J. R., Stoddart J. F.: *J. Am. Chem. Soc.* **2001**, *123*, 12632; d) Norgaard K., Jeppesen J. O., Laursen B. W., Simonsen J. B., Weygand M. J., Kjaer K., Stoddart J. F., Bjornholm T.: *J. Phys. Chem. B* **2005**, *109*, 1063.
72. a) Jang S. S., Jang Y. H., Kim Y.-H., Goddard W. A., Flood A. H., Laursen B. W., Tseng H.-R., Stoddart J. F., Jeppesen J. O., Choi J. W., Steuerman D. W., DeIonno E., Heath J. R.: *J. Am. Chem. Soc.* **2005**, *127*, 1563; b) Jang Y. H., Jang S. A., Goddard W. A.: *J. Am. Chem. Soc.* **2005**, *127*, 4959.
73. Laursen B. W., Nygaard S., Jeppesen J. O., Stoddart J. F.: *Org. Lett.* **2004**, *6*, 4167.
74. Although they will not be discussed here, zwitterionic rotaxanes and catenanes represent another interesting alternative to systems that possess a net charge.
75. a) Hamilton D. G., Davies J. E., Prodi L., Sanders J. K. M.: *Chem. Eur. J.* **1998**, *4*, 608; b) Zhang Q., Hamilton D. G., Feeder N., Teat S. J., Goodman J. M., Sanders J. K. M.: *New J. Chem.* **1999**, *23*, 897; c) Hamilton D. G., Prodi L., Feeder N., Sanders J. K. M.: *J. Chem. Soc., Perkin Trans. 1* **1999**, 1057; d) Lynch D. E., Hamilton D. G., Calos N. J., Wood B., Sanders J. K. M.: *Langmuir* **1999**, *15*, 5600; e) Hansen J. G., Feeder N., Hamilton D. G., Gunter M. J., Becher J., Sanders J. K. M.: *Org. Lett.* **2000**, *2*, 449; f) Gunter M. J., Bampos N., Johnstone K. D., Sanders J. K. M.: *New J. Chem.* **2001**, *25*, 166; g) Johnstone K. D., Bampos N., Sanders J. K. M., Gunter M. J.: *Chem. Commun.* **2003**, 1396; h) Pascu S. I., Jarrosson T., Naumann C., Otto S., Kaiser G., Sanders J. K. M.: *New J. Chem.* **2005**, *29*, 80.
76. Kaiser G., Jarrosson T., Otto S., Ng Y.-F., Bond A. D., Sanders J. K. M.: *Angew. Chem., Int. Ed.* **2004**, *43*, 1959.
77. Hamilton D. G., Montalti M., Prodi L., Fontani M., Zanello P., Sanders J. K. M.: *Chem. Eur. J.* **2000**, *6*, 608.
78. The authors assigned this peak to reduction of a free NpI unit based on comparisons with model compounds. As the neutral bistable [2]catenane is constantly in a rapid equilibrium between the two co-conformers, the authors proposed that reduction occurs when the molecule adopts the minor co-conformer where the PmI unit is encircled. See ref.[77].
79. A molecular shuttle has been reported in which a rigid electron-deficient tetracationic ring component shuttles between two electron-rich recognition sites in the dumbbell component with a barrier of ~13 kcal mol^{-1}. See ref.[19] and a) Anelli P.-L., Asakawa M., Ashton P. R., Bissell R. A., Clavier G., Gorski R., Kaifer A. E., Langford S. J., Mattersteig G., Menzer S., Philp D., Slawin A. M. Z., Spencer N., Stoddart J. F., Tolley M. S., Williams D. J.: *Chem. Eur. J.* **1997**, *3*, 1113. Reversing the recognition components, such that rigid electron-deficient, dicationic components are in the dumbbell compound and the ring component is an electron-rich flexible crown ether results in a barrier for shuttling of

~10 kcal mol^{-1}. See: b) Ashton P. R., Philp D., Spencer N., Stoddart J. F.: *J. Chem. Soc., Chem. Commun.* **1992**, 1124; c) Ashton P. R., Ballardini R., Balzani V., Bělohradský M., Gandolfi M. T., Philp D., Prodi L., Raymo F. M., Reddington M. V., Spencer N., Stoddart J. F., Venturi M., Williams D. J.: *J. Am. Chem. Soc.* **1996**, *118*, 4931.

80. Iijima T., Vignon S. A., Tseng H.-R., Jarrosson T., Sanders J. K. M., Marchioni F., Venturi M., Apostoli E., Balzani V., Stoddart J. F.: *Chem. Eur. J.* **2004**, *10*, 6375.
81. a) Asakawa M., Ashton P. R., Boyd S. E., Brown C. L., Gillard R. E., Kocian O., Raymo F. M., Stoddart J. F., Tolley M. S., White A. J. P., Williams D. J.: *J. Org. Chem.* **1997**, *62*, 26; b) Bravo J. A., Raymo F. M., Stoddart J. F., White A. J. P., Williams D. J.: *Eur. J. Org. Chem.* **1998**, 2565; c) Cabezon B., Cao J., Raymo F. M., Stoddart J. F., White A. J. P., Williams D. J.: *Chem. Eur. J.* **2000**, *6*, 2262.
82. In the coalescence method, the rate of exchange at the point of coalescence is calculated from the separation, $\Delta\upsilon$, between the two peaks at low temperature using the equation, $k_{ex} = (\pi\Delta\upsilon)/\sqrt{2}$. The rate constant, k_{ex}, is then entered into the Eyring equation, $\Delta G_c^{\ddagger} = -RT_c \ln (k_c h/k_B T_c)$, along with the coalescence temperature, T_c, in order to calculate the free energy of activation, $\Delta G_c^{\ddagger}$.
83. Vignon S. A., Jarrosson T., Iijima T., Tseng H.-R., Sanders J. K. M., Stoddart J. F.: *J. Am. Chem. Soc.* **2004**, *126*, 9884.
84. The K_a value for binding of $LiClO_4$ by [12]crown-4 at 298 K in MeCN is 2042 l mol^{-1}. See: de Namor A. F. D., Ng J. C. Y., Tanco M. A. L., Saloman M.: *J. Phys. Chem.* **1996**, *100*, 14485.
85. a) Jäger R., Schmidt T., Karbach D., Vögtle F.: *Synlett* **1996**, 8, 723; b) Yamamoto C., Okamoto Y., Schmidt T., Jäger R., Vögtle F.: J. Am. Chem. Soc. **1997**, 119, 10547; c) Vögtle F., Safarowsky O., Heim C., Affeld A., Braun O., Mohry A.: *Pure Appl. Chem.* **1999**, *71*, 247; d) Mohry A., Schwierz H., Vögtle F.: *Synthesis* **1999**, *10*, 1753; e) Reuter C., Mohry A., Sobanski A., Vögtle F.: *Chem. Eur. J.* **2000**, *6*, 1674; f) Li Q. Y., Vogel E., Parham A. H., Nieger M., Bolte M., Fröhlich R., Saarenketo P., Rissanen K., Vögtle F.: *Eur. J. Org. Chem.* **2001**, 4041.
86. a) Shinkai S., Ishihara M., Ueda K., Manabe O.: *J. Chem. Soc., Perkin Trans. 2* **1985**, 511; b) Pallavicini P. S., Perotti A., Poggi A., Seghi B., Fabbrizzi L.: *J. Am. Chem. Soc.* **1987**, *109*, 5139; c) Ueno A., Suzuki I., Osa T.: *J. Am. Chem. Soc.* **1989**, *111*, 6391; d) Minato S., Osa T., Ueno A.: *J. Chem. Soc., Chem. Commun.* **1991**, 107; e) Lednev I. K., Alfimov M. V.: *Supramol. Sci.* **1994**, *1*, 55; f) Nakamura M., Ikeda A., Ise N., Ikeda T., Ikeda H., Toda F., Ueno A.: *J. Chem. Soc., Chem. Commun.* **1995**, 721; g) Fabbrizzi L., Licchelli M., Pallavicini P., Parodi L.: *Angew. Chem., Int. Ed. Engl.* **1998**, *37*, 800; h) Nielsen M. B., Nielsen S. B., Becher J:. *Chem. Commun.* **1998**, 475; i) Nielsen M. B., Hansen J. G., Becher J.: *Eur. J. Org. Chem.* **1999**, 2807; j) Takenaka Y., Higashi M., Yoshida N.: *J. Chem. Soc., Perkin Trans. 2* **2002**, 615; k) Fabbrizzi L., Foti F., Licchelli M., Maccarini P. M., Sacchi D., Zema M.: *Chem. Eur. J.* **2002**, *8*, 4965.
87. Liu Y., Flood A. H., Moskowitz R. M., Stoddart J. F.: *Chem. Eur. J.* **2005**, *11*, 369.
88. Ashton P. R., Ballardini R., Balzani V., Boyd S. E., Credi A., Gandolfi M. T., Gómez-López M., Iqbal S., Philp D., Preece J. A., Prodi L., Ricketts H. G., Stoddart J. F., Tolley M. S., Venturi M., White A. J. P., Williams D. J.: *Chem. Eur. J.* **1997**, *3*, 152.
89. Liu Y., Bonvallet P. A., Vignon S. A., Khan S. I., Stoddart J. F.: *Angew. Chem., Int. Ed.* **2005**, *44*, 3050.
90. For examples of acyclic bis[2]catenanes, see: a) Ashton P. R., Reder A. S., Spencer N., Stoddart J. F.: *J. Am. Chem. Soc.* **1993**, *115*, 5286; b) Ashton P. R., Preece J. A., Stoddart

J. F., Tolley M. S.: *Synlett* **1994**, 789; c) Ashton P. R., Huff J., Parsons I. W., Preece J. A., Stoddart J. F., Tolley M. S., Williams D. J., White A. J. P.: *Chem. Eur. J.* **1996**, *2*, 123; d) Armaroli N., Rodgers M. A. J., Ceroni P., Balzani V., Dietrich-Buchecker C. O., Kern J.-M., Bailal A., Sauvage J.-P.: *Chem. Phys. Lett.* **1995**, *241*, 555.